DANMARKS OG GRØNLANDS GEOLOGISKE UNDERSØGELSE RAPPORT 2004/84

Palynology of the Upper Maastrichtian, Danish Central Graben

M-10X (Dan Field), E-5X (Tyra SE Field)

Poul Schiøler

GEOLOGICAL SURVEY OF DENMARK AND GREENLAND
MINISTRY OF THE ENVIRONMENT

GEUS

DANMARKS OG GRØNLANDS GEOLOGISKE UNDERSØGELSE RAPPORT 2004/84

Palynology of the Upper Maastrichtian, Danish Central Graben

M-10X (Dan Field), E-5X (Tyra SE Field)

A contribution to EFP-2001 (1313/01-0001)

Poul Schiøler

GEOLOGICAL SURVEY OF DENMARK AND GREENLAND
MINISTRY OF THE ENVIRONMENT

GEUS

Contents

Abstract

A biostratigraphic and palynofacies analysis of a closely-spaced sample succession from cored sections through the Maastrichtian to Danian chalks in the wells M-10X and E-5X shows that the Maastrichtian part of the cores correlate with the Upper Maastrichtian *Isabelidinium cooksoniae* to *Palynodinium grallator* dinoflagellate Zones. The base of the core from M-10X is biostratigraphically somewhat lower than that of the E-5X core. Due to the absence of dinoflagellates from samples above the *P. grallator* Zone the uppermost Maastrichtian to Danian interval could not be correlated to any dinoflagellate zones.

The chalks were deposited in a relatively stable, low-productivity, oligotrophic, marine environment relatively far from terrestrial source areas. The lower two-thirds of the cores, from core base to the basal *P. grallator* Zone was deposited under stable marine conditions during a slight and gradual sea-level lowering with a sea-level minimum reached at the base of the *P. grallator* Zone. Throughout this interval, productivity was in an overall decline from a maximum near the base of the M-10X core, in the basal *Palaeocystodinium denticulatum* Zone, to a minimum in the *Hystrichostrogylon borisii* and basal *P. grallator* Zones. Sea level rose abruptly again in the lower part of the *P. grallator* Zone and remained high to the top of that zone. A productivity rise followed this sea-level rise. The second sea-level high was possibly punctuated by a second, short-lived sea-level lowering that took place in the middle part of the *P. grallator* Zone.

Based on correlation with the Maastrichtian type section in the ENCI Quarry, Limburg, The Netherlands, the sea-level low at the base of the *P. grallator* Zone can be correlated with the sequence boundary at the Horizon van Kanne in the ENCI Quarry section and dated to 65.5 Ma.

Introduction

The aim of the present palynological study is to contribute to a better understanding of the formation of the North Sea Upper Maastrichtian chalks and the timing of depositional events in the chalk interval. For this purpose, a closely-spaced succession of samples from the cored sections of the M-10X and E-5X wells (Fig. 1) has been studied with focus on dinoflagellate biostratigraphy and palynofacies characterisation of the depositional environment.

Although subordinate in quantity to calcareous microfossils and nannofossils, organic-walled dinoflagellate cysts (dinoflagellates hereafter) usually occur in sufficient quantity in the NW European chalks to provide a means for biostratigraphic dating and correlation that matches that of calcareous microfossils, both in detail and reliability (see references in Schiøler & Wilson 1993). However, only very few studies document the dinoflagellate biostratigraphy of the North Sea chalks (Costa 1985; Costa & Davey 1992; Schiøler 1993; Schiøler & Wilson 1993), and although palynofacies and palyno-environmental studies of the NW European Late Cretaceous chalk succession have been carried out (Schiøler *et al.* 1997; Pearce *et al.* 2003), a palynofacies analysis on kerogen from the North Sea chalks has not been attempted before. A palynofacies analysis of the core successions from the M-10X and E-5X wells with focus on sea-level changes and variations in palaeo-watermass productivity is attempted in the present contribution.

Material and Methods

A total of 102 core samples were collected from M-10X and 57 from E-5X. On average, the sample interval is 3´. As the samples are from the oil/gas reservoir zone, the crushed samples were flushed with a mixture of 95% dichlormethan and 5% methanol for 24 hours in a soxhlet extraction column in order to remove hydrocarbons from the samples. The cleansed samples were spiked with *Lycopodium* tablets and subsequently digested in hydrochloric and hydrofluoric acid following standard palynological preparation procedures (cf. Batten 1999); the residue was sieved at 11 µm. A brief oxidation (2 min in 36% nitric acid) was carried out on all residues. The residues were heavy-liquid separated using zinc chloride and mounted in glycerine jelly on microscope slides.

Two datasets were obtained from two sets of visual kerogen counts; approximately 300 particles larger than 6 µm was recorded in the first count. The first count encompassed the following six categories: black particles, brown phytoclasts, leaf cuticles, resin, fungal hyphae and palynomorphs. Inspection under incident light showed that the majority of black particles were pyrite; they are termed pyrite particles herein. The term brown phytoclast encompasses herein particles with signs of plant anatomy (shape, structure) that appear orange to dark brown; the term also includes particles with a brown edge that are otherwise opaque. The kerogen group "amorphous organic matter", which is normally counted in palynofacies analysis, was not counted in this study as doubt arose whether this category could be separated with certainty from residual hydrocarbons (see below). Palynomorphs encompass a variety of alga cysts, sporomorphs and other acid-resistant organism remains.

The second count concerned palynomorphs only. Approximately 100 palynomorphs were counted in each sample. The following eight groups were counted: dinoflagellates (total of determinable and indeterminable), other phytoplankton (mainly acritarchs and members of the green algae genus *Palambages*), foraminifera inner linings, fungal spores, thick-walled trilete spores, other non-saccate sporomorphs, saccate pollen, and a group of highly degraded palynomorphs presumably of algal origin. Non-marine microplankton was not observed. In the second count, dinoflagellates were identified to species level when possible for qualitative biostratigraphical purpose and for calculation of %*Impagidinium* group dinoflagellates and the peridinioid/non-peridinioid ratio (see below).

Below, depths are core depths in decimal feet. The count data for all samples are listed in Appendices 1 and 2. On the basis of the counts, a number of palynofacies parameters were calculated; these are dealt with in detail below.

Palynology

The palynology of the majority of samples from the base of the studied core sections to c. 11 feet below the hardground at the top of the Tor Formation (top Tor Hardground) is characterised by a moderately diverse dinoflagellate assemblage with subordinate acritarchs. Gonyaulacoid dinoflagellates dominate the dinoflagellate assemblage. Terrestrially derived brown phytoclasts are present in moderate numbers in most samples and dominate in many samples. Sporomorphs, leaf cuticles, resin and organic-walled foraminifera inner linings are extremely rare. The preservational state of the palynomorphs ranges from poor (most samples) to moderate (fewer samples) to excellent (very few samples). Granular, yellowish brown, amorphous matter, sometimes resembling small vesiculate spheres, swamps the kerogen assemblage in most samples,. This amorphous matter is thought to represent residual hydrocarbons and is therefore not considered further herein. The relative abundance of dinoflagellates and brown phytoclasts indicate deposition in a fully marine environment with a terrestrial influx from relatively remote continental source areas.

Samples from the uppermost 10.3´ of the Tor Formation in M-10X, as well as the overlying Danian samples studied, are barren of marine palynomorphs. In samples from the uppermost 14.2´ in E-5X, dinoflagellates are extremely rare, only a few cosmopolitan species were encountered, and these may be reworked from sediments below. Apart from the poor, and probably reworked, dinoflagellate microflora in E-5X, the samples from the uppermost Maastrichtian to lowermost Danian interval contain only dominant black particulate matter (predominantly consisting of pyrite particles), few brown phytoclasts and very rare sporomorphs. The almost complete disappearance of *in situ* dinoflagellates from this part of the core is enigmatic. The absence of dinoflagellates could be an effect of chalk diagenesis subsequent to deposition or it may have been caused by primary absence of dinoflagellate cysts from the sediments. Based on the absence of marine palynomorphs, this interval could be interpreted in palynofacies terms as representing marginal marine to almost non-marine conditions. However, such an interpretation would clearly be in conflict with micro- and nannofossil evidence (see contributions elsewhere in this volume). Therefore, a palynofacies interpretation of the concerned interval is not considered reliable, and the samples from this interval are not treated further herein.

Dinoflagellate biostratigraphy

A dinoflagellate zonation for the Maastrichtian strata of the Dan Field was proposed by Schiøler & Wilson (1993, Fig. 2). The well M-10X was one of five wells on which that zonation was based. Subsequent biostratigraphic work has shown that this zonation is also applicable outside the Dan Field (Schiøler *et al.* 1997); therefore the zonation scheme of Schiøler & Wilson is used herein.

M-10X

The top of the *Isabelidinium cooksoniae* (Ico) Zone is at 6629.33′, at the highest occurrence (HO) of the nominate species. The base of the Ico Zone is at the HO of *Triblastula utinensis*. As the latter species was not encountered in the core, it may be inferred that the base of the Ico Zone was not reached. The top of the *Palaeocystodinium denticulatum* (Pde) Zone, that overlies the Ico Zone, is at the lowest occurrence (LO) of *Hystrichostrogylon borisii*, at 6552.25′. The top of *the Hystrichostrogylon borisii* (Hbo) Zone, that overlies the Pde Zone is at the base of the overlying *Palynodinium grallator* (Pgr) Zone, at 6503.25′, at the LO of the nominate species. Technically, the top of the Pgr Zone is at the HO of *P. grallator*. This normally coincides with the top of the Tor Formation and the Maastrichtian–Danian boundary. However, in M-10X samples from the uppermost 10.3′ of the Tor Formation as well as all study samples above this level are barren of dinoflagellates. Therefore, the top of the Pgr Zone must be placed at 6449.50′, 10.5′ below the Maastrichtian–Danian boundary at 6439.0′.

The Pgr Zone was subdivided into two subzones by Hansen (1977); a lower *Tanyosphaeridium magdalium* (Tma) Subzone and an upper *Thalassiphora pelagica* (Tpe) Subzone, separated at the LO of the dinoflagellate *Thalassiphora pelagica*. In a previous biostratigraphic study of core samples from M-10X, the base of the Tpe Subzone was located at 6473′ in that core (Schiøler & Wilson 1993). The Danian samples studied herein could not be assigned to any dinoflagellate zones, as they are all barren. The stratigraphic distribution of key dinoflagellates in M-10X is shown in Fig. 3.

E-5X

The LO of *H. borisii* and the base of the Hbo Zone in the E-5X core is at 6926.17′. *Isabelidinium cooksoniae* was not encountered; thus, the base of the core is in the Pde Zone. The base of the Pgr Zone is at 6872.66′, at the LO of *P. grallator*. As in M-10X, the HO of *P. grallator* (and the top of the Pgr Zone) is at 6833.5′, 14.2′ below the top of the Tor Formation (at 6819.3′), at the base of a barren interval that ranges to the top of the section. The Pgr Zone could not be subdivided in E-5X as the index species for the Tpe Subzone was not encountered in the core. As in M-10X, all Danian samples are barren for age-diagnostic dinoflagellates. The distribution of key dinoflagellates in E-5X is shown in Fig. 4.

Correlation of the wells

The two wells can be correlated by means of the above-mentioned zone index events. Further constraints come from quantitative dinoflagellate data: three conspicuous acmes of dinoflagellate species were observed in M-10X and two of these can be found at similar stratigraphic levels in E-5X. In the Pde Zone, an acme of *P. denticulatum* can be recognised in both wells and may be used for correlation. Two acmes of *P. grallator* occur in the Pgr Zone in M-10X. The highest of these, located directly below the palynologically barren interval near the top Tor Formation, is present in E-5X also. The lowest acme of *P. grallator*, in the lower part of the Pgr Zone in M-10X, was not observed in E-5X. However, there is a core gap in the lower part of the Pgr Zone in E-5X from which no palynological data

exist. It is therefore possible that the lower acme of *P. grallator* is located in this core gap. A correlation of the two cores based on dinoflagellate biostratigraphy is proposed in Fig. 5. It is seen from Fig. 5, that the thickness of the Hbo Zones is broadly similar in the two wells, whereas the Pgr Zone in M-10X is much thicker than in E-5X. This may be due either to different sedimentation rates in the two wells, a hiatus or the presence of a normal fault in E-5X. If a hiatus or a normal fault is located in the lower part of the Pgr Zone, these features offer an alternative, or supplementary, explanation for the absence for the lower acme of *P. grallator* in E-5X.

The dinoflagellate zonation used herein has been previously applied to the Maastrichtian type section in Limburg, The Netherlands, by Schiøler *et al.* (1997) and a correlation of the two cores with units in that section is proposed in Fig. 5. The thicker of the two cored sections, in M-10X, correlates as a minimum with the Schiepersberg to Meerssen Members of the Maastricht Formation, but may include the Gronsveld and Valkenburg Members from the base of the Maastricht Formation, as well as the uppermost part of the Lanaye Member. All these members can in turn be correlated with the upper *B. junior* to *B. casimirovensis* belemnite zones of Late Maastrichtian age (Jeletzky 1951; Birkelund 1957). In the Mastrichtian type section, the HO of *Triblastula utinensis* is in the middle part of the Lanaye Member. As *T. utinensis* was not recorded in M-10X, strata correlatable with the lower part of the Lanaye Member are not encountered in the latter core section.

The HO of *I. cooksoniae* is at the top of the Schiepersberg Member in the ENCI Quarry. This species occurs in M-10X, but not in E-5X. Thus, it may be inferred that layers correlatable with the Schiepersberg Member, as well as lower members of the Maastricht Formation, are not present in E-5X, and therefore, the E-5X section correlates with the Emael to Meerssen Members, upper *B. junior* to *B. casimirovensis* belemnite zones (Fig. 5).

Significance of the kerogen groups and pyrite

Changes in the kerogen assemblages in the two core sections are interpreted in terms of changes in relative sea level. This builds on the assumption that successive changes in the absolute and relative abundance of certain kerogen and palynomorph groups reflect progradation and backstepping of the coastline. The basis for this is a fast growing literature documenting the linkage between changes in relative sea-level and changes in the palynological assemblage (e.g. Partridge 1976; Brinkhuis & Zachariasse 1988; Habib & Miller 1989; Gorin and Steffen 1991; Eshet *et al.* 1992; Steffen & Gorin 1993; Versteegh 1994; Powell *et al.* 1995; Tyson 1995, 1996; Schiøler *et al.* 1997, 2002; Jaramillo & Oboh-Ikuenobe 1999).

Changes in the proportion of heterotrophic to autotrophic dinoflagellates have been interpreted in terms of changes in palaeoproductivity.

In most settings, the formation of pyrite begins in the sediment under anoxic conditions. The top of the pyrite formation depth is controlled by the depth of the anoxic zone below the sediment–water interface (Berner 1984). As pyrite formation is also dependent on the presence of organic matter, sulphate and detrital iron, changes in the concentration of any

of these compounds affect the amount of pyrite formed. In pelagic, calcareous sediments deposited in a marine environment, far from the shoreline, the limiting factor for pyrite formation is the availability of detrital iron (Berner 1984). Hence, the concentration of pyrite in samples from such settings may be inferred to correlate with the amount of detrital iron available when the sediment was deposited. As detrital iron is exclusively derived from a terrigenous source, changes in the concentration of pyrite may in turn be interpreted to correlate with changes in terrigenous influx and therefore correlate with changes in distance to shoreline, i.e. relative sea-level changes.

The parameters used herein for palynofacies analysis are explained below and are shown in Figs 6–25. Two types of trendlines have been added to the data points in the figures. A moving average (period of three) trend line (in green) has been superposed to smoothen the curve. A polynomial (order of six) trend line (in blue) has been superposed in order to visualise long term trends in the data.

Marine/non-marine ratio

In a near-shore setting, a shift towards a higher marine/non-marine ratio is characteristic of marine transgression and indicates decline in freshwater influx (e.g. Tyson 1995; Li and Habib 1996). Building on this, a shift towards a lower marine/non-marine ratio in an open marine setting may be inferred to indicate an increase in freshwater influx resulting from coastline progradation.

The palynomorph assemblage counted in the first count is totally dominated by dinoflagellate cysts. The $\log_{10}$ palynomorphs/non-marine ratios was calculated on the basis of results from the first count as the sum of all marine palynomorphs (dinoflagellates, other marine algae, foraminifera inner linings and a group of degraded palynomorphs thought to primarily represent remains of dinoflagellates) divided by the sum of non-marine kerogen (brown phytoclasts, leaf cuticles, resin, fungal hyphae and non-marine palynomorphs). The palynomorph count from count 1, which encompasses marine as well as non-marine palynomorphs, was split into marine and non-marine components by multiplication with the proportion of marine to non-marine palynomorphs obtained from the second count. The $\log_{10}$ marine/non-marine ratios for the two wells are shown in Figs 6 and 7.

Concentration and relative abundance of organic-walled phytoplankton

The organic-walled phytoplankton from the samples consists almost entirely of dinoflagellate cysts and acritarchs, with dinoflagellates being overwhelmingly dominant. High abundance (absolute or relative) of these groups generally indicate a neritic marine environment with limited continental influence (e.g. Muller 1959; Davey & Rogers 1975; Morzadec-Kerfourn 1977; Habib *et al.* 1994; Tyson 1995; Below & Kirsch 1997). However, in distal shelf areas with stable stratified watermasses, the concentration of dinoflagellate cysts may decline (Tyson 1995). The concentration of organic-walled phytoplankton in the two wells is shown in Figs 8 and 9 as specimens g^{-1}. The data is based on count data from the second count.

The relative abundance of the organic-walled phytoplankton group was calculated on the basis of the palynomorph count from the first count, corrected for the proportion of organic-walled phytoplankton to all other palynomorphs based on the second count. The relative abundance of the organic-walled phytoplankton was then calculated as a % of all particles counted in the first count and is shown in Figs 10 and 11.

Concentration and relative abundance of brown phytoclasts

A shift towards a higher concentration of brown phytoclasts is characteristic of marine regression and indicates an increase in freshwater influx (Tyson 1995). The concentration of brown phytoclasts in the two wells is shown in Figs 12 and 13 as particles g^{-1}. The relative abundance of brown phytoclasts, as % of all particles counted in the first count is shown in Figs 14 and 15.

Concentration and relative abundance of pyrite

As the limiting factor for pyrite formation in the present setting is availability of detrital iron (Berner, 1984), an increase in the concentration of pyrite may be interpreted as the result of coastline progradation and a decrease may be interpreted as a result of coastline backstepping. The concentration of pyrite in the two wells is shown in Figs 16 and 17 as particles g^{-1}. The relative abundance of pyrite, as % of all particles counted in the first count is shown in Figs 18 and 19.

%*Impagidinium* group

This group combines dinoflagellate taxa from the similar genera *Impagidinium* and *Pterodinium*. Abundance of *Impagidinium* indicates an outer neritic to oceanic environment (Wall *et al.* 1977; Harland 1983; Brinkhuis *et al.* 1992; Edwards & Andrle 1992; Shaozhi & Harland 1993; Brinkhuis 1994; Versteegh 1994; Matthiessen 1995). An increase in %*Impagidinium* is therefore interpreted as an indication of shoreline backstepping and a decrease is taken as an indication of shoreline progradation. The relative abundance of the *Impagidinium* group in the two wells is shown in Figs 20 and 21 as percentage of all dinoflagellates counted in the second count.

Organic-walled phytoplankton diversity

The highest diversity of living dinoflagellate cysts assemblages are found in warm water estuarine to neritic facies although generally, dinoflagellate cyst diversity increases in an offshore direction from estuarine to slope facies (Wall *et al.* 1977) and decreases with falling salinity (Wall *et al.* 1977; Tyson 1995). As an estuarine setting can be excluded for the study intervals, an increase in dinoflagellate diversity may be taken as an indication of shoreline backstepping or a temperature increase, or both. The significance of changes in acritarch diversity is not well known, but it may be assumed that it follows that of dinoflag-

ellate cysts as the majority of acritarch cysts most likely represent resting spores of marine algae. The organic-walled phytoplankton diversity data shown in Figs 22 and 23 combines dinoflagellate and acritarch species. As dinoflagellates strongly dominate the organic-walled phytoplankton assemblage in the study samples, the above relationship between diversity and distance from shoreline and/or temperature change are considered applicable to the present dataset.

Peridinioid/non-peridinioid ratio

Peridinioid dinoflagellate cysts constitute one of two morphologically distinct dinoflagellate cyst main groups. Peridinioid cysts are probably derived from protoperidinioid dinoflagellates; a group dominated by heterotrophic species. Protoperidinioids dominate the living dinoflagellate assemblage in water masses with high levels of nutrients where the primary productivity is high, e.g. in upwelling areas (Powell *et al.* 1992). The other main group of dinoflagellate cysts consists of gonyaulacoid dinoflagellates, which primarily represent cysts of autotrophic dinoflagellates. The peridinioid/gonyaulacoid ratio has therefore been used as a proxy for productivity in the water mass (Eshet *et al.* 1994). The non-peridinioid group used in the $\log_{10}$ peridinioid/non-peridinioid ratio shown in Figs 24 and 25 combines all gonyaulacoid dinoflagellates with rare acritarchs. As for the diversity parameter, not much is known about the correlation between acritarchs and productivity. However, considering the scarcity of acritarchs in the samples, it is considered valid to use the peridinioid/non-peridinioid ratio as a productivity proxy.

Results

A comparison of the calculated parameters from the base of the E-5X core to the uppermost part of the Tor Formation shows a good overall pair-wise correlation between the two wells (Figs 6–25). This is most clearly seen by comparing the two sets of trendlines in the figures.

Amongst the parameters used herein as sea-level proxies, the marine/non-marine ratio, %organic-walled phytoplankton and %*Impagidinium* are key parameters as they directly reflect progradation and backstepping of the shoreline. In E-5X, the vertical changes of the key sea-level parameters (except %*Impagidinium*) as well as %brown phytoclasts and organic-walled phytoplankton diversity have greater amplitude than in M-10X (compare Figs 6 and 7, 10 and 11, 14 and 15, 22 and 23).

The concentration of phytoplankton is at an overall stable low through the cored section, from c. 600 to c. 1000 specimens g^{-1} (Figs 8 and 9). In comparison, the concentration of dinoflagellates in recent mud sediments from mid-Atlantic shelf settings are 3000–4000 specimens g^{-1} (Wall *et al.* 1977), with much higher concentrations, up to 20,000 specimens g^{-1}, in localised "seed beds" and in front of estuaries (McMinn 1990, Anderson *et al.* 1982). Thus, the sediments studied herein may be interpreted as having been deposited under relatively stable, low-productivity, oligotrophic conditions.

The organic-walled phytoplankton diversity in M-10X oscillates around 20 species per sample without much variation whereas E-5X values varies from c. 30 species per sample in the uppermost Pde–lowermost Hbo Zones to minimum values below 10 species per sample at the base of the Pgr Zone (Figs 22 and 23). In general, the diversity can be considered moderate to low and supports the suggestion of deposition under oligotrophic conditions.

Gonyaulacoid cyst types dominate over peridinioid types by a factor of 10 to 100 in both cores (Figs 24 and 25), further supporting an oligotrophic environment.

Based on the results shown in Figs 6–25, the study section in both wells may be divided into a lower interval (interval 1) characterised by a relatively uniform palynological pattern with abundant dinoflagellates and overall stable values for most parameters, and an upper interval (interval 2) characterised by relatively rapid changes in key parameters. The boundary between the two major intervals may be placed at the base of the Pgr Zone or directly above it. The uppermost part of the upper interval (uppermost Tor Formation and upwards) sees the abrupt, almost complete disappearance of marine palynomorphs from all samples.

Interval 1 (base of sections to base of Pgr Zone)

With the exception of the %*Impagidinium* parameter in E-5X, key proxies for sea-level change show an overall slight declining trend in both wells from a relative sea-level high at

the base of the section, in the uppermost Ico Zone, to a relative sea-level low in the basal part of the Pgr Zone (Figs 6, 7, 10, 11, 20). In M-10X, a sub-interval of maximum sea-level is interpreted near the base of the Pde Zone and the base of the cored section, between 6629.33′ and 6615.33′ based on a succession of maximum values for key sea-level proxies (Figs 6, 10, 20). The sub-interval is under- and overlain by slightly lower values of these parameters. This stratigraphic sub-interval was not cored in E-5X. In the latter core, maximum sea-level values are reached slightly higher in the succession between 6963.33′ and 6948.08′, near the top of the Pde Zone (Figs 7, 11, 21). In M-10x, slightly elevated values for two key sea-level proxies in the interval 6582.58'–6552.25' also indicate a sea-level high near the top of the Pde Zone (Figs 6, 20). In E-5X, %*Impagidinium* does not show a declining trend through interval 1 (but indeed shows a sharp drop at the top of the interval, at the base of the Pgr Zone), but rather indicates stable marine conditions through interval 1. In M-10X minimum values for key sea-level proxies are reached in the relatively narrow sub-interval 6505.08′–6499.00′ (Figs 6, 10, 20). Two thin incipient hardgrounds were observed in that interval (Ineson 2004, this volume), one at 6500.00′, the other at 6497.00′. A candidate sequence boundary is positioned at the lower hardground, at 6500.00′. In E-5X, minimum sea-level proxy values cluster in the interval 6877.66′–6865.25′ (Figs 7, 11, 21), with the exception of a single high value at 6869.33′ for %*Impagidinium* (Fig. 21). However, this high value is overlain by very low values at 6866.25′ and 6859.83′ and is considered a data outlier. No hardgrounds were observed in the interval of lowest sea-level in E-5X; a candidate sequence boundary is positioned on the basis of palynofacies indications alone, at 6874.00', between the samples at 6873.33 and 6872.66. it is notable that the inferred minimum sea-level and candidate sequence boundary are located at the same biostratigraphic level in both wells, at the base of the Pgr Zone.

The overall slight regressive trend observed up through interval 1 is supported by an increase in both concentration and %brown phytoclasts up through the interval (Figs 12–15).

The concentration of pyrite shows a steady increase from values around 1000 particles g^{-1} in the basal part of interval 1 in both wells to levels between 2000–4000 particles g^{-1} at the top of interval 1, further supporting a slight but steady regressive trend (Figs 16–19).

The peridinioid/gonyaulacoid ratio (Figs 24 and 25) decreases slightly from maximum values at the base of the Pde Zone (only exposed in M-10X in the sub-interval 6629.33′–6612.66′) to a minimum level through most of the Hbo Zone (6548.92′–6511.50′in M-10X, 6919.17′–6890.66′ in E-5X). This indication of a relative productivity low occurs at the same level in both wells and is followed by a slightly increasing trend for the peridinioid/gonyaulacoid ratio that continues upwards into the overlying interval 2 (see section below). This trend is supported by changes in the concentration of phytoplankton cysts g^{-1} as indicated by the polynomial trend line that moves from a relative high (in the range 800–3000 particles g^{-1}) in the middle part of the Pde Zone in M-10X through a low (in the range 400–1000 particles g^{-1}) in the upper part of the Pde Zone and most of the Hbo Zone, to higher values (in the range 200–1400 particles g^{-1}) towards the top of that zone, above 6514.50′ (Figs 8 and 9).

In M-10X, the organic-walled phytoplankton diversity undergoes a slight decrease up through the interval (Fig. 22), whereas the decrease is more pronounced in E-5X (Fig. 23).

Due to the dual nature of the diversity parameter, this decrease may be interpreted as indicating either coastline progradation or decreasing water temperature, or both. Thus the data from the two wells indicate an overall sea-level and/or temperature high in the Pde Zone (located in the middle part of that zone in M-10X and in the upper part of that zone in E-5X) and a sea-level and/or temperature low in the basal Pgr Zone.

Interval 2 (base of Pgr Zone to base of barren interval)

This interval is characterised by having more variation in parameters than the underlying interval 1. From the base of interval 2, in the basal Pgr Zone, the marine/non-marine ratio and the organic-walled phytoplankton abundance (both relative and absolute) shift abruptly from low values in the basal part of the Pgr Zone to maximum values in the lower part of the zone (Figs 6, 7, 10, 11). This shift begins at 6487.25´ in M-10X and at 6869.25 in E-5X and ends at 6477.00´ in M-10X and at 6866.25´ in E-5X. The high values for the sea-level proxies at this level are followed by a sudden fall to minimum values in both wells (at 6475.17´ in M-10X and at 6859.83´ in E-5X). This inferred sea-level fall coincides approximately with the Tma–Tpe Subzone boundary at 6472.33 in M-10X (Subzone boundary not identified in E-5X) and is maintained until another shift to high values take place (at 6460.00´ in M-10X and at 6836.83´ in E-5X). The relatively high values continue to the top of the zone where virtually all marine palynomorphs disappear abruptly a short distance below top Tor Formation (at 6448.17´ in M-10X and at 6830.00´ in E-5X). Based on these higher frequency changes in the sea-level proxies in both wells, interval 2 may be interpreted as representing parts of two short-term cycles of sea-level rise and fall. The interval starts with a sea-level low in the basal Pgr Zone, followed by a sea-level rise in the lower part of that zone. Then follows a similarly rapid sea-level fall that continues through the middle part of the zone until a final sea-level rise takes place that lasts at least until 10–14´ below the top Tor Formation after which the palynological data disappear. This development is supported by the trend seen in %*Impagidinium* in E-5X and, less clearly, in M-10X (Figs 21, 20).

The presence of two subcycles in Interval 2 is supported by relatively high values of concentration of brown phytoclasts around the Tma–Tpe Subzone boundary in M-10X (Fig. 12). In E-5X, there are not many data points available, but two high values at 6847.83´ and 6845.83´ may support a sea-level low in the middle part of Interval 2 (Fig. 13). In M-10X, the absolute concentration of brown phytoclasts in Interval 2 is higher than in interval 1. This indicates that even during peak transgression in the interval, the coastline was closer to that well than it was during interval 1.

In both wells, the absolute abundance of pyrite has highest values at the base and at the top of Interval 2 but low values in the middle part of the Interval (Figs 16 and 17). As the high values in the top occur within the barren interval, the pyrite pattern from this well supports the suggestion of a sea-level low at the base of the interval and a shift to a sea-level high in the lower part of the interval. As the concentration of pyrite remains low in the palynologically productive interval, there is no support for the second sea-level low around the Tma–Tpe Subzone boundary.

In both wells the peridinioid/gonyaulacoid ratio (Figs 24 and 25) is characterised by a pattern of low values at the base of the Pgr Zone that gives way to high values in the middle part of the zone. High values persist until the dinoflagellates disappear at the base of the barren interval. This indicates a relative productivity high in the middle and upper part of Interval 2. In the M-10X well there is an indication of a productivity fall around the Tma–Tpe Subzone boundary, coeval with the sea-level fall indicated by other parameters.

From a low in the basal part of Interval 2 the organic-walled phytoplankton diversity shows an increasing trend up through the Pgr Zone in both wells (albeit more pronounced in E-5X than in M-10X) with maximum values reached shortly below the base of the barren interval (Figs 22 and 23). It is notable that the average diversity in Interval 2 of the two cores is lower than in interval 1. This possibly indicates a shallower setting and/or colder climate for Interval 2. Relative sea-level curves for the two study sections as well as productivity indications are proposed in Figs 26 and 27.

In conclusion, the palynofacies interpretation of the two wells points to a pelagic deposition in an overall stable, low-productivity, oligotrophic watermass, probably with the E-5X well in a slightly shallower depositional setting than M-10X. From the base of the cored sections, deposition took place during a slight and gradual sea-level lowering with a sea-level minimum reached in the basal Pgr Zone. Throughout this relatively stable interval, productivity was in overall decline with minimum values reached in the Hbo Zone and basal Pgr Zones. The sea-level rose quickly again in the lower part of the Pgr Zone to a high that was lower than that of the previous sea-level. The second sea-level high persisted to the top of the studied sections, possibly punctuated by a second, short-lived sea-level low that took place in the middle part of the Pgr Zone, spanning the boundary between the Tma and Tpe subzones. A productivity rise accompanied the sea-level rise that took place from the basal Pgr zone. Although productivity temporarily reached values higher than during any previous period covered by the study interval in the upper part of the Pgr Zone, on average it was lower during Interval 2 than during Interval 1. Palynofacies interpretation of the remaining, upper part of the core was precluded by the abrupt and almost complete disappearance of marine palynomorphs from the samples a short distance below the top Tor Formation and the Cretaceous-Palaeogene boundary. A combined sea-level curve for the study area is proposed in Fig. 28.

Discussion

The type of the Maastrichtian Stage, the ENCI Quarry section in Limburg, The Netherlands, was studied for palynofacies by Schiøler *et al.* (1997) with the aim of mapping relative sea-level changes through the late Maastrichtian interval. The authors were able to establish a sea-level curve for the interval and compared it with the Haq-curve of eustatic sea-level change. On their sea-level curve, the authors identified parts of four sedimentary cycles in the ENCI section (Fig. 28). Three of the cycles may be correlated with the third order cycles UZA 4.5, TA 1.1 and TA 1.2 of Haq *et al.* (1988), the fourth is caused by regional tectonic relaxation and is not shown on the Haq chart (Schiøler *et al.* 1997). The lowermost cycle identified by Schiøler *et al.* as UZA 4.5 of Haq *et al.* (1988), is at the Horizon van Lichtenberg, below the two North Sea core sections. Next cycle terminates at a sequence boundary at the Horizon van Romontbos, at the HO *of I. cooksoniae*. This level can be correlated with the M-10X core. However, according to Schiøler *et al.* that cycle is of higher order and controlled by local tectonic relaxation. Accordingly, it cannot be identified in the two North Sea cores. The sequence boundary at the conspicuous hardground Horizon van Kanne is situated directly above the LO of *P. grallator*, and was interpreted as a sequence boundary developed during a significant sea-level fall (Schiøler *et al.* 1995). The sequence boundary at Horizon van Kanne was identified as the base of the TA 1.2 cycle of Haq *et al.* (1988) by Schiøler *et al.* (1997). Setting the age of the Maastrichtian–Palaeogene boundary to 65.0 Ma (Hardenbol *et al.*, 1998), the sea-level fall represented by the Horizon van Kanne could be dated to 65.5 Ma by Schiøler *et al.*, based on astronomically calibrated 20 ky cycles recorded in the ENCI section by Zijlstra (1994). The sea-level fall represented by Horizon van Kanne can be correlated to both North Sea sections using the LO of *P. grallator* and correlates with the sea-level fall identified at the base of the Pgr Zone on palynofacies evidence. In M-10X, two closely spaced incipient hardgrounds are present at 6497′ and 6500′; a few feet above the base of the *P. grallator* Zone, at 6503.25′ (Ineson 2004). This provides the possibility of directly correlating the Horizon van Kanne with the lower hardground in M-10X, at 6500′. In E-5X, hardgrounds have not been observed near the base of the *P. grallator* Zone. However, as mentioned above, the palynological results indicate that the basal part of the *P. grallator* Zone may be missing in E-5X. Hence, it is therefore possible that the sea-level fall inferred from the type Maastrichtian section is the same sea-level fall that affected the two North Sea wells and removed sediments from the lower part of the Pgr Zone in E-5X and created the two incipient hardgrounds in M-10X.

Acknowledgements

Many of the figures were prepared by Stefan Sølberg (GEUS), for which he is thanked. Constructive criticism by Jon Ineson (GEUS) improved the manuscript considerably. The Danish Energy Authority is thanked for support through grant No. 1313/01-0001.

References

Anderson, D.M., Aubrey, D.G., Tyler, M.A. & Coats, D.W. 1982: Vertical and horizontal distributions of dinoflagellate cysts in sediments. Limnology and Oceanography **27**, 757–765.

Batten, D.J. 1999: Small palynomorphs. In: Jones, T.P. & Rowe, N.P. (eds): *Fossil plants and spores: modern techniques*, 15–19. Geological Society, London.

Below, R., Kirsch, K.-H. 1997: Die kerogen-facies der tonstein-blättertonstein rhythmite des Ober-Barrême/Unter-Apt im Niedersächsischen Becken (Norddeutschland) am beispiel der bohrung Hoheneggelsen KB 50. Palaeontographica, Abt. B **242**, 1–90.

Berner, R.A. 1984: Sedimentary pyrite formation: an update. Geochimica Cosmochimica Acta **48**, 605–615.

Birkelund, T. 1957: Upper Cretaceous Belemnites from Denmark. Biol. Skr. Dan. Vid. Selsk. **9**(1), 69 pp.

Brinkhuis, H. 1994: Late Eocene to Early Oligocene dinoflagellate cysts from the Priabonian type-area (northeast Italy): biostratigraphy and paleoenvironmental interpretation. Palaeogeography, Palaeoclimatology, Palaeoecology **107**, 121–163.

Brinkhuis, H. & Zachariasse, W.J. 1988: Dinoflagellate cysts, sea-level changes and planktonic foraminifers across the Cretaceous-Tertiary boundary at El Haria, northwest Tunisia. Marine Micropaleontology **13**, 153–191.

Brinkhuis, H., Powell, A. J., Zevenboom, D. 1992: High-resolution dinoflagellate cyst stratigraphy of the Oligocene/Miocene transition interval in northwest and central Italy. In: Head, M.J., Wrenn, J.H. (eds): Neogene and Quaternary dinoflagellate cysts and acritarchs: American Association of Stratigraphic Palynologists Foundation, Dallas, 219–258.

Costa, L. I. 1985: Dinoflagellate cyst stratigraphy in the Upper Cretaceous of the Central Graben, Norwegian North Sea. North Sea Chalk Symposium, Copenhagen: 1–9.

Costa, L. I. & Davey, R. J. 1992: Dinoflagellate cysts of the Cretaceous System. In: A. J. Powell (ed.): A Stratigraphic Index of Dinoflagellate Cysts. Chapman and Hall, London, 99–154.

Davey, R.J. & Rogers, J. 1975: Palynomorph distribution in recent offshore sediments along two traverses off South West Africa. Marine Geology **18**, 213–225.

Edwards, L.E. & Andrle, V.A.S. 1992: Distribution of selected dinoflagellate cysts in modern marine sediments. In: Head, M. J., Wrenn, J.H. (eds): Neogene and Quaternary dinoflagellate cysts and acritarchs. American Association of Stratigraphic Palynologists Foundation, Dallas, 259–288.

Eshet, Y., Moshkovitz, S., Habib, D., Benjamini, C. & Magaritz, M. 1992: Calcareous nannofossil and dinoflagellate stratigraphy across the Cretaceous/Tertiary boundary at Hor Hahar, Israel. Marine Micropaleontology **18**, 199–229.

Eshet, Y., Almogi-Labin, A. & Bein, A. 1994: Dinoflagellate cysta, paleoproductivity and upwelling systems: a Late Cretaceous example from Israel. Marine Micropaleontology **23**, 231–240.

Gorin, G.E. & Steffen, D. 1991: Organic facies as a tool for recording eustatic variations in marine fine-grained carbonates - example of the Berriasian stratotype at Berrias (Ardèche, SE France). Palaeogeography, Palaeoclimatology, Palaeoecology **85**, 303–320.

Habib, D. & Miller, J.A. 1989: Dinoflagellate species and organic facies evidence of marine transgression and regression in the Atlantic Coastal Plain. Palaeogeography, Palaeoclimatology, Palaeoecology **74**, 23–47.

Habib, D., Eshet, Y. & Van Pelt, R. 1994: Palynology of sedimentary cycles. In: Traverse, A. (ed.): Sedimentation of organic particles. Cambridge University Press, Cambridge, 311–335.

Hansen, J. M. 1977: Dinoflagellate stratigraphy and echinoid distribution in Upper Maastrichtian and Danian deposits from Denmark. Bulletin of the Geological Society of Denmark **26**, 1–26.

Haq, B. U., Hardenbol, J. & Vail, P. R. 1988: Mesozoic and Cenozoic chronostratigraphy and cycles of sea-level change. In: C. K. Wilgus, B. S. Hastings, H. Posamentier, J. Van Vagoner, C. A. Ross, C. G. St. C. Kendal (eds): Sea-level changes: an integrated approach. SEPM Spec. Publ. **42**, 71–108.

Hardenbol, J., Thierry, J., Farley, M.B., Jacquin, T., de Graciansky, P.-C. & Vail, P.R. 1998: Mesozoic and Cenozoic sequence chronostratigraphic chart. In: de Graciansky, P.-C., Hardenbol, J., Jacquin, T., Vail, P.R., Farley, M.B (eds): Mesozoic and Cenozoic sequence stratigraphy of European Basins. SEPM Special Publication **60**, 3–13.

Harland, R. 1983: Distribution maps of recent dinoflagellate cysts in bottom sediments from the North Atlantic Ocean and adjacent seas. Palaeontology **26**, 321–387.

Ineson, J.R. 2004: Sedimentology of the Upper Maastrichtian chalk, Danish Central Graben. Danmarks og Grønlands Geologiske Undersøgelse Rapport **2004/89**.

Jaramillo, C.A. & Oboh-Ikuenobe, F.E. 1999: Sequence stratigraphic interpretations from palynofacies, dinocyst and lithological data of Upper Eocene–Lower Oligocene strata in southern Mississippi and Alabama, U.S. Gulf Coast. Palaeogeography, Palaeoclimatology, Palaeoecology **145**, 259–302.

Jeletzky, J. A. 1951: Die Stratigraphie und Belemnitenfauna des Obercampan und Maastricht Westfalens, Nordwestdeutschlands und Dänemarks sowie einige algemeine Gliederungsprobleme der jüngeren borealen Oberkreide Eurasiens. Beih. Geol. Jb. **1**, 142 pp.

Li, H. & Habib, D. 1996: Dinoflagellate stratigraphy and its response to sea level change in Cenomanian–Turonian sections of the Western Interior of the United States. Palaios **11**, 15–30.

Matthiessen, J. 1995: Distribution pattern of dinoflagellate cysts and other organic-walled microfossils in recent Norwegian-Greenland Sea sediments. Marine Micropaleontology **24**, 307–334.

McMinn, A. 1990: Recent dinoflagellate cyst distribution in Eastern Australia. Review of Palaeobotany and Palynology **65**, 305–310.

Morzadec-Kerfourn, M.-T. 1977: Les kystes de dinoflagellés dans les sédiments récents le long des côtes Bretonnes. Revue de Micropaléontologie **20**, 157–166.

Muller, J. 1959: Palynology of recent Orinoco delta and shelf sediments: reports of the Orinoco Shelf Expedition; Volume **5**. Micropaleontology **5**, 1–32.

Partridge, A.D. 1976: The geological expression of eustacy in the Early Tertiary of the Gippsland Basin. APEA Journal **1976**, 73–79.

Pearce, M.A., Jarvis, I., Swan, A.R.H., Murphy, A.M., Tocher, B.A. & Edmunds, W.M. 2003: Integrating palynological and geochemical data in a new approach to palaeoecological studies: Upper Cretaceous of the Banterwick Barn Chalk borehole, Berkshire, UK. Marine Micropaleontology **47**(3-4), 271–306.

Powell, A.J., Lewis, J. & Dodge, J.D. 1992: The palynological expression of post-Palaeogene upwelling, a review. In: Upwelling systems: evolution since the Early Miocene, C.P. Summerhayes, W.L. Prell & C.K. Emeis (eds): Geological Society of London, Special Publication **64**, 215–26.

Powell, A.J., Brinkhuis, H. & Bujak, J.P. 1995: Upper Paleocene–Lower Eocene dinoflagellate cyst sequence biostratigraphy of SE England. In: Knox, R.W.O'B., Corfield, R., Dunay R.E. (eds): Correlation of the early Paleogene in Northwest Europe. Geological Society (London) Special Publication **101**, 145–183.

Schiøler, P. 1993: New species of dinoflagellate cysts from Maastrichtian-Danian chalks of the Danish North Sea. Journal of Micropalaeontology **12**(1), 99–112.

Schiøler, P. & Wilson, G.J. 1993: Maastrichtian dinoflagellate zonation in the Dan Field, Danish North Sea. Review of Palaeobotany and Palynology **78**, 321–351.

Schiøler, P., Brinkhuis, H., Roncaglia, L. & Wilson, G.J. 1997: Dinoflagellate biostratigraphy and sequence stratigraphy in the type Maastrichtian (Late Cretaceous), ENCI Quarry, The Netherlands. Marine Micropaleontology **31**, 65–95.

Schiøler, P., Crampton, J.S. & Laird, M.G. 2002: Palynofacies and sea-level changes in the middle Coniacian–Campanian (Late Cretaceous) of the East Coast Basin, New Zealand. Palaeogeography, Palaeoclimatology, Palaeoecology **188**(3–4), 101–125.

Shaozhi, M. & Harland, R. 1993: Quaternary organic-walled dinoflagellate cysts from the South China Sea and their paleoclimatic significance. Palynology **17**, 47–65.

Steffen, D. & Gorin, G.E. 1993: Sedimentology of organic matter in Upper Tithonian–Berriasian deep-sea carbonates of southeast France: evidence of eustatic control. In: Katz, B., Pratt, L. (eds): Source rocks in a sequence stratigraphic framework. AAPG Studies in Geology **37**, 49–65.

Surlyk, F. 1970: Die Stratigraphie des Maastricht von Dänemark und Norddeutschland aufgrund von Brachiopoden. Newsl. Stratigr. **1**(2), 7–16.

Tyson, R.V. 1995: Sedimentary organic matter. Organic facies and palynofacies. Chapman and Hall, London.

Tyson, R.V. 1996: Sequence stratigraphical interpretation of organic facies variations in marine siliciclastic systems: general principles and application to the onshore Kimmeridge Clay Formation, UK. In: Hesselbo, S., Parkinson, N. (eds): Sequence stratigraphy in British geology. Geological Society (London) Special Publication **103**, 75–96.

Versteegh, G.J.M. 1994: Recognition of cyclic and non-cyclic environmental changes in the Mediterranean Pliocene: A palynological approach. Marine Micropaleontology **23**, 147–183.

Wall, D., Dale, B., Lohmann, G.P. & Smith, W.K. 1977: The environmental and climatic distribution of dinoflagellate cysts in modern marine sediments from regions in the North and South Atlantic oceans and adjacent seas. Marine Micropaleontology **2**, 121–200.

Zijlstra, J.J.P. 1994: Sedimentology of the Late Cretaceous and Early Tertiary (Tuffaceous) chalk of northwest Europe. Geologica Ultraiect. **119**, 1–192.

Figures

Fig. 1. Late Cretaceous structural framework of the Danish Central Graben showing the position of the M-10X and E-5X wells within the Dan and Tyra fields, respectively (figure from Ineson 2004, this volume).

Fig. 2. Correlation of selected Maastrichtian biostratigraphic zonation schemes from the North German, Danish and North Sea areas. Tpe=*Thalassiphora pelagica* Subzone; Tma=*Tanyosphaeridium magdalium* Subzone; Hbo=*Hystrichostrogylon borisii* Zone; Pde=*Palaeocystodinium denticulatum* Zone; Ico=*Isabelidinium cooksoniae* Zone; Cut=*Cannosphaeropsis utinensis* Subzone; Aac=*Alterbidinium acutulum* Subzone; Eha=*Eatonicysta hapala* Subzone (figure from Schiøler & Wilson, 1993).

Fig. 3. Distribution of key dinoflagellates in the M-10X well. B=barren sample.

Fig. 4. Distribution of key dinoflagellates in the E-5X well. B=barren sample.

Fig. 5. Correlation of the cored sections from M-10X and E-5X with the type Maastrichtian section in the ENCI Quarry, Limburg, The Netherland, based on dinoflagellates (ENCI stratigraphy from Schiøler *et al.*, 1997). MD = log depth, CD = core depth.

Fig. 6. Marine/non-marine ratio in the M-10X core. The ratio is calculated as $\log_{10}$ of the the sum of marine palynomorphs (dinoflagellates, acritarchs, other marine algae, foraminifera inner linings and degraded palynomorphs) divided by all terrestrially derived palynomorphs (brown phytoclasts, leaf cuticles, resin, fungal hyphae, terrestrial sporomorphs) from the first particle count (see text for further detail on the calculation). Horizontal lines indicate zone boundaries. Zone abbreviations as in Fig. 2. A short term trendline (moving average, period of three) and a long term trendline (sixth order polynomial) are superposed on the data in green and blue, respectively.

Fig. 7. Marine/non-marine ratio in the E-5X core. The ratio is calculated as in Fig. 6. Horizontal lines and trend lines as in Fig. 6. Zone abbreviations as in Fig. 2.

Fig. 8. Concentration of organic-walled phytoplankton as specimens g^{-1} dry sediment in the M-10X core. Note the complete disappearance of this fossil group above the sample at 6440.50´. Horizontal lines and trend lines as in Fig. 6. Zone abbreviations as in Fig. 2.

Fig. 9. Concentration of organic-walled phytoplankton as specimens g^{-1} dry sediment in the E-5X core. Note the complete disappearance of this fossil group above the sample at 6839.25´. Horizontal lines and trend lines as in Fig. 6. Zone abbreviations as in Fig. 2.

Fig. 10. Abundance of organic-walled phytoplankton relative to all counted particles from the first count in the M-10X core, calculated on basis of the palynomorph count from count 1 multiplied with the ratio of organic-walled phytoplankton against all palynomorphs from count 2. Horizontal lines and trend lines as in Fig. 6. Zone abbreviations as in Fig. 2.

Fig. 11. Abundance of organic-walled phytoplankton relative to all counted particles from the first count in the E-5X core, calculated on basis of the palynomorph count from count 1 multiplied with the ratio of organic-walled phytoplankton against all palynomorphs from count 2. Calculation as in Fig. 11. Horizontal lines and trend lines as in Fig. 6. Zone abbreviations as in Fig. 2.

Fig. 12. Concentration of brown phytoclasts as particles g^{-1} dry sediment in the M-10X core. Horizontal lines and trend lines as in Fig. 6. Zone abbreviations as in Fig. 2.

Fig. 13. Concentration of brown phytoclasts as particles g^{-1} dry sediment in the E-5X core. Horizontal lines and trend lines as in Fig. 6. Zone abbreviations as in Fig. 2.

Fig. 14. Abundance of brown phytoclasts relative to all counted particles from the first count in the M-10X core. Horizontal lines and trend lines as in Fig. 6. Zone abbreviations as in Fig. 2.

Fig. 15. Abundance of brown phytoclasts relative to all counted particles from the first count in the E-5X core. Horizontal lines and trend lines as in Fig. 6. Zone abbreviations as in Fig. 2.

Fig. 16. Concentration of pyrite particles g^{-1} dry sediment in the M-10X core. Horizontal lines and trend lines as in Fig. 6. Zone abbreviations as in Fig. 2.

Fig. 17. Concentration of pyrite particles g^{-1} dry sediment in the E-5X core. Horizontal lines and trend lines as in Fig. 6. Zone abbreviations as in Fig. 2.

Fig. 18. Abundance of pyrite particles relative to all counted particles from the first count in the M-10X core. Horizontal lines and trend lines as in Fig. 6. Zone abbreviations as in Fig. 2.

Fig. 19. Abundance of pyrite particles relative to all counted particles from the first count in the E-5X core. Horizontal lines and trend lines as in Fig. 6. Zone abbreviations as in Fig. 2.

Fig. 20. Abundance of *Impagidinium* group dinoflagellates (*Impagidinium* and *Pterodinium*) relative to all counted dinoflagellates from the second count in the M-10X core. Horizontal lines and trend lines as in Fig. 6. Zone abbreviations as in Fig. 2.

Fig. 21. Abundance of *Impagidinium* group dinoflagellates (*Impagidinium* and *Pterodinium*) relative to all counted dinoflagellates from the second count in the E-5X core. Horizontal lines and trend lines as in Fig. 6. Zone abbreviations as in Fig. 2.

Fig. 22. Diversity of marine phytoplankton (dinoflagellates and acritarchs) in the M-10X core as number of taxa in a sample. Horizontal lines and trend lines as in Fig. 6. Zone abbreviations as in Fig. 2.

Fig. 23. Diversity of marine phytoplankton (dinoflagellates and acritarchs) in the E-5X core as number of taxa in a sample. Horizontal lines and trend lines as in Fig. 6. Zone abbreviations as in Fig. 2.

Fig. 24. Ratio of peridinioid to non-peridiniod dinoflagellate specimens in the M-10X core. Non-peridinioid taxa combines gonyaulacoid dinoflagellates with rare acritarch species. Horizontal lines and trend lines as in Fig. 6. Zone abbreviations as in Fig. 2.

Fig. 25. Ratio of peridinioid to non-peridiniod dinoflagellate specimens in the E-5X. Non-peridinioid taxa combines gonyaulacoid dinoflagellates with rare acritarch species. Horizontal lines and trend lines as in Fig. 6. Zone abbreviations as in Fig. 2.

Fig. 26. Inferred sea-level curve and productivity indications for M-10X. MD = log depth, CD = core depth.

Fig. 27. Inferred sea-level curve and productivity indications for E-5X. MD = log depth, CD = core depth.

Fig. 28. Comparison between the sea-level changes inferred from the present study, the relative sea-level changes inferred from the Type Maastrichtian at ENCI Quarry, Limburg, The Netherlands by Schiøler *et al.* (1997) and the short term (third order) eustatic cycles of Haq *et al.* (1988). The North Sea sea-level curved is based on the combined evidence from the wells M-10X and E-5X. A higher order cycle controlled by local tectonism occurs between Romontbos and Kanne Horizons in the ENCI section. Geochronology based on astronomical calibration from Zijlstra (1994). It is notable that both the North Sea curve and the ENCI curve shows a marked sea-level fall at the LO of *Palynodinium grallator*, at the Horizon van Kanne in the ENCI section. HS = highstand, LS = lowstand, MFS = maximum flooding surface, SB = sequence boundary, TR = transgression (figure modified from Schiøler *et al.* 1997).

Appendices

Appendix 1. Palynofacies count data and calculated parameters from M-10X.

Appendix 2. Palynofacies count data and calculated parameters from E-5X.

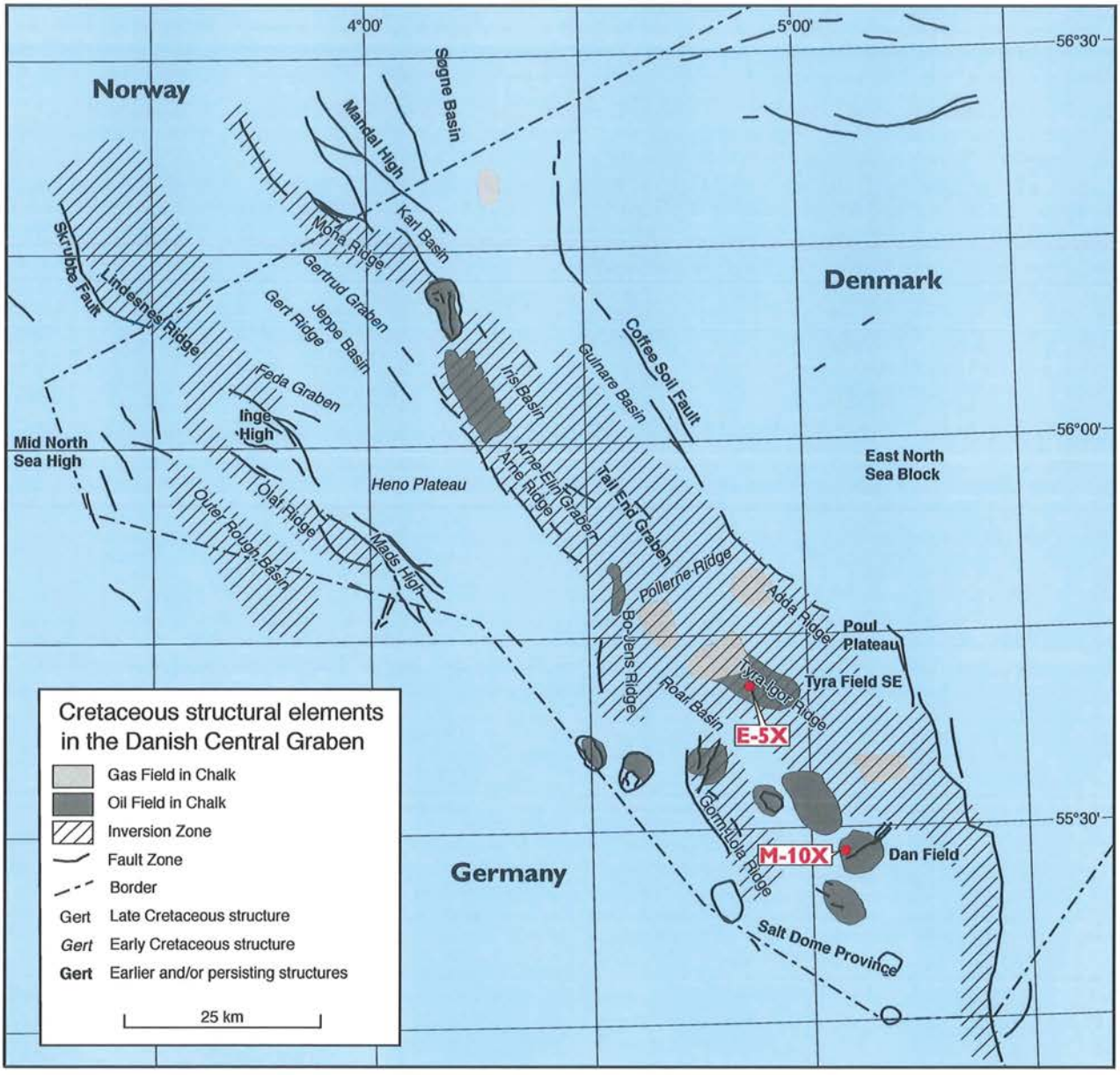
4°00'
5°00'
56°30'
56°00'
55°30'
Norway
Denmark
Germany
Søgne Basin
Mandal High
Karl Basin
Mona Ridge
Gertrud Graben
Gert Ridge
Jeppe Basin
Skrubbe Fault
Lindesnes Ridge
Feda Graben
Inge High
Mid North Sea High
Heno Plateau
Outer Rough Basin
Olaf Ridge
Mads High
Iris Basin
Arne-Elin Graben
Arne Ridge
Gulnare Basin
Coffee Soil Fault
Tail End Graben
Pollerne Ridge
Bo Jens Ridge
Adda Ridge
Poul Plateau
Tyra Field SE
Tyra-Igor Ridge
Roar Basin
E-5X
M-10X
Dan Field
Gorm Tilda Ridge
Salt Dome Province
East North Sea Block
Cretaceous structural elements in the Danish Central Graben
Gas Field in Chalk
Oil Field in Chalk
Inversion Zone
Fault Zone
Border
Gert Late Cretaceous structure
Gert Early Cretaceous structure
Gert Earlier and/or persisting structures
25 km

Fig

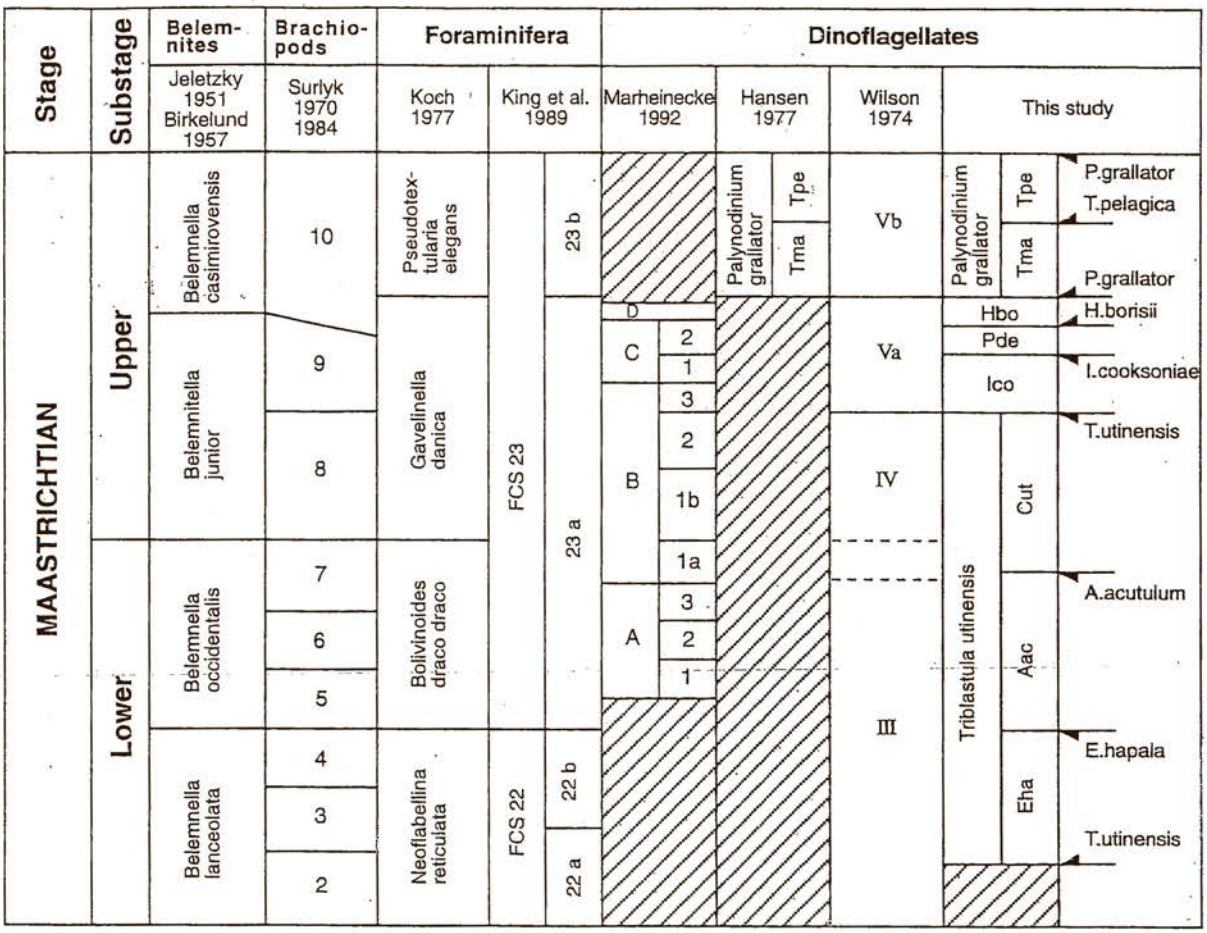
Stage
Substage
Belem-nites
Brachio-pods
Foraminifera
Dinoflagellates
Jeletzky 1951 Birkelund 1957
Surlyk 1970 1984
Koch 1977
King et al. 1989
Marheinecke 1992
Hansen 1977
Wilson 1974
This study
MAASTRICHTIAN
Upper
Lower
Belemnella casimirovensis
Belemnitella junior
Belemnella occidentalis
Belemnella lanceolata
10
9
8
7
6
5
4
3
2
Pseudotex-tularia elegans
Gavelinella danica
Bolivinoides draco draco
Neoflabellina reticulata
FCS 23
FCS 22
23 b
23 a
22 b
22 a
D
C
B
A
2
1
3
2
1b
1a
3
2
1
Palynodinium grallator
Tpe
Tma
Vb
Va
IV
III
Hbo
Pde
Ico
Triblastula utinensis
Cut
Aac
Eha
P.grallator
T.pelagica
P.grallator
H.borisii
I.cooksoniae
T.utinensis
A.acutulum
E.hapala
T.utinensis

Fig. 2

M-10X			key dinoflagellates						Dinoflagellate zone (Schieler & Wilson 1993)	
core depth (f)	core depth (dec. f)	log depth (dec. f)	*I. cooksoniae*	*P. denticulatum*	*H. borisii*	*P.grallator*	*T. pelagica*	event		
6433' 4"	6433.33	6438.83	B	B	B	B				(no zones)
6433' 7"	6433.58	6439.08	B	B	B	B				
6434' 7"	6434.58	6440.08	B	B	B	B				
6436' 10"	6436.83	6442.33	B	B	B	B				
6438' 2"	6438.17	6443.67	B	B	B	B				
6438' 10"	6438.83	6444.33	B	B	B	B				
6439'	6439.00	6444.50	B	B	B	B				
6439' 4"	6439.33	6444.83	B	B	B	B				
6440' 6"	6440.60	6446.10	B	B	B	B				
6441' 11"	6441.92	6447.42	B	B	B	B				
6443' 5"	6443.41	6448.91	B	B	B	B				
6444' 10"	6444.83	6450.33	B	B	B	B				
6446' 6"	6446.50	6452.00	B	B	B	B				
6448' 2"	6448.17	6453.67	B	B	B	B				
6449' 6"	6449.50	6455.00	0	0	6	12		HO *P. grallator*	Tpe	Pgr
6451' 10"	6451.83	6457.33	0	0	0.25	20.75				
6454' 4"	6454.33	6459.83	0	0	6.5	22		2nd acme Pgr		
6456' 9"	6456.75	6462.25	0	0	1	27.75				
6458' 2"	6458.17	6463.67	0	0	1	43.5				
6460' 0"	6460.00	6465.50	0	0	2	1.75				
6463'	6463.00	6468.50	B	B	B	B				
6465' 3"	6465.25	6470.75	0	0	1	1				
6467' 8"	6467.66	6473.16	0	0	0	0				
6472' 4"	6472.33	6477.83	0	0	1	1		LO *T. pelagica*		
6475' 2"	6475.17	6480.67	0	0	0	4.25			Tma	
6477' 0"	6477.00	6482.50	0	0	0	55.75				
6481'	6481.00	6486.50	0	0	0	30.5		1st acme Pgr		
6483' 10"	6483.83	6489.33	0	0	1	0				
6487' 3"	6487.25	6492.75	0	0	0	0				
6489' 6"	6489.50	6495.00	0	0	0	0				
6491' 6"	6491.50	6497.00	B	B	B	B				
6495' 6"	6495.50	6501.00	B	B	B	B				
6499' 0"	6499.00	6504.50	0	0	0	0				
6502' 4"	6502.33	6507.83	0	0	0	3.25				
6503' 3"	6503.25	6508.75	0	0	?	4.5		LO *P. grallator*		
6505' 1"	6505.08	6510.58	0	0	0	0				Hbo
6507' 8"	6507.66	6513.16	0	0	0	0				
6511' 6"	6511.50	6517.00	0	0	0	0				
6514' 6"	6514.50	6520.00	0	0	0	0				
6516' 8"	6516.66	6522.16	0	0	0	0				
6519' 5"	6519.41	6524.91	B	B	B	B				
6522' 3"	6522.25	6527.75	B	B	B	B				
6525' 3"	6525.25	6530.75	0	0	0	0				
6528' 11"	6528.92	6534.42	0	0	1	0				
6531'	6531.00	6536.50	0	0	0	0				
6533' 2"	6533.17	6538.67	0	0	0	0				
6539' 11"	6539.92	6545.42	B	B	B	B				
6542' 7"	6542.58	6548.08	B	B	B	B				
6546' 5"	6546.41	6551.91	0	0	0	0				
6548' 11"	6548.92	6554.42	0	0	2	0				
6552' 3"	6552.25	6557.75	0	0	0.5	0		LO *H. borisii*		
6554' 10"	6554.83	6560.33	0	0	0	0				Pde
6557' 7"	6557.58	6563.08	0	0	0	0				
6560' 9"	6560.75	6566.25	0	0	0	0				
6563' 5"	6563.41	6568.91	0	0	0	0				
6564' 9"	6564.66	6570.16	0	0	0	0				
6568' 3"	6568.25	6573.75	0	1	0	0				
6571' 2"	6571.17	6576.67	0	0	0	0				
6573' 8"	6573.66	6579.16	0	0	0	0				
6577' 1"	6577.08	6582.58	0	x	0	0				
6579' 10"	6579.83	6585.33	0	0	0	0				
6582' 7"	6582.58	6588.08	0	1	0	0				
6586' 3"	6586.25	6591.75	0	0.5	0	0				
6590'	6590.00	6595.50	0	4.5	0	0		acme Pde		
6592' 2"	6592.17	6597.67	0	1.5	0	0				
6598' 6"	6598.50	6604.00	B	B	B	B				
6601' 7"	6601.58	6607.08	0	0	0	0				
6604' 11"	6604.92	6610.42	0	0	0	0				
6608' 1"	6608.08	6613.58	0	0	0	0				
6610'	6610.00	6615.50	1	1.5	0	0				
6611' 7"	6611.58	6617.08	0	0	0	0				
6612' 4"	6612.33	6617.83	0	0	0	0				
6612' 8"	6612.66	6618.16	0	0	0	0				
6613' 1"	6613.08	6618.58	0	0	0	0				
6613' 6"	6613.50	6619.00	0	0	0	0				
6614' 1"	6614.08	6619.58	0	0	0	0				
6614' 5"	6614.41	6619.91	0	0	0	0				
6614' 9"	6614.75	6620.25	0	0	0	0				
6615'	6615.00	6620.50	0	0	0	0				
6615' 4"	6615.33	6620.83	0	0	0	0				
6615' 7"	6615.58	6621.08	0	0	0	0				
6615' 11"	6615.92	6621.42	0	1	0	0				
6616' 3"	6616.25	6621.75	0	0	0	0				
6616' 7"	6616.58	6622.08	0	0	0	0				
6617' 2"	6617.17	6622.67	0	0	0	0				
6617' 7"	6617.58	6623.08	0	0	0	0				
6618'	6618.00	6623.50	0	0.25	0	0				
6618' 5"	6618.41	6623.91	0	3	0	0				
6618' 7"	6618.58	6624.08	0	0	0	0				
6619'	6619.00	6624.50	0	0	0	0				
6619' 5"	6619.41	6624.91	0	0	0	0				
6623'	6623.00	6628.50	0	0	0	0				
6626' 5"	6626.41	6631.91	0	0	0	0				
6629' 4"	6629.33	6634.83	11.5	0	0	0		HO *I. cooksoniae*		Ico
6631' 8"	6631.66	6637.16	2.5	0	0	0				
6634' 5"	6634.41	6639.91	0	0	0	0				
6637' 4"	6637.33	6642.83	0	0	0	0				
6641'	6641.00	6646.50	1	0	0	0				
6644'	6644.00	6649.50	0	0	0	0				
6647'	6647.00	6652.50	0	0	0	0				
6648' 6"	6648.50	6654.00	0	0	0	0				
6652' 7"	6652.58	6658.08	0	0	0	0				
6655' 7"	6655.58	6661.08	0	0	0	0				

Fig. 3

E-5X			key dinoflagellates				Dinoflagellate zone (Schiøler & Wilson 1993)
core depth (f)	core depth (dec. f)	log depth (dec. f)	*P. denticulatum*	*H. borisii*	*P.grallator*	event	
6809' 3"	6809.25	6814.00	B	B	B		(no zones)
6812' 5"	6812.41	6817.16	B	B	B		
6814' 2"	6814.17	6818.92	B	B	B		
6817' 7"	6817.58	6822.33	B	B	B		
6818' 8"	6818.66	6823.41	B	B	B		
6820'	6820.00	6824.75	B	B	B		
6821' 1"	6821.08	6825.83	B	B	B		
6823' 4"	6823.33	6828.08	B	B	B		
6824' 10"	6824.83	6829.58	B	B	B		
6826' 8"	6826.66	6831.41	B	B	B		
6827' 11"	6827.92	6832.67	B	B	B		
6830'	6830.00	6834.75	B	B	B		
6833' 6"	6833.50	6838.25	0	1	47.25	HO *P. grallator*	Pgr
6836' 10"	6836.83	6841.58	0	1	7.25	2nd acme Pgr	
6839' 3"	6839.25	6844.00	0	0	16.5		
6841' 11"	6841.92	6846.67	0	0	2		
6845' 10"	6845.83	6850.58	0	0	1.5		
6847' 10"	6847.83	6852.58	0	0	1		
6859' 10"	6859.83	6864.58	0	0	0		
6863' 4"	6863.33	6868.08	0	0	0		
6866' 3"	6866.25	6871.00	0	0	0		
6869' 4"	6869.33	6874.08	0	0	1.5		
6872' 8"	6872.66	6877.41	0	0	0.75	LO *P. grallator*	
6875' 4"	6875.33	6880.08	0	0	0		Hbo
6877' 8"	6877.66	6882.41	0	1	0		
6881' 5"	6881.40	6886.15	0	0	0		
6883' 11"	6883.92	6888.67	0	0	0		
6887' 3"	6887.25	6892.00	0	0	0		
6889' 4"	6889.33	6894.08	0	0	0		
6890' 8"	6890.66	6895.41	0	0	0		
6894'	6894.00	6898.75	0	2	0		
6897' 11"	6897.92	6902.67	0	0	0		
6900' 9"	6900.75	6905.50	0	1	0		
6903' 9"	6903.75	6908.50	0	0	0		
6906' 10"	6906.83	6911.58	0	0	0		
6910' 3"	6910.25	6915.00	0.5	0	0		
6912' 5"	6912.41	6917.16	0	1	0		
6916' 4"	6916.33	6921.08	0	1.5	0		
6919' 2"	6919.17	6923.92	1	0	0		
6920' 9"	6920.75	6925.50	0	0	0		
6923' 10"	6923.83	6928.58	0	0	0		
6926' 2"	6926.17	6930.92	0	6	0	LO *H. borisii*	
6928' 7"	6928.58	6933.33	2	0	0		Pde
6932' 5"	6932.41	6937.16	0	0	0		
6935' 10"	6935.8	6940.58	0	0	0		
6938' 4"	6938.33	6943.08	0	0	0		
6941' 2"	6941.17	6945.92	0	0	0		
6943' 3"	6943.25	6948.00	0	0	0		
6948' 1"	6948.08	6952.83	0	0	0		
6950' 5"	6950.41	6955.16	0	0	0		
6952' 11"	6952.92	6957.67	1	0	0		
6956' 10"	6956.83	6961.58	3	0	0		
6960' 2"	6960.17	6964.92	4	0	0	acme Pde	
6963' 2"	6963.17	6967.92	2	0	0		
6965'2"	6965.17	6969.92	2	0	0		
6968' 7"	6968.58	6973.33	0	0	0		
6972' 2"	6972.17	6976.92	0	0	0		
6975' 2"	6975.17	6979.92	2	0	0		

Fig. 4

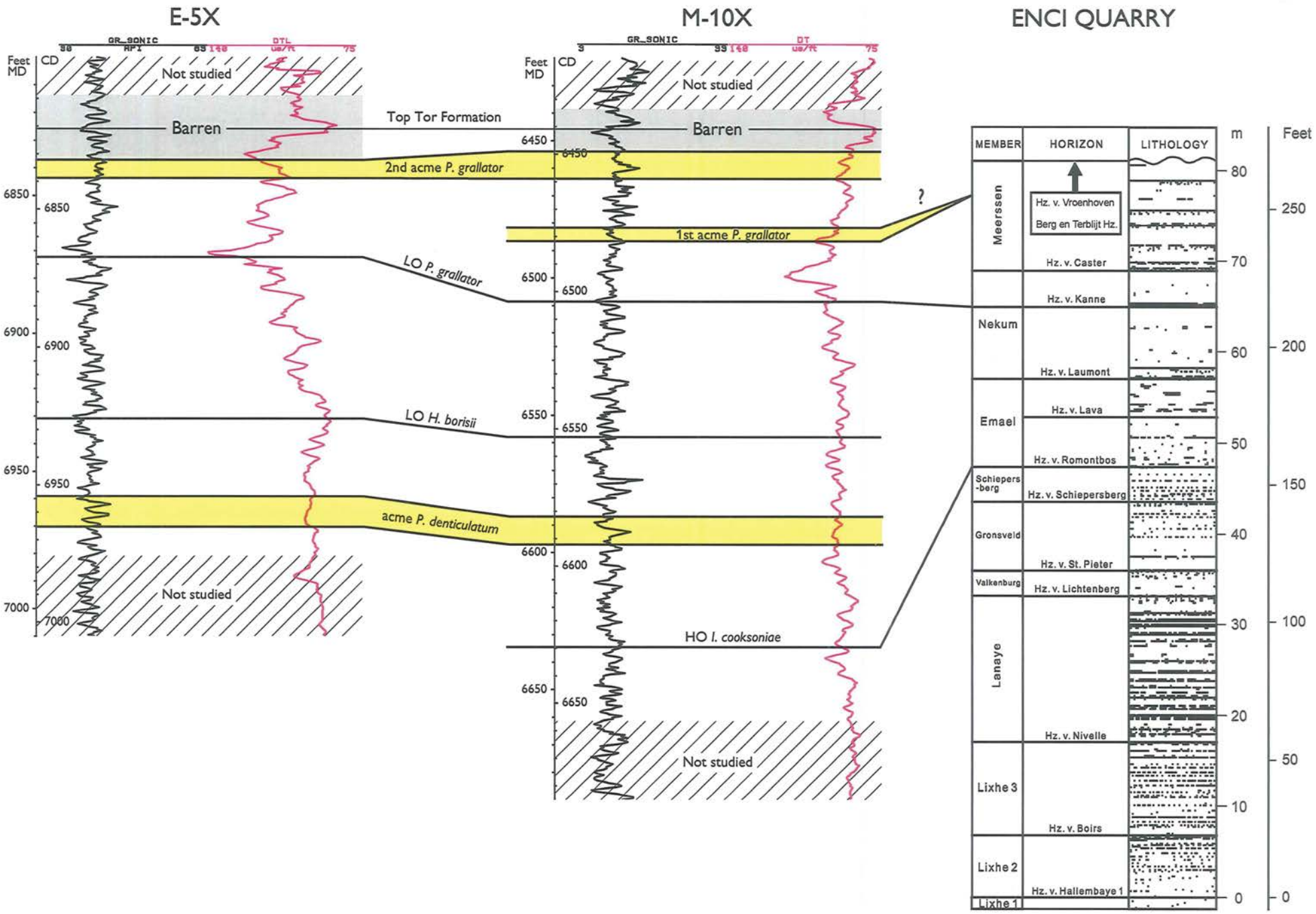
E-5X
M-10X
ENCI QUARRY
GR_SONIC
DTL
DT
Feet MD
CD
Not studied
Barren
Top Tor Formation
2nd acme P. grallator
1st acme P. grallator
LO P. grallator
LO H. borisii
acme P. denticulatum
HO I. cooksoniae
?
6450
6500
6550
6600
6650
6850
6900
6950
7000
MEMBER
HORIZON
LITHOLOGY
m
Feet
Meerssen
Hz. v. Vroenhoven
Berg en Terblijt Hz.
Hz. v. Caster
Hz. v. Kanne
Nekum
Hz. v. Laumont
Emael
Hz. v. Lava
Hz. v. Romontbos
Schiepers-berg
Hz. v. Schiepersberg
Gronsveld
Hz. v. St. Pieter
Valkenburg
Hz. v. Lichtenberg
Lanaye
Hz. v. Nivelle
Lixhe 3
Hz. v. Boirs
Lixhe 2
Hz. v. Hallembaye 1
Lixhe 1
80
70
60
50
40
30
20
10
0
250
200
150
100
50
0

Fig. 5

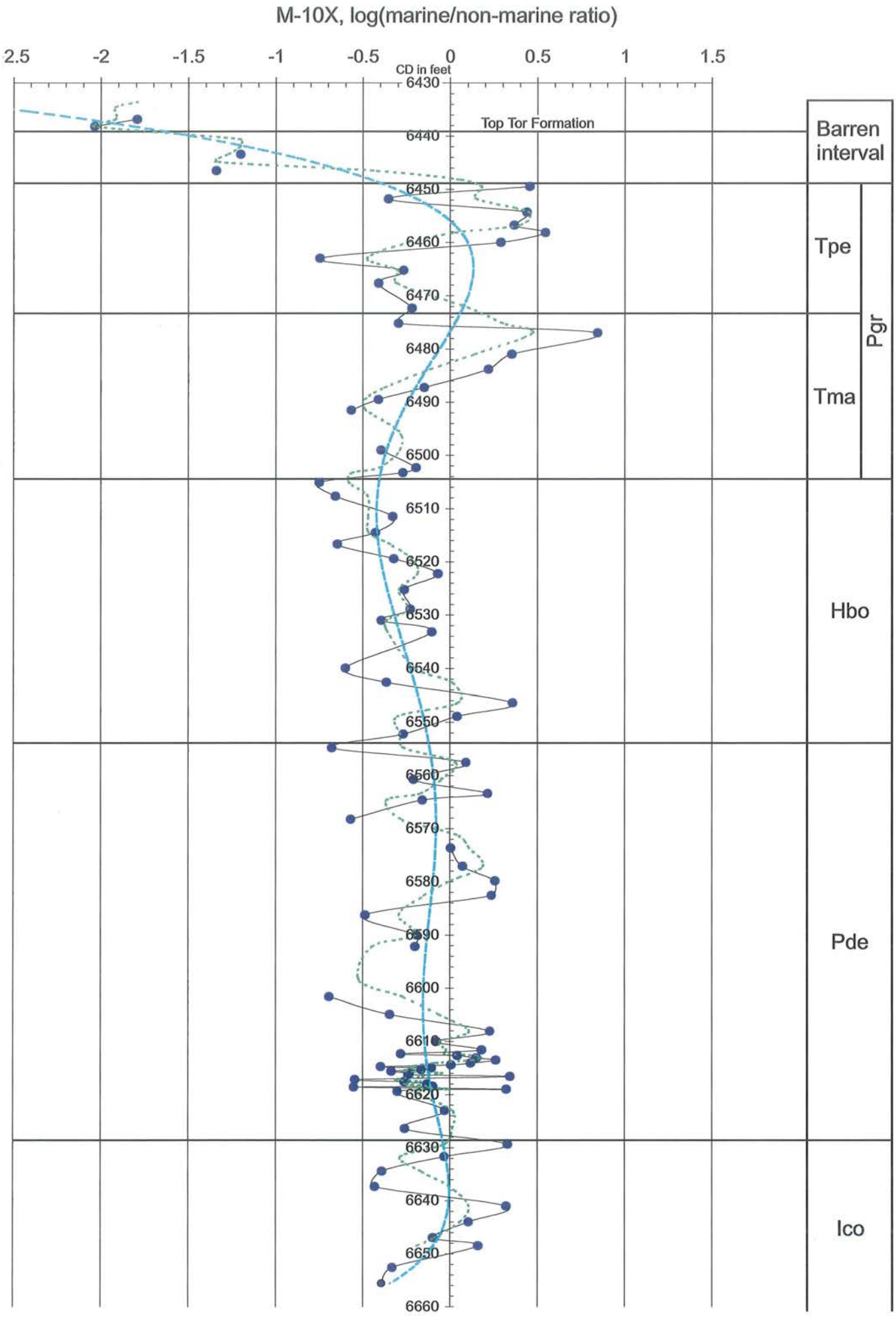
M-10X, log(marine/non-marine ratio)
2.5
-2
-1.5
-1
-0.5
0
0.5
1
1.5
CD in feet
6430
6440
6450
6460
6470
6480
6490
6500
6510
6520
6530
6540
6550
6560
6570
6580
6590
6600
6610
6620
6630
6640
6650
6660
Top Tor Formation
Barren interval
Tpe
Tma
Pgr
Hbo
Pde
Ico

Fig. 6

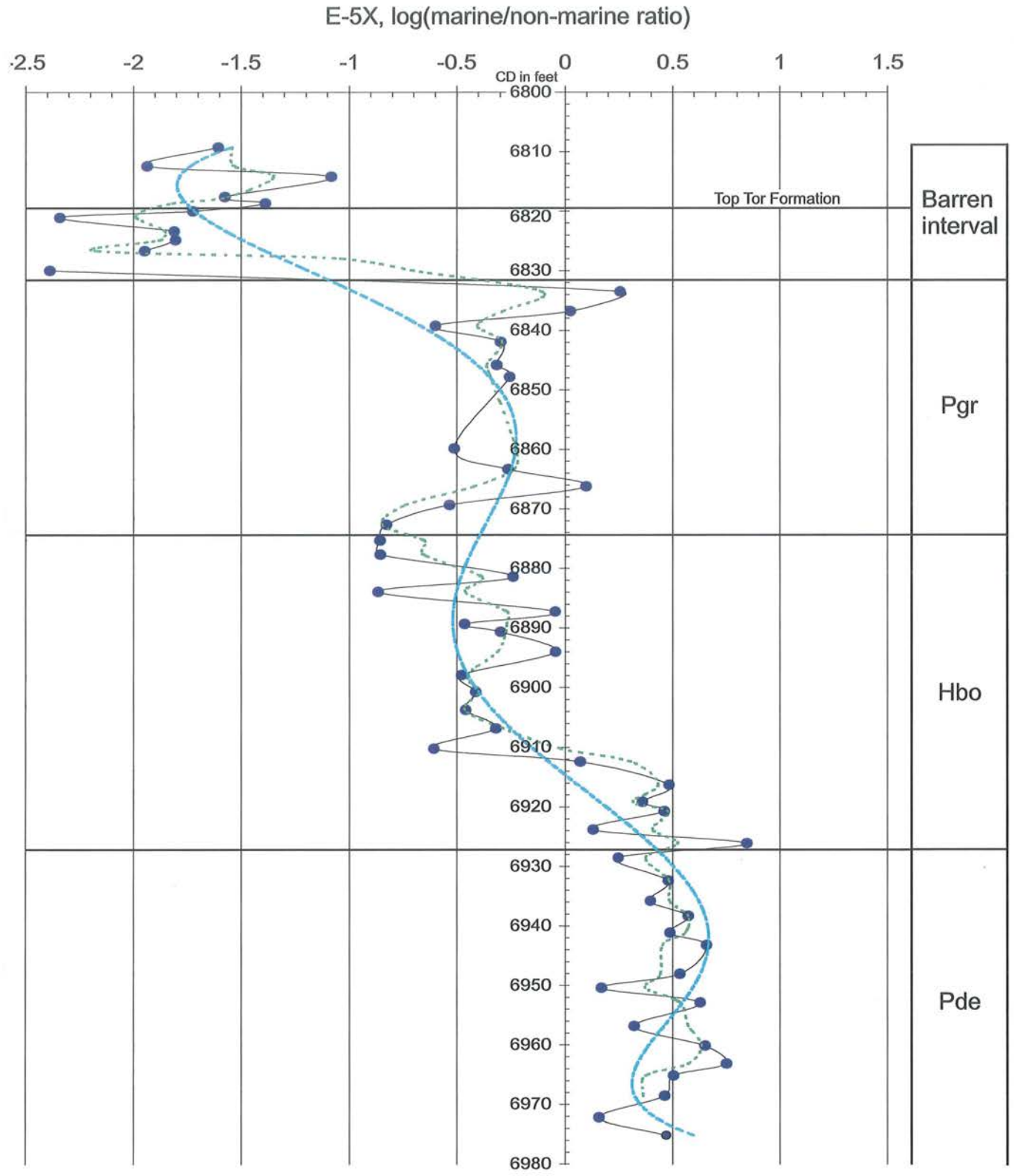
E-5X, log(marine/non-marine ratio)
-2.5
-2
-1.5
-1
-0.5
0
0.5
1
1.5
CD in feet
6800
6810
6820
6830
6840
6850
6860
6870
6880
6890
6900
6910
6920
6930
6940
6950
6960
6970
6980
Top Tor Formation
Barren interval
Pgr
Hbo
Pde

Fig. 7

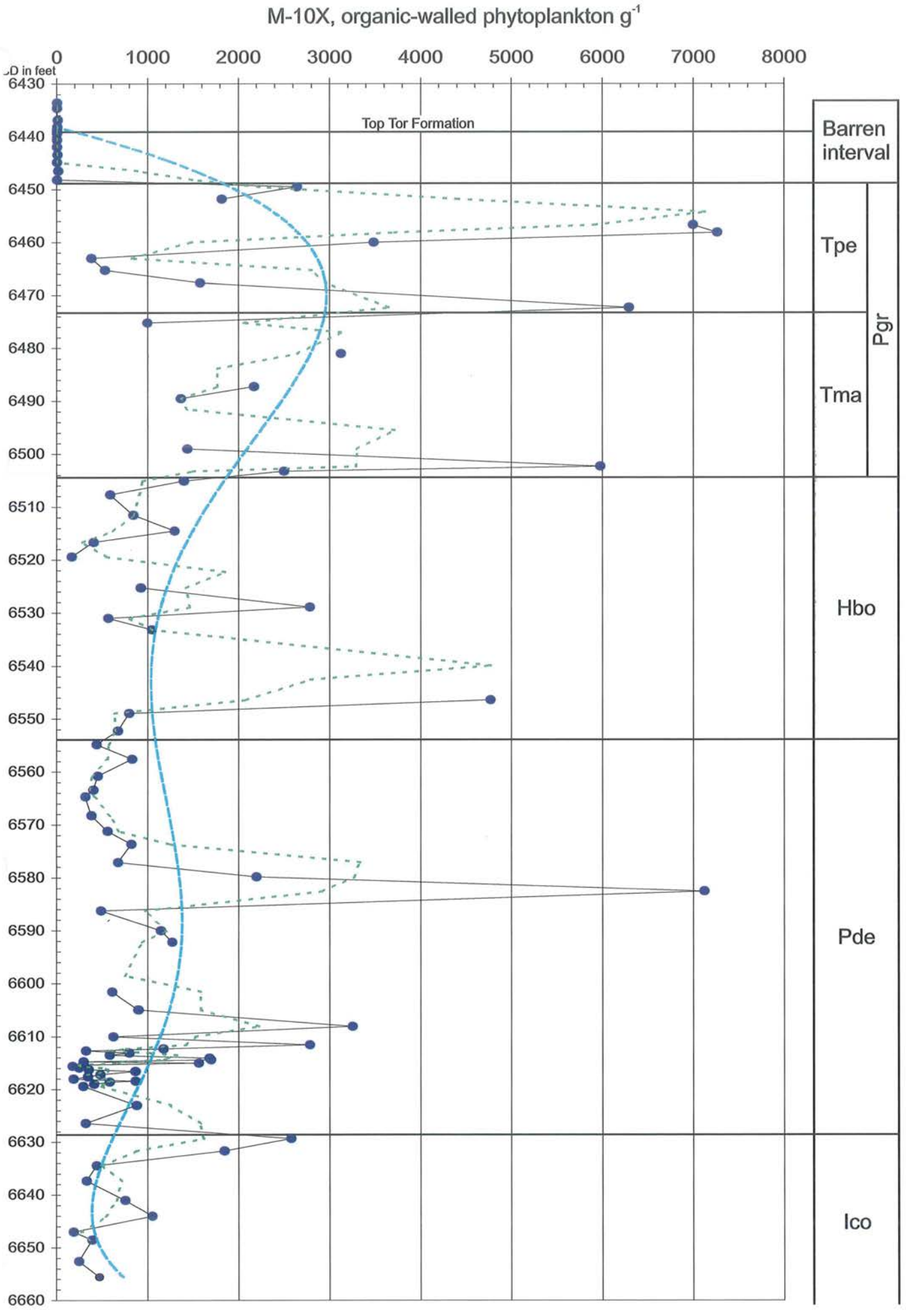
M-10X, organic-walled phytoplankton g-1
0
1000
2000
3000
4000
5000
6000
7000
8000
D in feet
6430
6440
6450
6460
6470
6480
6490
6500
6510
6520
6530
6540
6550
6560
6570
6580
6590
6600
6610
6620
6630
6640
6650
6660
Top Tor Formation
Barren interval
Tpe
Tma
Pgr
Hbo
Pde
Ico

Fig. 8

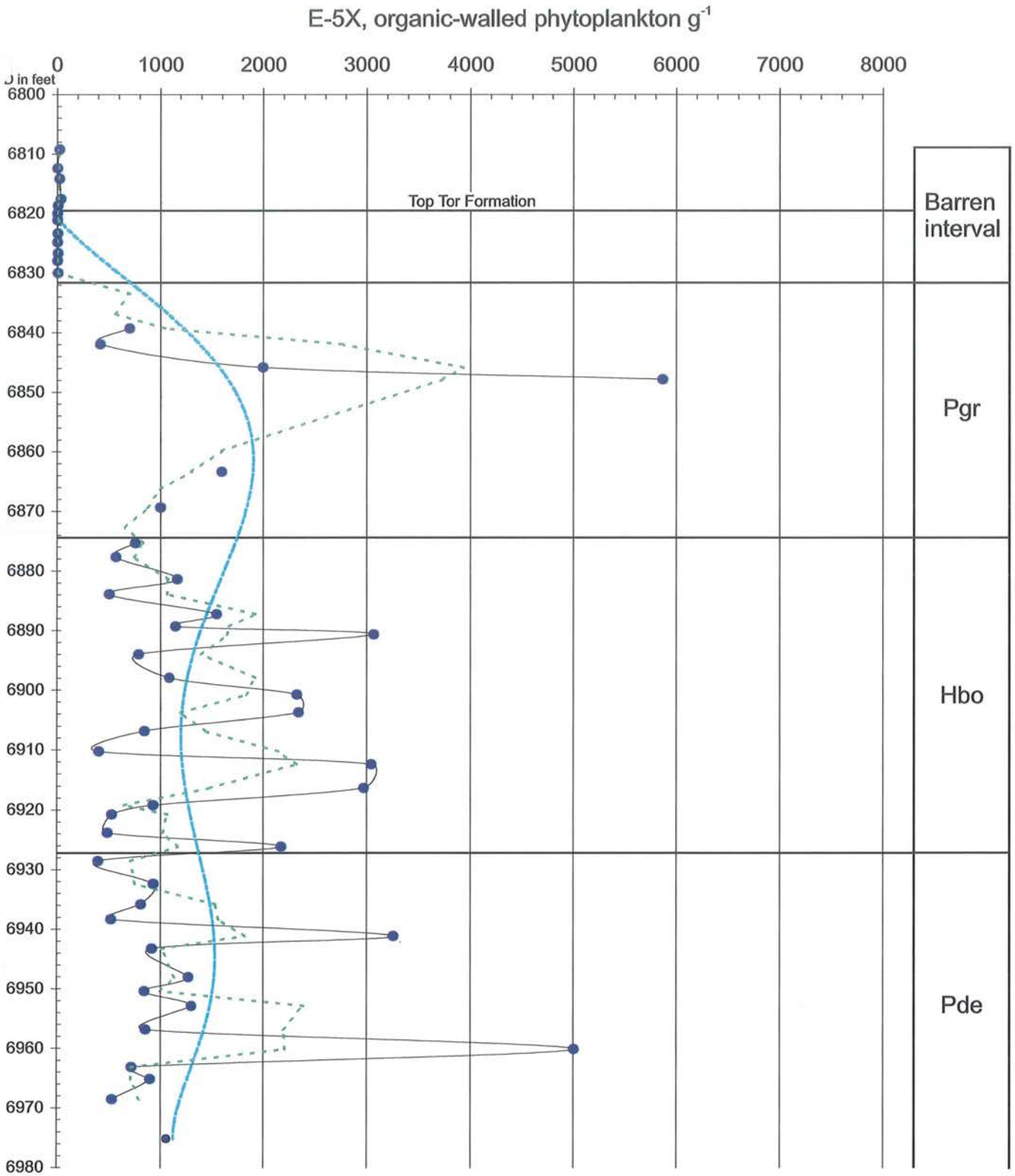
E-5X, organic-walled phytoplankton g-1
0
1000
2000
3000
4000
5000
6000
7000
8000
D in feet
6800
6810
6820
6830
6840
6850
6860
6870
6880
6890
6900
6910
6920
6930
6940
6950
6960
6970
6980
Top Tor Formation
Barren interval
Pgr
Hbo
Pde

Fig. 9

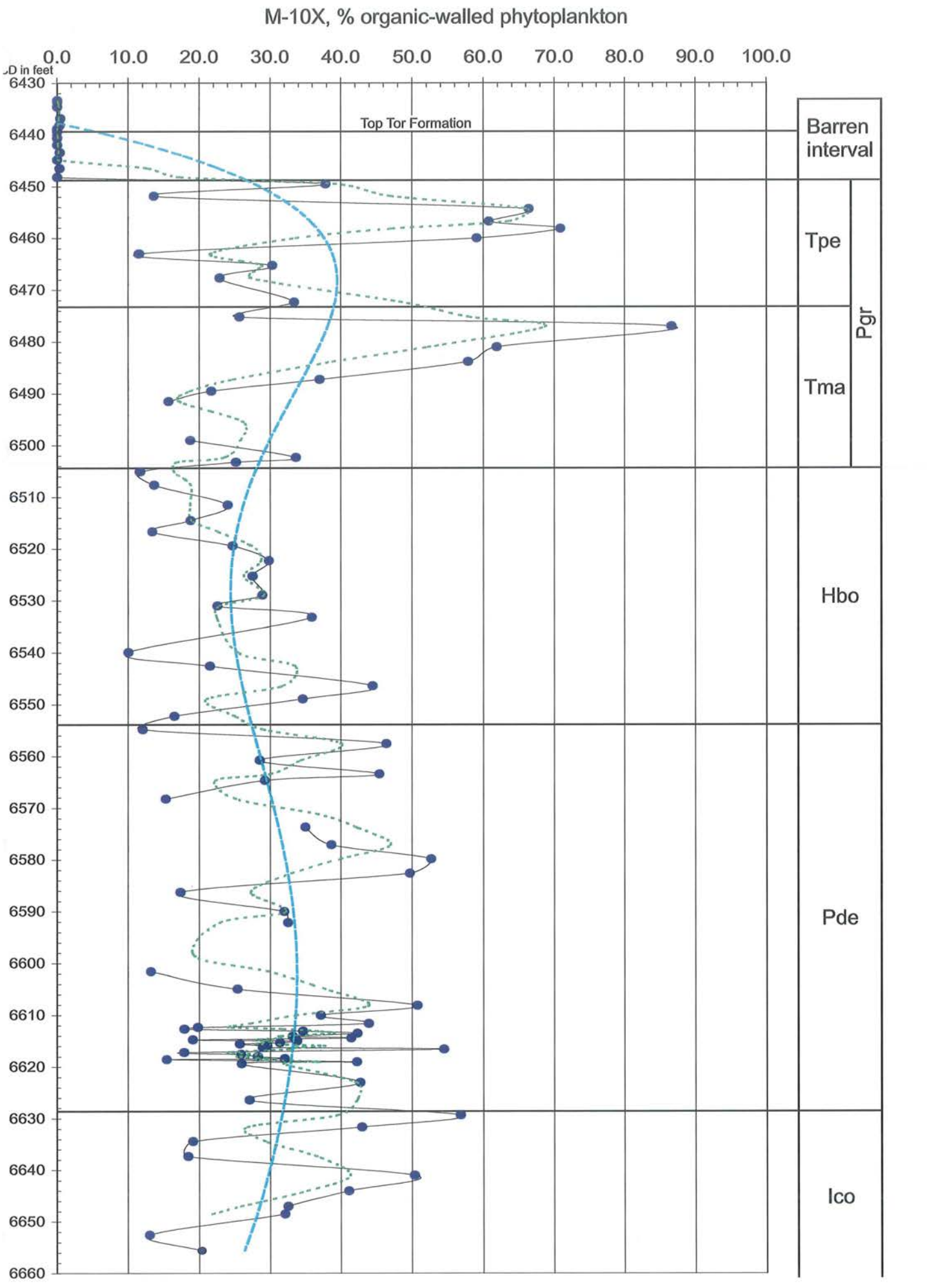
M-10X, % organic-walled phytoplankton
0.0
10.0
20.0
30.0
40.0
50.0
60.0
70.0
80.0
90.0
100.0
D in feet
6430
6440
6450
6460
6470
6480
6490
6500
6510
6520
6530
6540
6550
6560
6570
6580
6590
6600
6610
6620
6630
6640
6650
6660
Top Tor Formation
Barren interval
Tpe
Tma
Pgr
Hbo
Pde
Ico

Fig. 10

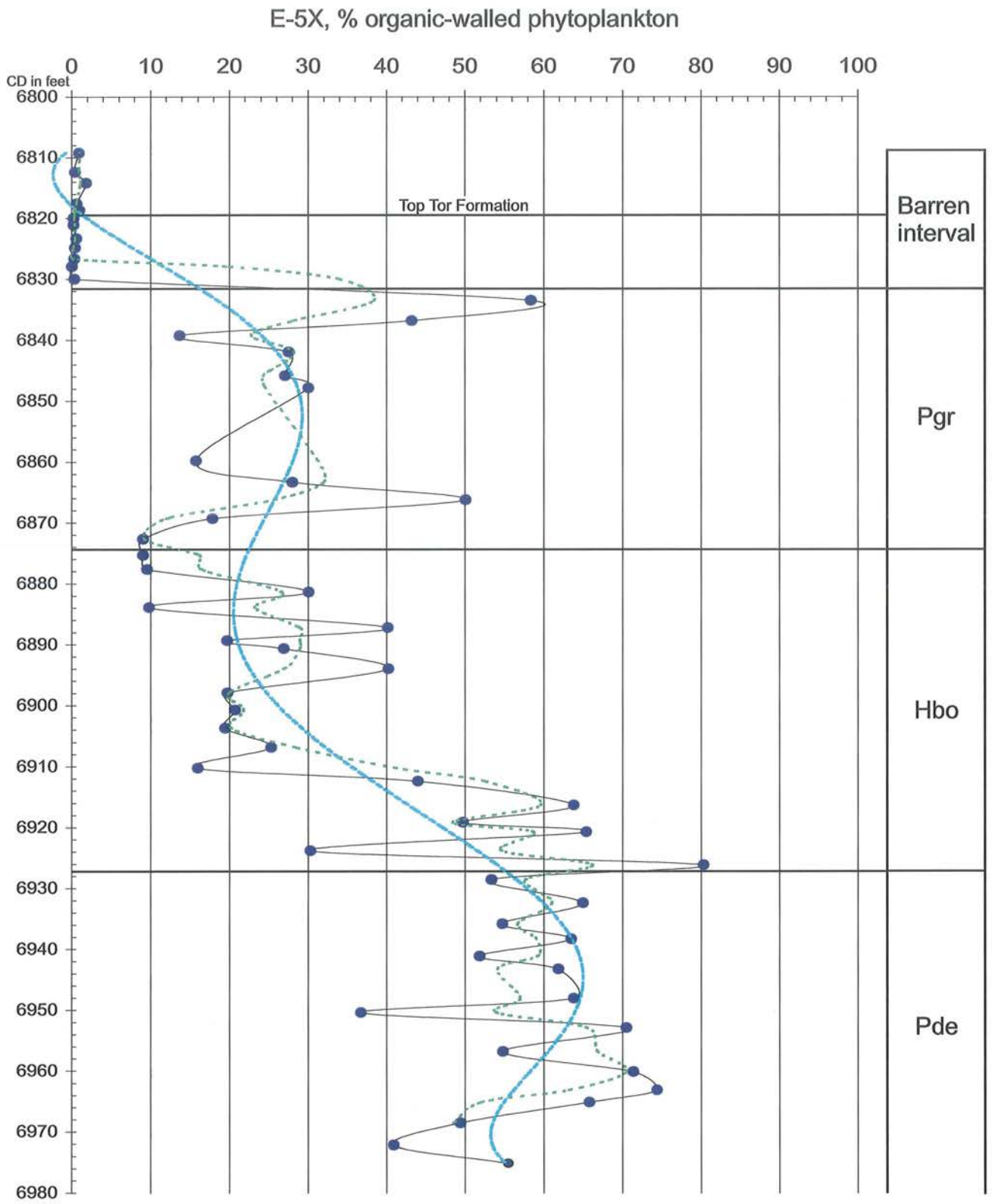
E-5X, % organic-walled phytoplankton
0
10
20
30
40
50
60
70
80
90
100
CD in feet
6800
6810
6820
6830
6840
6850
6860
6870
6880
6890
6900
6910
6920
6930
6940
6950
6960
6970
6980
Top Tor Formation
Barren interval
Pgr
Hbo
Pde

Fig. 11

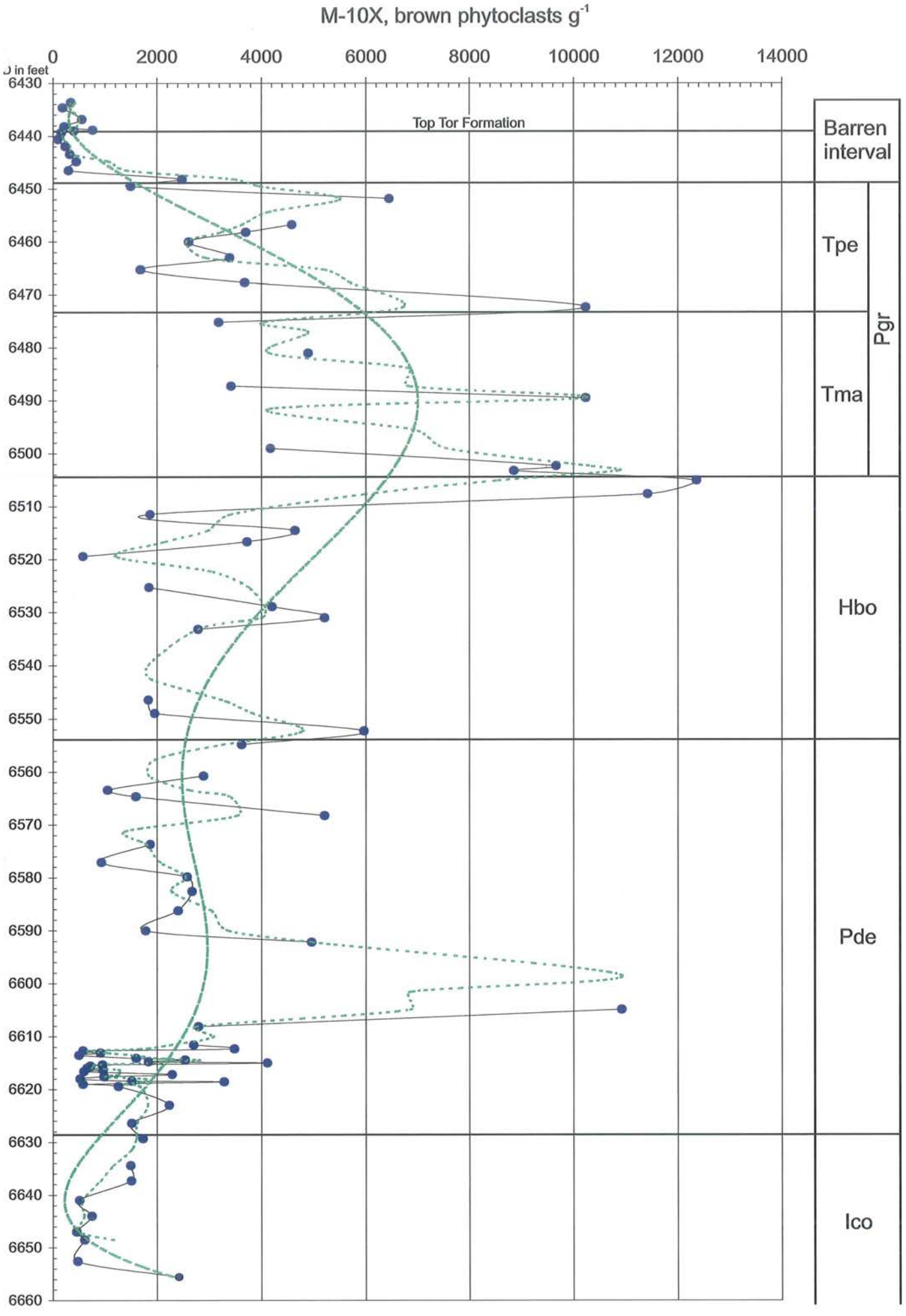
M-10X, brown phytoclasts g-1
0
2000
4000
6000
8000
10000
12000
14000
D in feet
6430
6440
6450
6460
6470
6480
6490
6500
6510
6520
6530
6540
6550
6560
6570
6580
6590
6600
6610
6620
6630
6640
6650
6660
Top Tor Formation
Barren interval
Tpe
Tma
Pgr
Hbo
Pde
Ico

Fig. 12

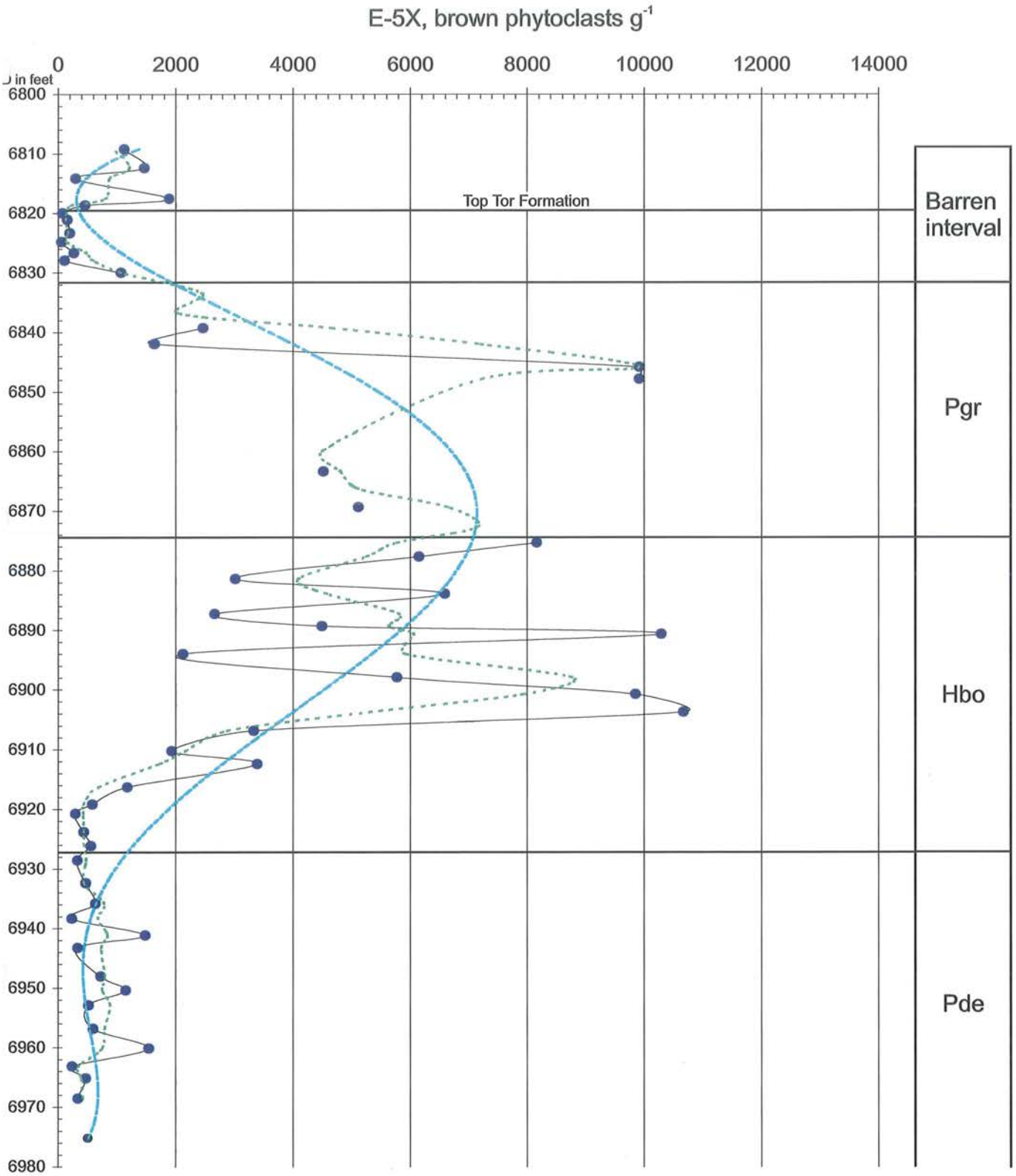
E-5X, brown phytoclasts g-1
0
2000
4000
6000
8000
10000
12000
14000
in feet
6800
6810
6820
6830
6840
6850
6860
6870
6880
6890
6900
6910
6920
6930
6940
6950
6960
6970
6980
Top Tor Formation
Barren interval
Pgr
Hbo
Pde

Fig. 13

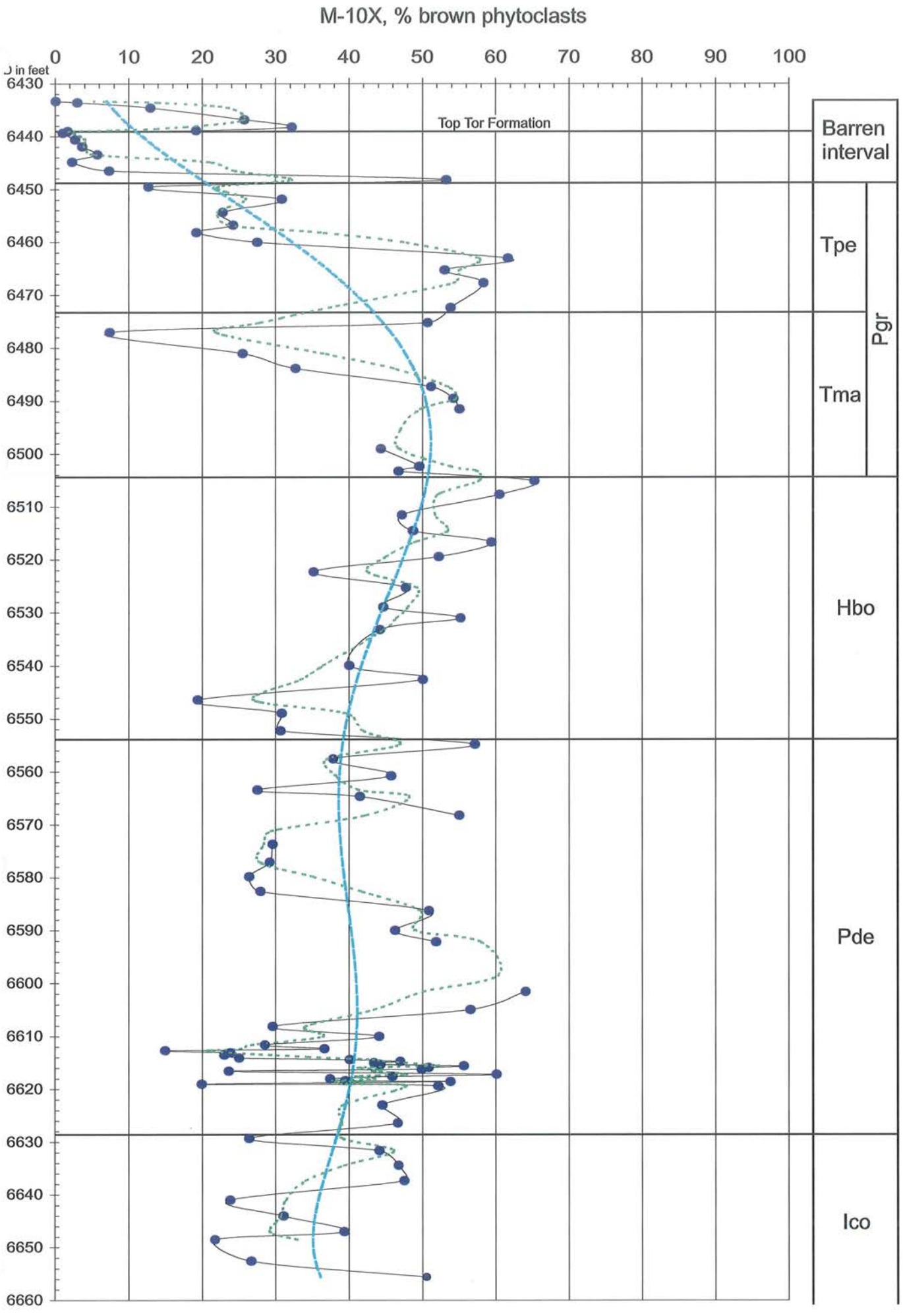
M-10X, % brown phytoclasts
0
10
20
30
40
50
60
70
80
90
100
D in feet
6430
6440
6450
6460
6470
6480
6490
6500
6510
6520
6530
6540
6550
6560
6570
6580
6590
6600
6610
6620
6630
6640
6650
6660
Top Tor Formation
Barren interval
Tpe
Tma
Pgr
Hbo
Pde
Ico

Fig. 14

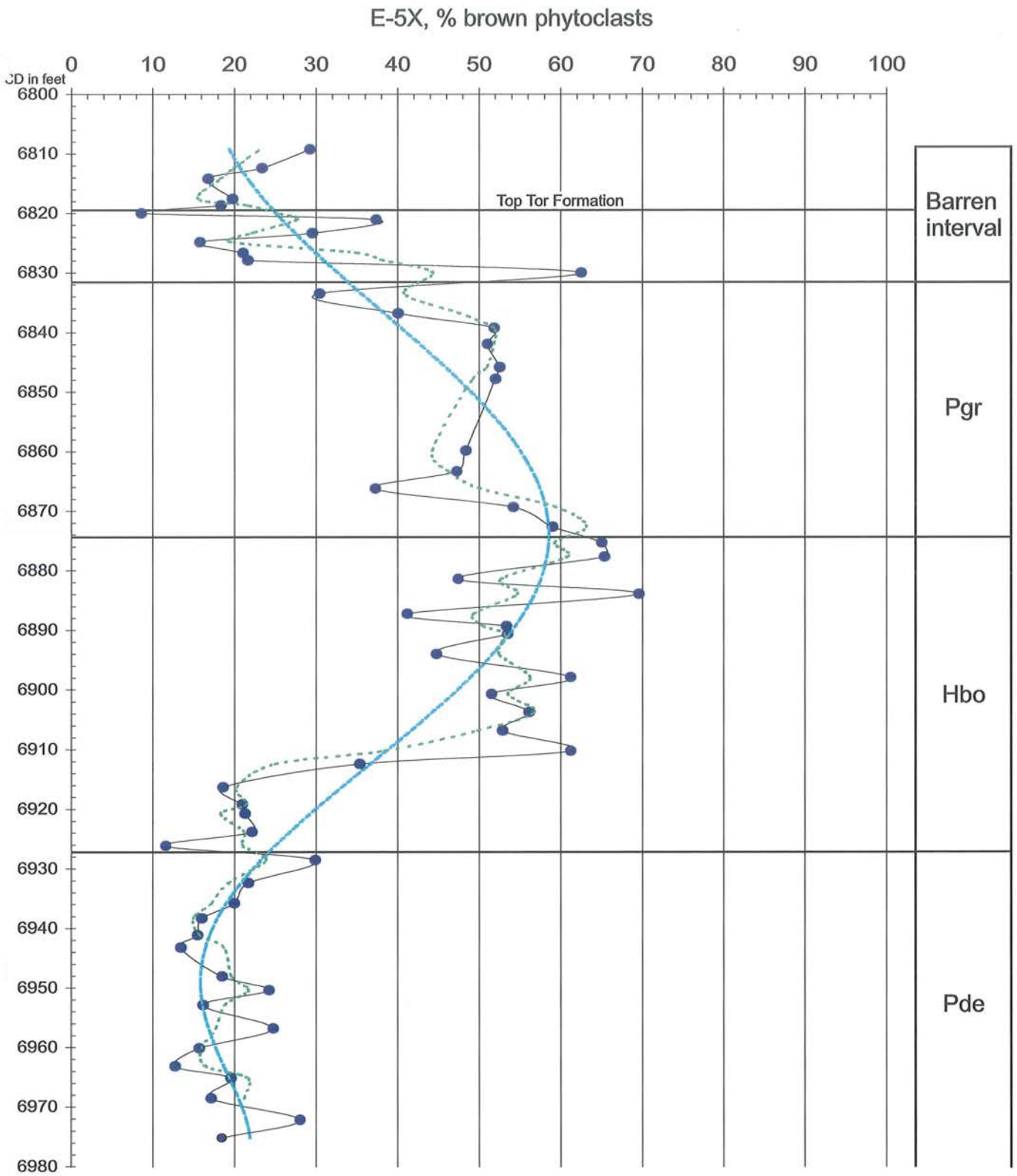
E-5X, % brown phytoclasts
0
10
20
30
40
50
60
70
80
90
100
CD in feet
6800
6810
6820
6830
6840
6850
6860
6870
6880
6890
6900
6910
6920
6930
6940
6950
6960
6970
6980
Top Tor Formation
Barren interval
Pgr
Hbo
Pde

Fig. 15

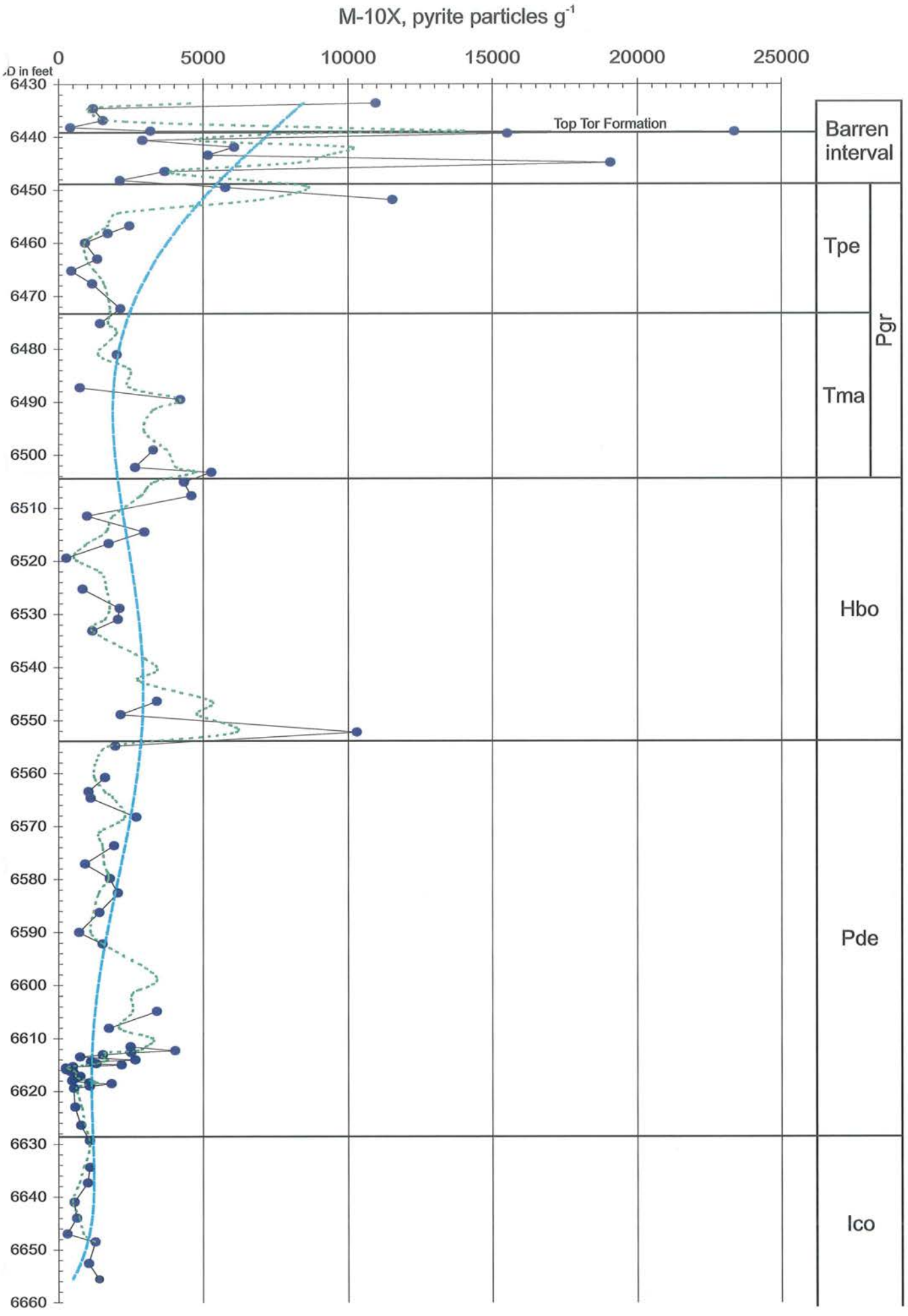
M-10X, pyrite particles g-1
0
5000
10000
15000
20000
25000
D in feet
6430
6440
6450
6460
6470
6480
6490
6500
6510
6520
6530
6540
6550
6560
6570
6580
6590
6600
6610
6620
6630
6640
6650
6660
Top Tor Formation
Barren interval
Tpe
Tma
Pgr
Hbo
Pde
Ico

Fig. 16

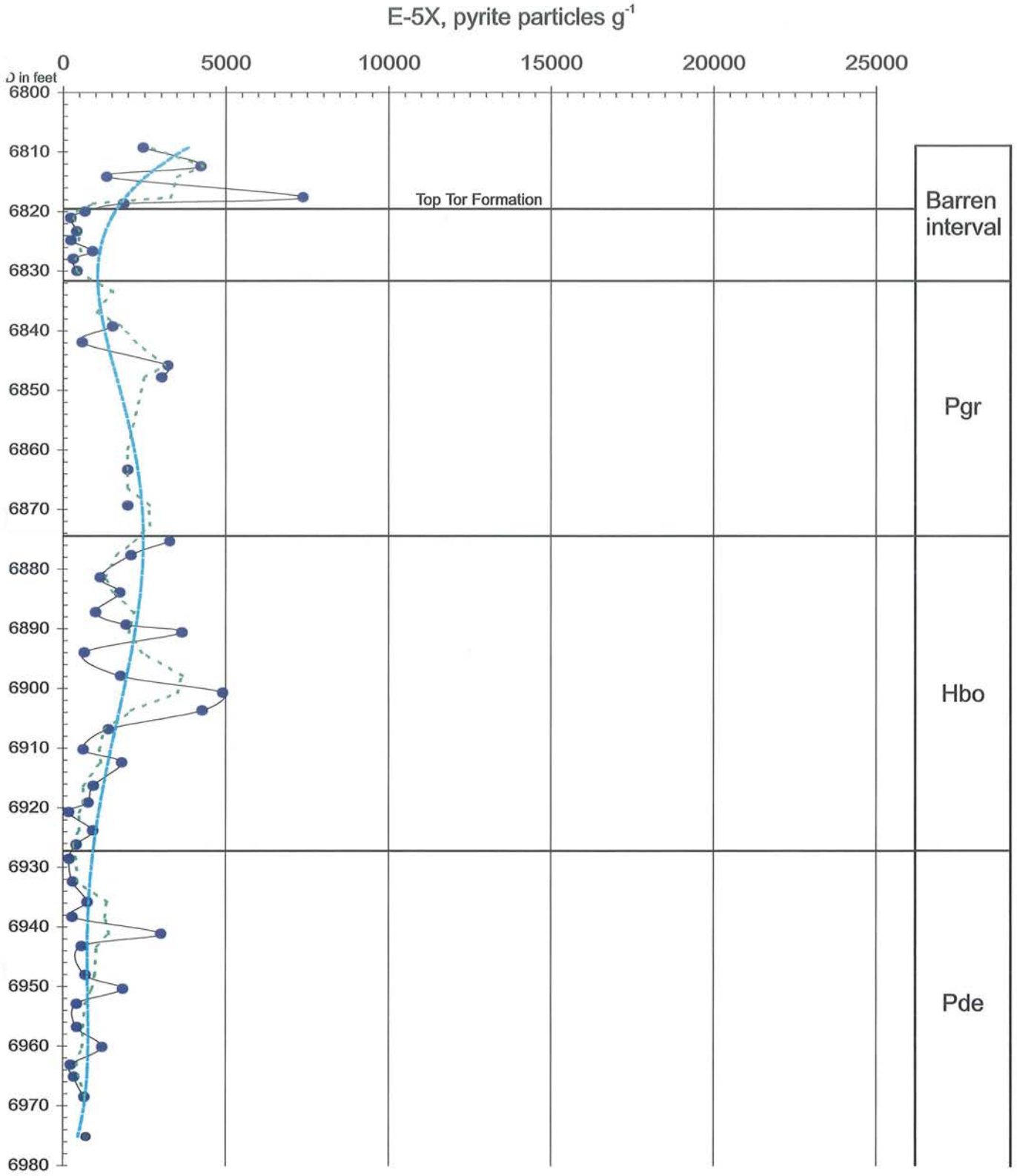
E-5X, pyrite particles g-1
0
5000
10000
15000
20000
25000
D in feet
6800
6810
6820
6830
6840
6850
6860
6870
6880
6890
6900
6910
6920
6930
6940
6950
6960
6970
6980
Top Tor Formation
Barren interval
Pgr
Hbo
Pde

Fig. 17

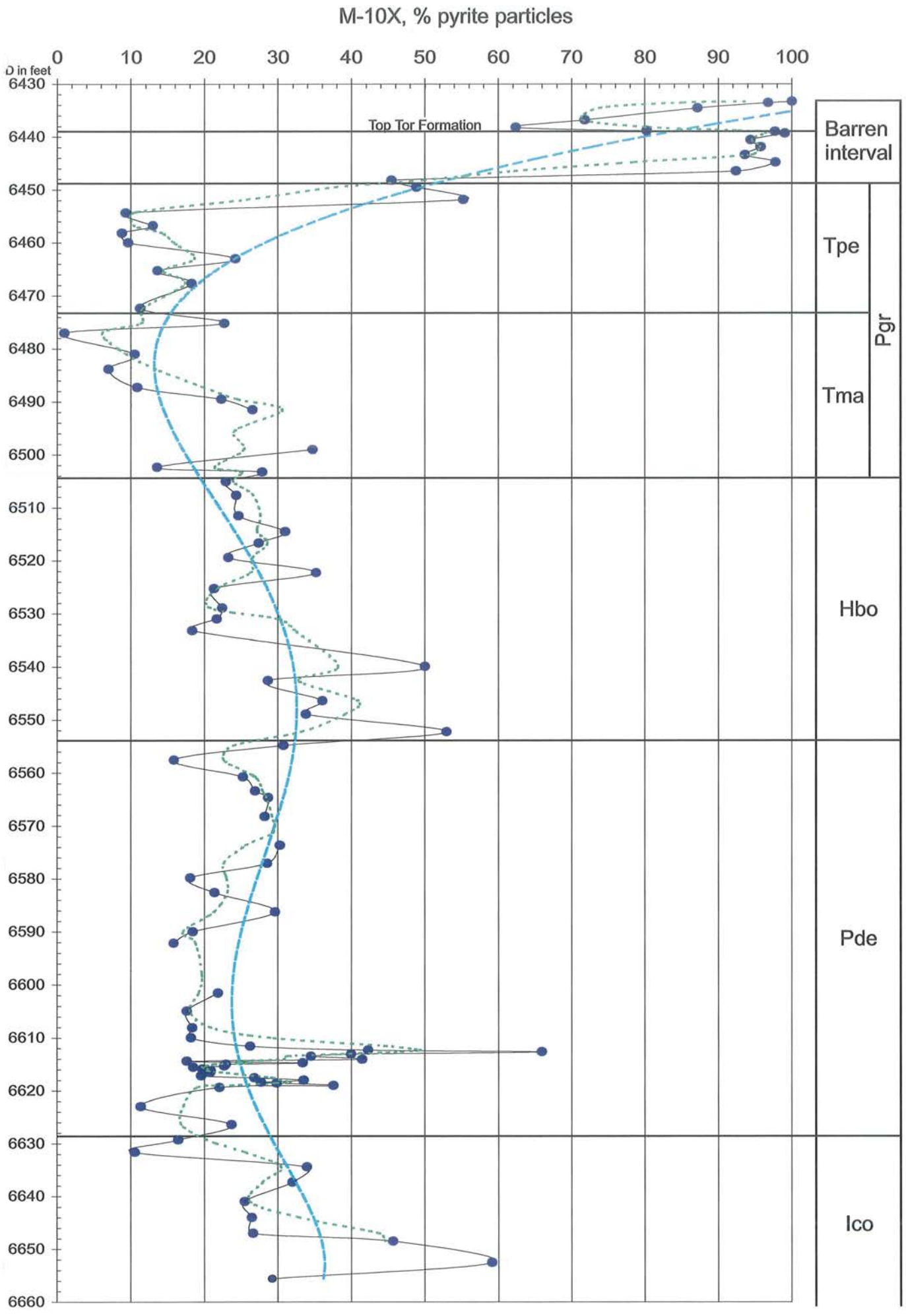
M-10X, % pyrite particles
0
10
20
30
40
50
60
70
80
90
100
D in feet
6430
6440
6450
6460
6470
6480
6490
6500
6510
6520
6530
6540
6550
6560
6570
6580
6590
6600
6610
6620
6630
6640
6650
6660
Top Tor Formation
Barren interval
Tpe
Tma
Pgr
Hbo
Pde
Ico

Fig. 18

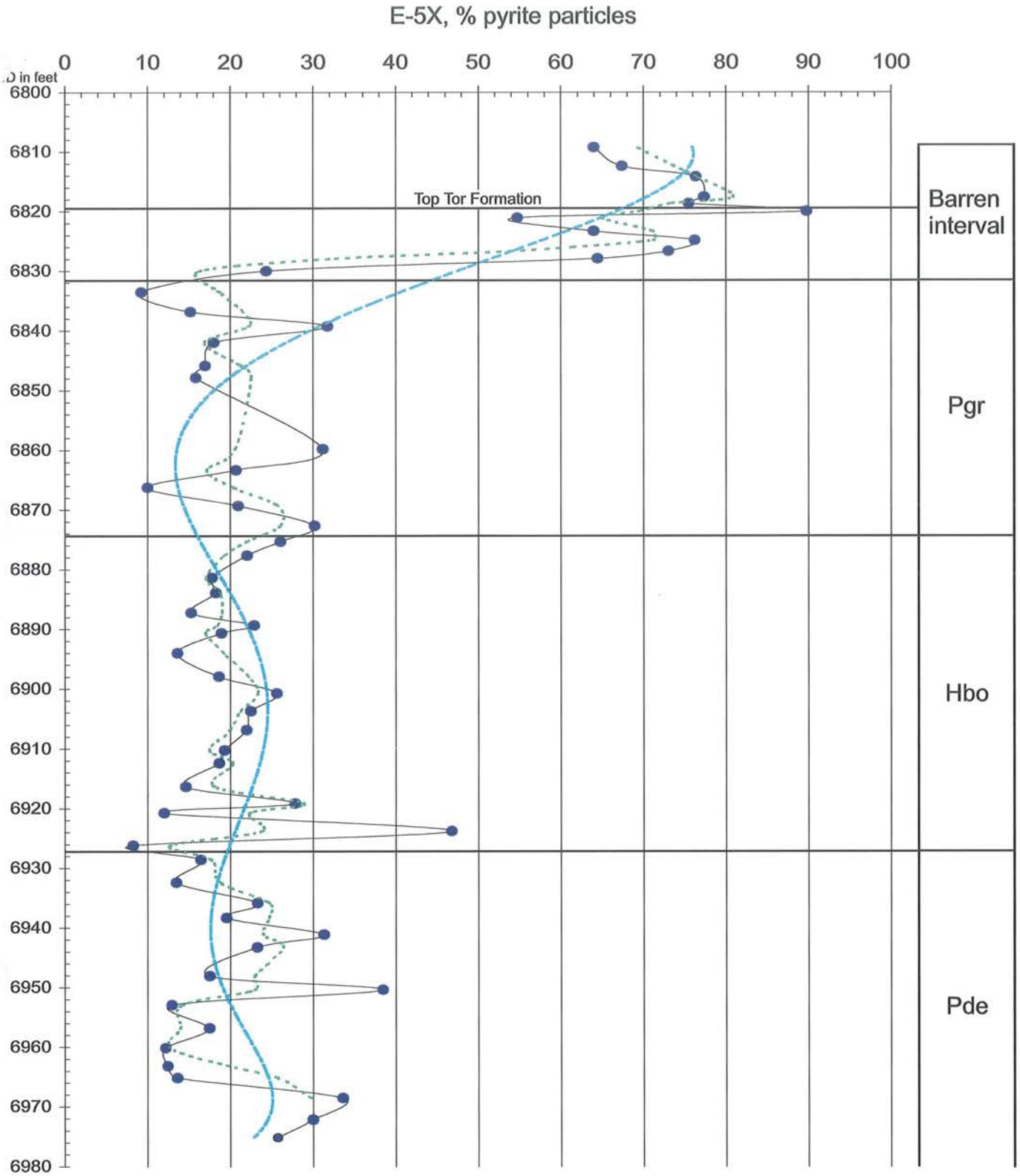
E-5X, % pyrite particles
0
10
20
30
40
50
60
70
80
90
100
D in feet
6800
6810
6820
6830
6840
6850
6860
6870
6880
6890
6900
6910
6920
6930
6940
6950
6960
6970
6980
Top Tor Formation
Barren interval
Pgr
Hbo
Pde

Fig. 19

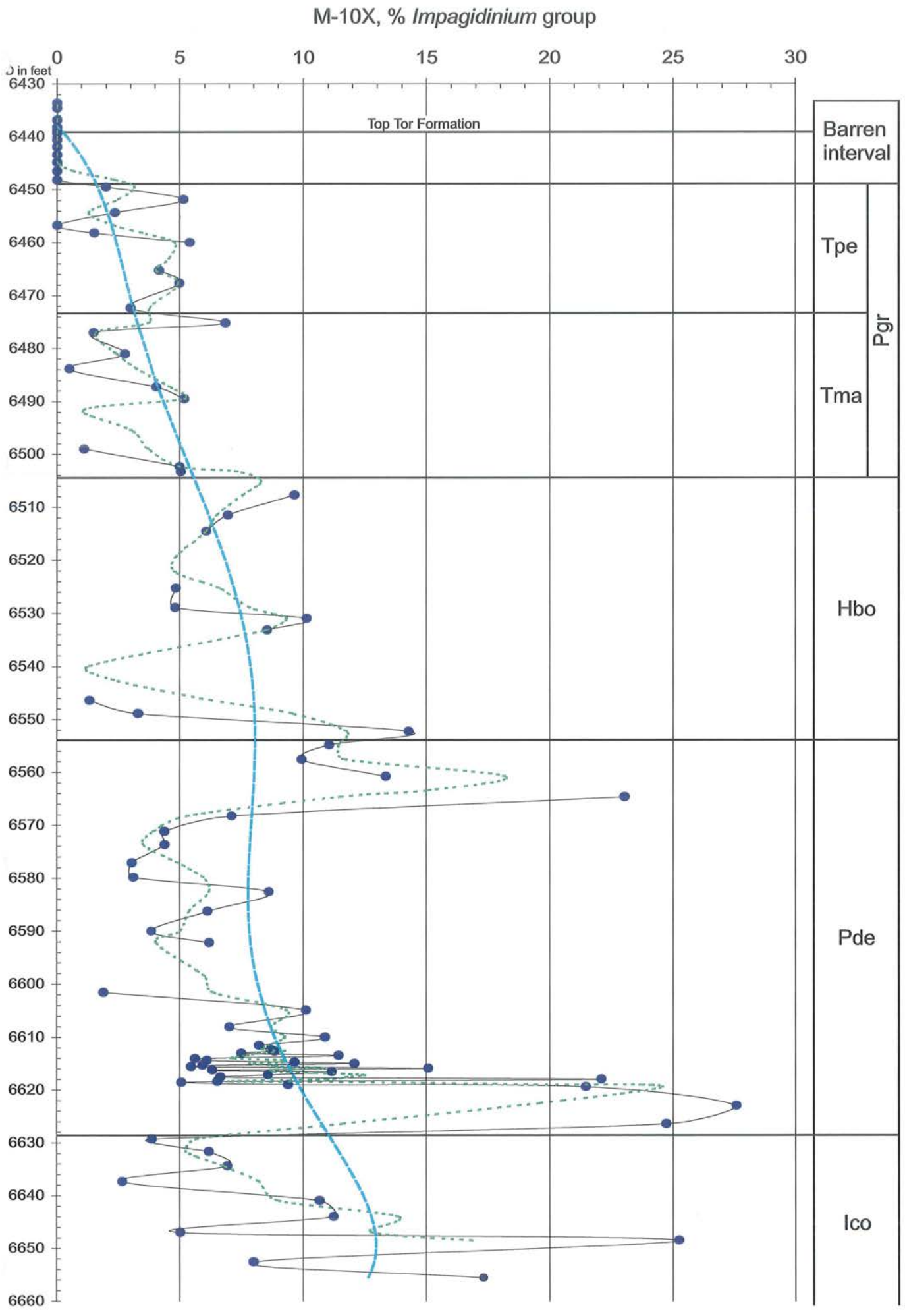
M-10X, % *Impagidinium* group
0
5
10
15
20
25
30
D in feet
6430
6440
6450
6460
6470
6480
6490
6500
6510
6520
6530
6540
6550
6560
6570
6580
6590
6600
6610
6620
6630
6640
6650
6660
Top Tor Formation
Barren interval
Tpe
Tma
Pgr
Hbo
Pde
Ico

Fig. 20

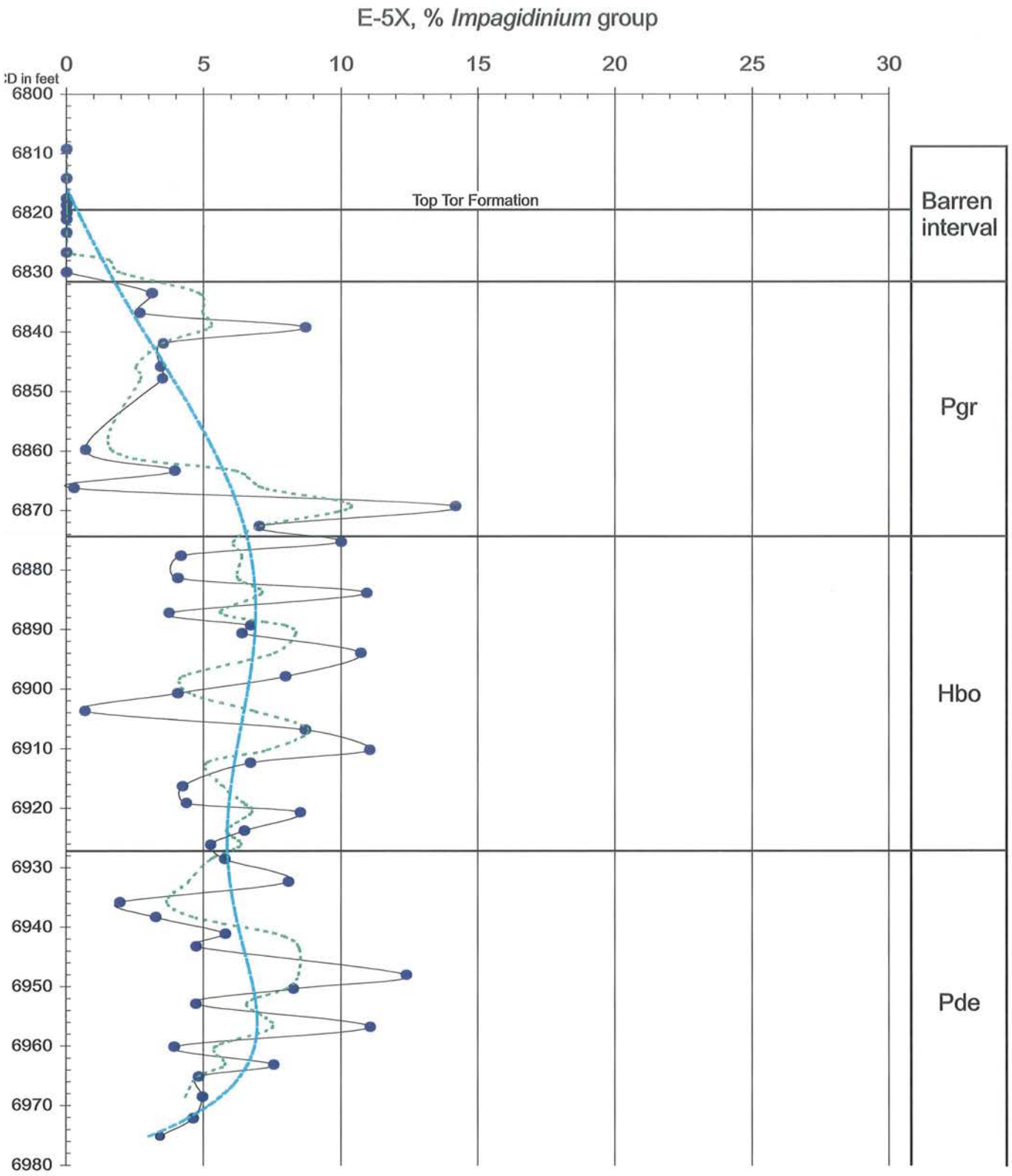
E-5X, % *Impagidinium* group
0
5
10
15
20
25
30
:D in feet
6800
6810
6820
6830
6840
6850
6860
6870
6880
6890
6900
6910
6920
6930
6940
6950
6960
6970
6980
Top Tor Formation
Barren interval
Pgr
Hbo
Pde

Fig. 21

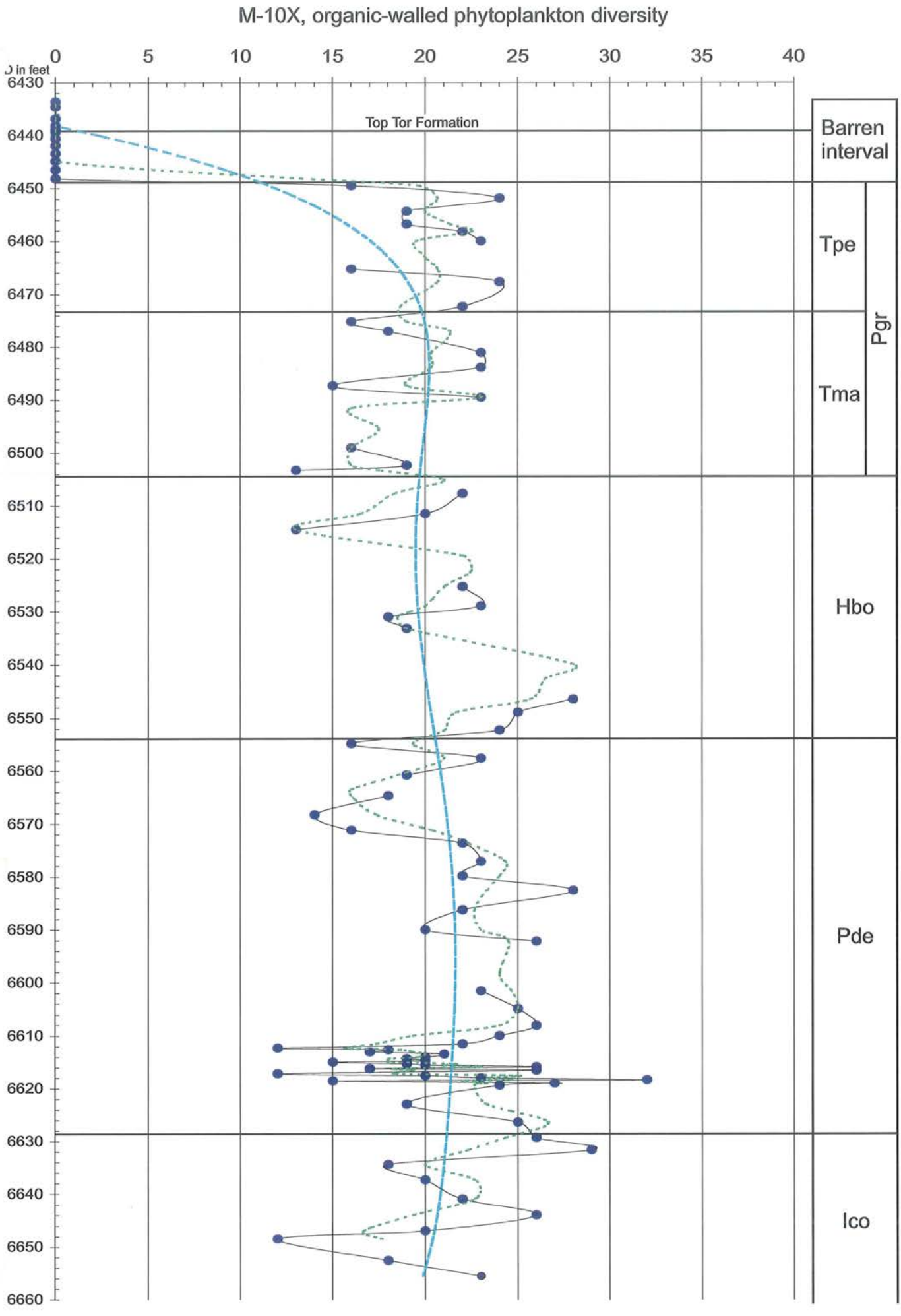
M-10X, organic-walled phytoplankton diversity
0
5
10
15
20
25
30
35
40
D in feet
6430
6440
6450
6460
6470
6480
6490
6500
6510
6520
6530
6540
6550
6560
6570
6580
6590
6600
6610
6620
6630
6640
6650
6660
Top Tor Formation
Barren interval
Tpe
Tma
Pgr
Hbo
Pde
Ico

Fig. 22

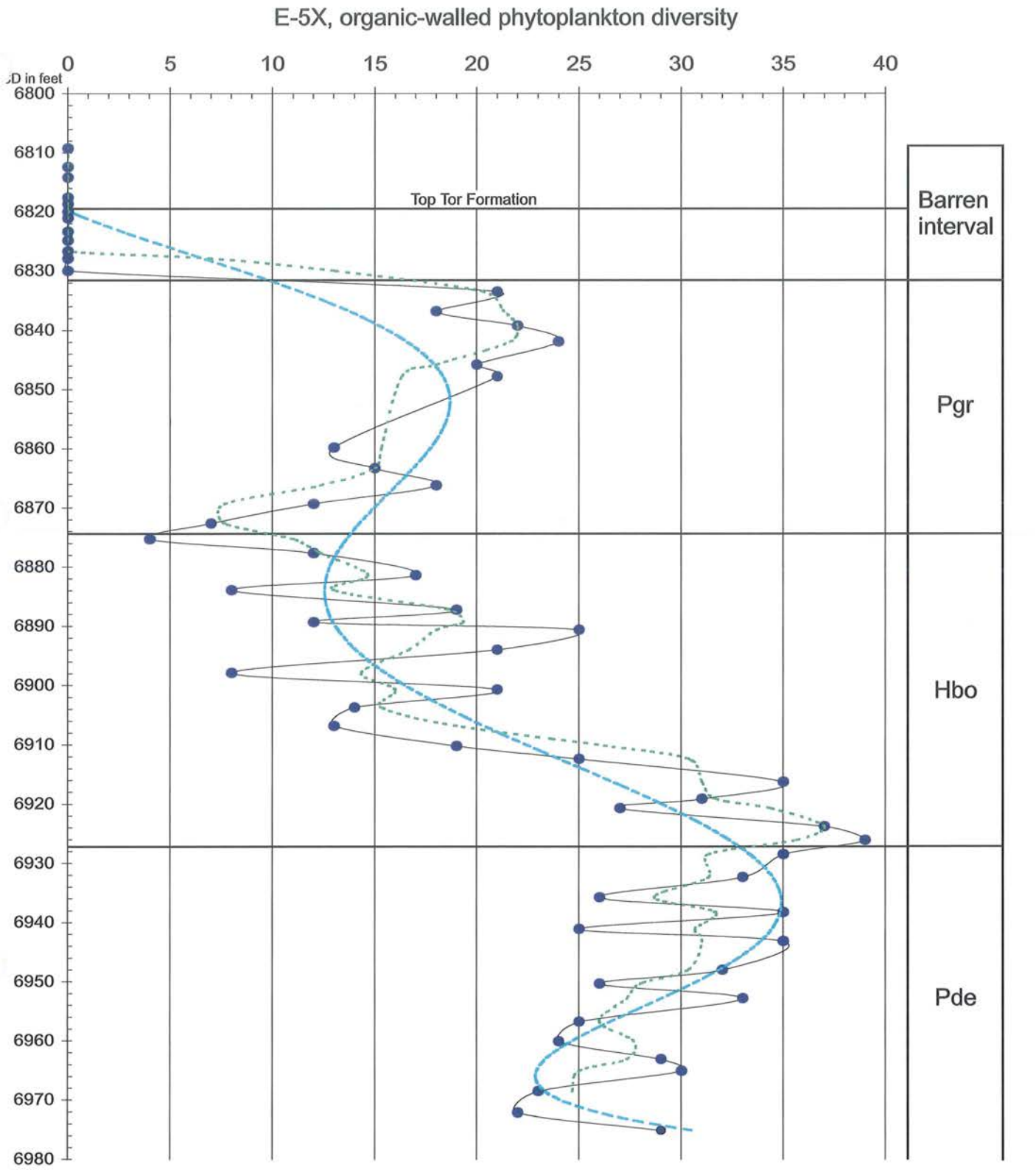
E-5X, organic-walled phytoplankton diversity
0
5
10
15
20
25
30
35
40
D in feet
6800
6810
6820
6830
6840
6850
6860
6870
6880
6890
6900
6910
6920
6930
6940
6950
6960
6970
6980
Top Tor Formation
Barren interval
Pgr
Hbo
Pde

Fig. 23

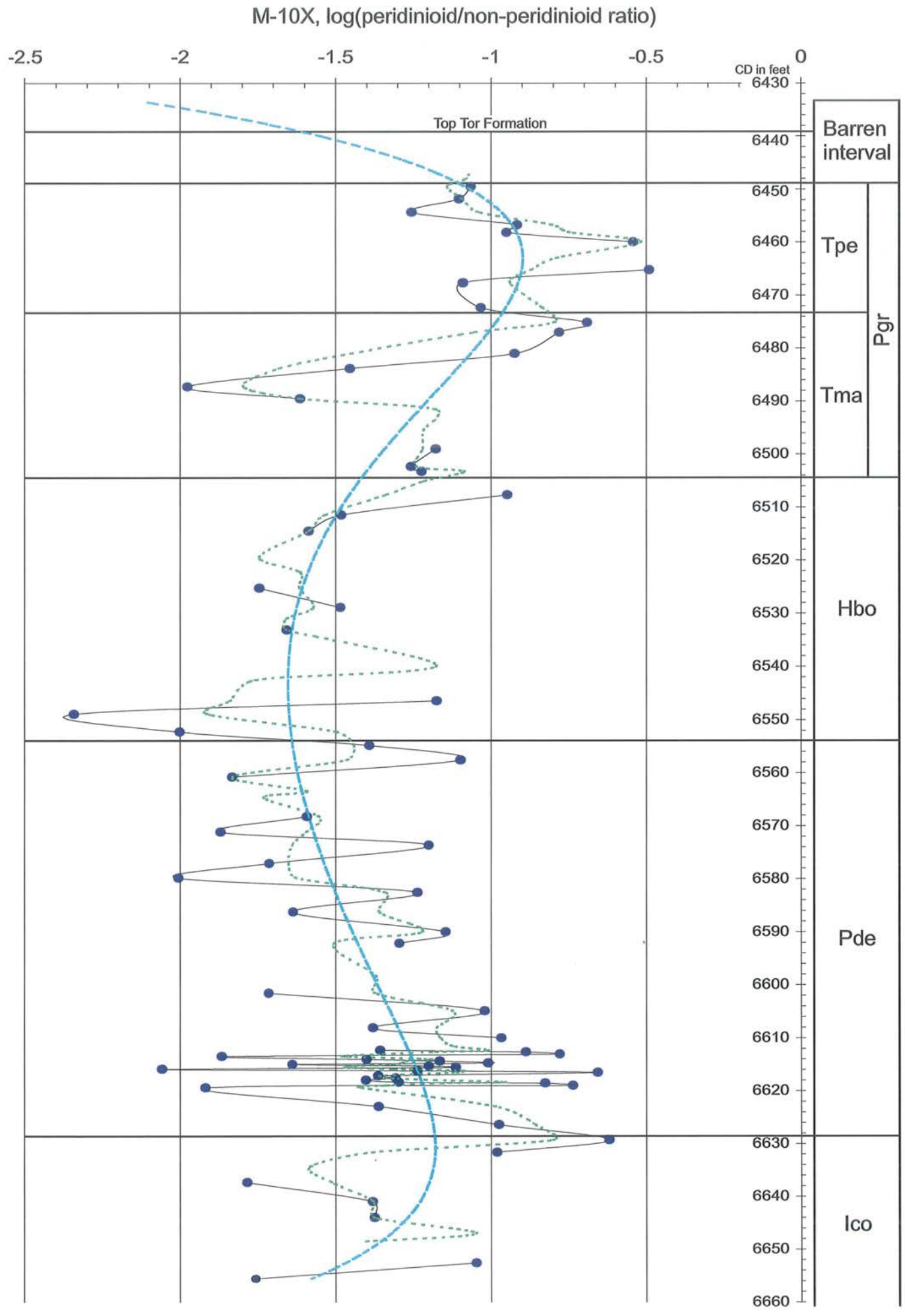
M-10X, log(peridinioid/non-peridinioid ratio)
-2.5
-2
-1.5
-1
-0.5
0
CD in feet
6430
6440
6450
6460
6470
6480
6490
6500
6510
6520
6530
6540
6550
6560
6570
6580
6590
6600
6610
6620
6630
6640
6650
6660
Top Tor Formation
Barren interval
Tpe
Tma
Pgr
Hbo
Pde
Ico

Fig. 24

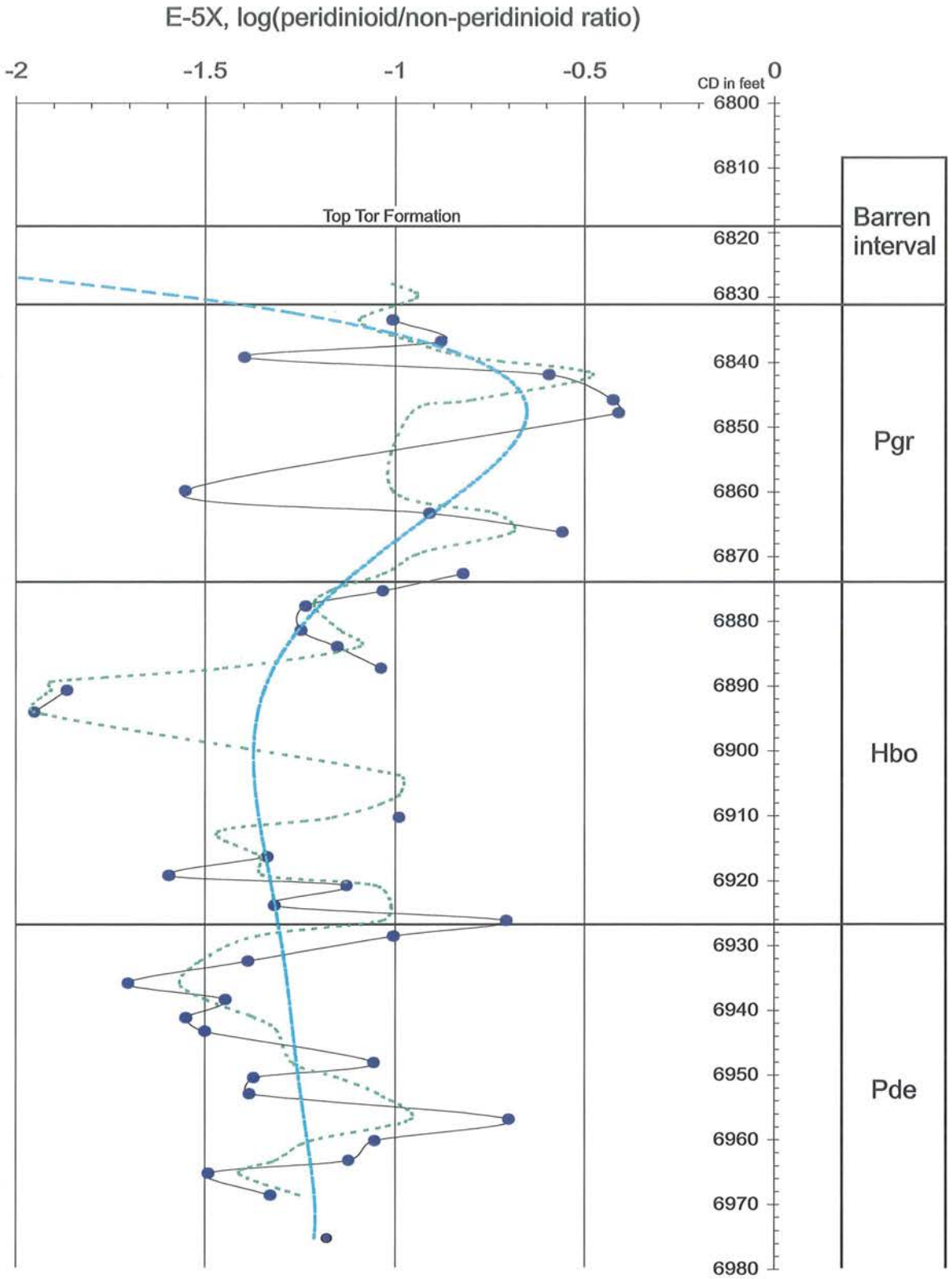
E-5X, log(peridinioid/non-peridinioid ratio)
-2
-1.5
-1
-0.5
0
CD in feet
6800
6810
6820
6830
6840
6850
6860
6870
6880
6890
6900
6910
6920
6930
6940
6950
6960
6970
6980
Top Tor Formation
Barren interval
Pgr
Hbo
Pde

Fig. 25

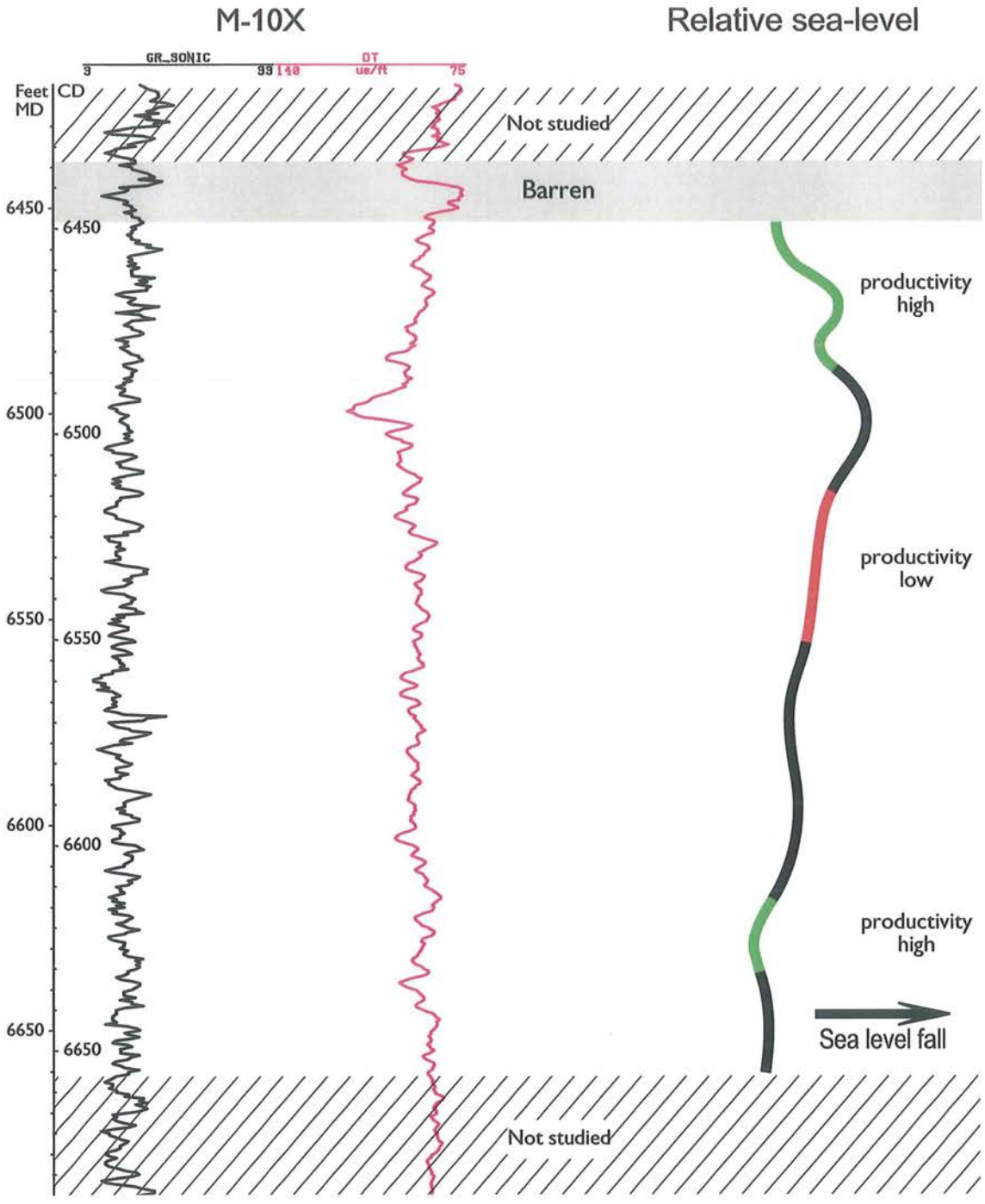
M-10X
Relative sea-level
GR_SONIC
3
93
140
DT
us/ft
75
Feet
MD
CD
6450
6500
6550
6600
6650
Not studied
Barren
productivity
high
productivity
low
productivity
high
Sea level fall
Not studied

Fig. 26

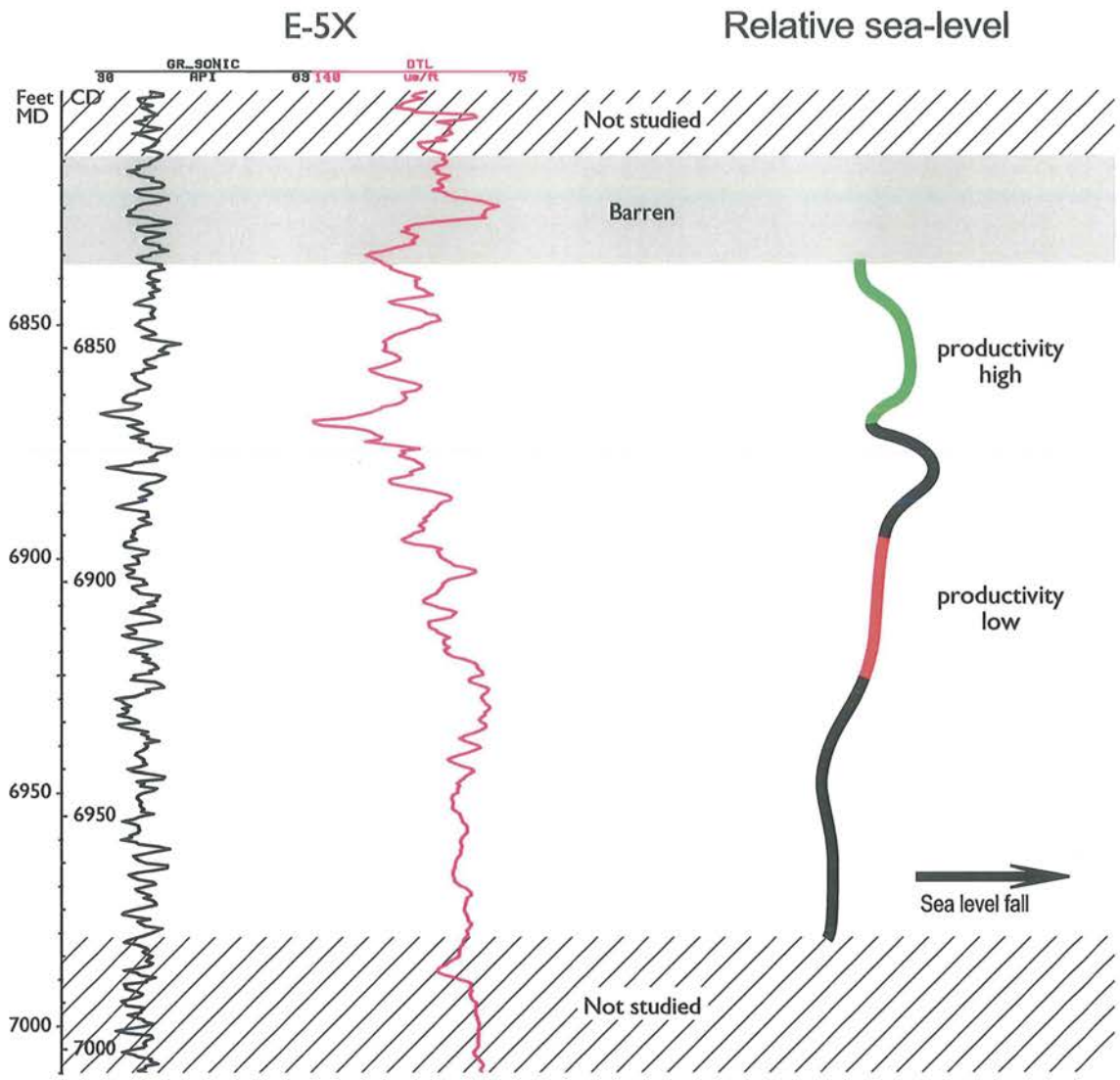
E-5X
Relative sea-level
GR_SONIC
30
API
60 140
DTL
us/ft
75
Feet
MD
CD
Not studied
Barren
6850
6850
productivity
high
6900
6900
productivity
low
6950
6950
Sea level fall
Not studied
7000
7000

Fig. 27

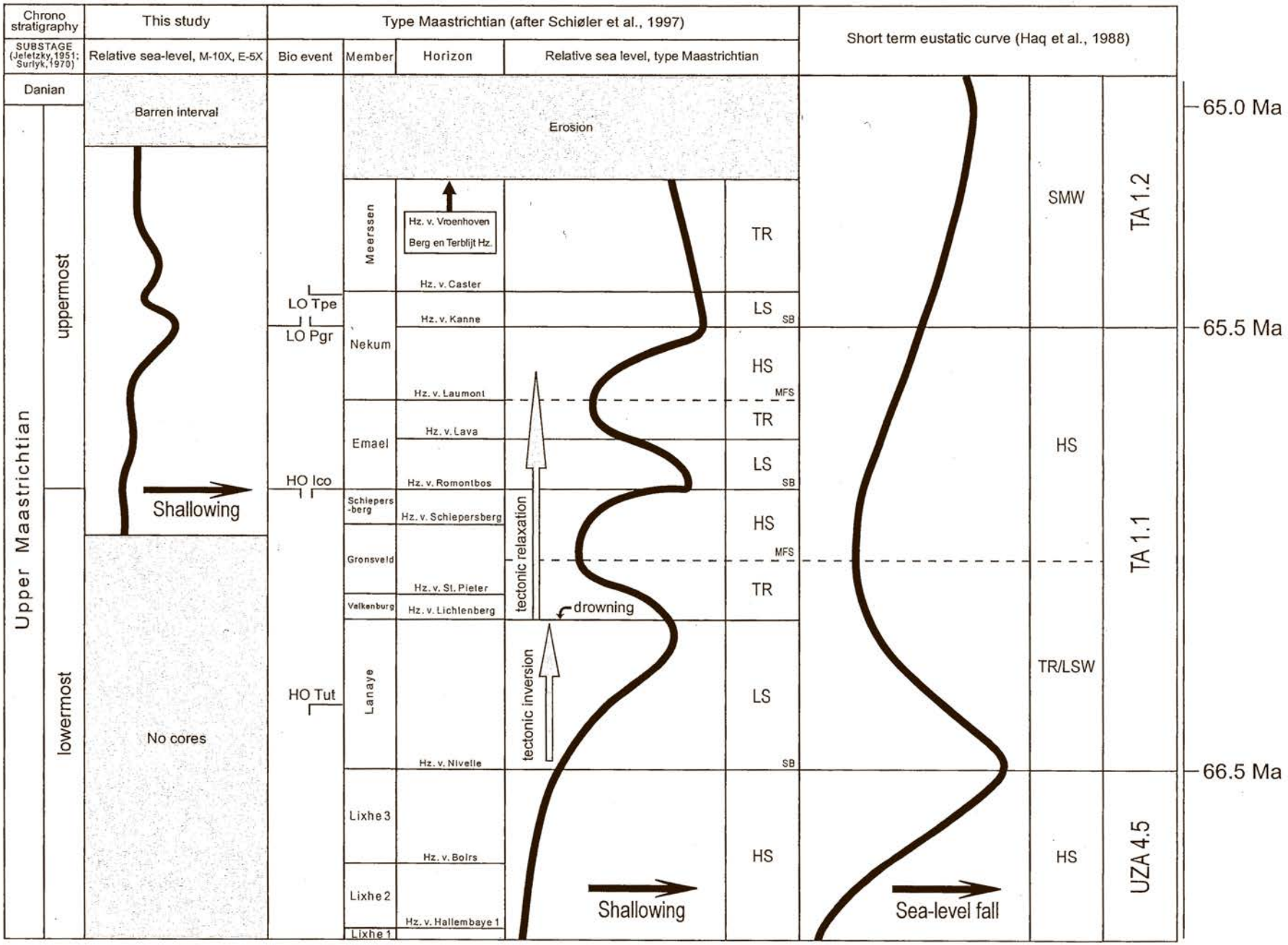
Chrono stratigraphy
This study
Type Maastrichtian (after Schiøler et al., 1997)
Short term eustatic curve (Haq et al., 1988)
SUBSTAGE (Jeletzky,1951; Surlyk,1970)
Relative sea-level, M-10X, E-5X
Bio event
Member
Horizon
Relative sea level, type Maastrichtian
Danian
Upper Maastrichtian
uppermost
lowermost
Barren interval
Shallowing
No cores
Erosion
Meerssen
Hz. v. Vroenhoven
Berg en Terblijt Hz.
Hz. v. Caster
LO Tpe
LO Pgr
Hz. v. Kanne
Nekum
Hz. v. Laumont
Emael
Hz. v. Lava
Hz. v. Romontbos
HO Ico
Schiepers -berg
Hz. v. Schiepersberg
Gronsveld
Hz. v. St. Pieter
Valkenburg
Hz. v. Lichtenberg
HO Tut
Lanaye
Hz. v. Nivelle
Lixhe 3
Hz. v. Bolrs
Lixhe 2
Hz. v. Hallembaye 1
Lixhe 1
TR
LS
SB
HS
MFS
TR
LS
SB
HS
MFS
TR
LS
SB
HS
tectonic relaxation
drowning
tectonic inversion
Shallowing
Sea-level fall
SMW
HS
TR/LSW
HS
TA 1.2
TA 1.1
UZA 4.5
65.0 Ma
65.5 Ma
66.5 Ma

Fig. 28

Depths			1st count, kerogen particles and pyrite								2nd count, palynomorphs										
core depth (f)	core depth (decimal f)	log depth (f)	black particles	brown phytoclasts	leaf cuticles	resin	fungal hyphae	palynomorphs	SUM	*Lycopodium* spores	dinoflagellates	other marine algae	foraminifera linings	non-mar. algae, fungal spores and sclerotia	degraded palynomorphs	thick-walled sporomorphs	other non-saccate sporomorphs	saccate pollen	zoomorphs	SUM	*Lycopodium* spores
6433' 4"	6433.33	6438.83	300	0	0	0	0	0	300	0	0.0	0.0	0	0	0	0.0	0.0	0.0	0	0.0	0
6433' 7"	6433.58	6439.08	295	9	0	0	0	1	305	2	0.0	0.0	0	0	0	0.0	1.0	0.0	0	1.0	2
6434' 7"	6434.58	6440.08	176	26	0	0	0	0	202	11	0.0	0.0	0	0	0	0.0	0.0	0.0	0	0.0	11
6436' 10"	6436.83	6442.33	226	81	1	0	0	7	315	11	1.3	0.0	0	0	0	0.0	4.0	0.0	1	6.3	11
6438' 2"	6438.17	6443.67	182	94	0	0	5	11	292	34	1.0	0.0	0	7	0	0.0	1.0	0.0	2	11.0	34
6438' 10"	6438.83	6444.33	239	57	0	0	0	2	298	6	0.0	0.0	0	0	0	0.0	0.0	0.0	2	2.0	6
6439'	6439.00	6444.50	296	5	0	2	0	0	303	1	0.0	0.0	0	0	0	0.0	0.0	0.0	0	0.0	1
6439' 4"	6439.33	6444.83	309	3	0	0	0	0	312	2	0.0	0.0	0	0	0	0.0	0.0	0.0	0	0.0	2
6440' 6"	6440.60	6446.10	284	8	1	7	0	1	301	11	0.0	0.0	0	0	0	0.0	0.0	0.0	0	0.0	11
6441' 11"	6441.92	6447.42	290	11	0	2	0	0	303	3	0.0	0.0	0	0	0	0.0	0.0	0.0	0	0.0	3
6443' 5"	6443.41	6448.91	247	15	1	0	0	1	264	3	0.3	0.0	0	0	0	0.0	0.0	0.0	0	0.3	3
6444' 10"	6444.83	6450.33	304	7	0	0	0	0	311	1	0.0	0.0	0	0	0	0.0	0.0	0.0	0	0.0	1
6446' 6"	6446.50	6452.00	278	22	0	0	0	1	301	5	1.0	0.0	0	0	0	0.0	0.0	0.0	0	1.0	5
6448' 2"	6448.17	6453.67	135	158	0	3	0	1	297	4	0.0	0.0	0	0	0	0.0	0.0	0.0	0	0.0	4
6449' 6"	6449.50	6455.00	147	38	0	0	0	116	301	2	101.0	2.0	0	0	0	0.0	2.0	0.0	0	105.0	3
6451' 10"	6451.83	6457.33	170	95	0	0	0	43	308	1	107.0	0.0	1	1	0	0.0	0.0	1.0	0	110.0	4
6454' 4"	6454.33	6459.83	28	69	0	1	0	205	303	0	106.3	0.0	0	0	0	0.0	0.0	1.0	1	108.3	0
6456' 9"	6456.75	6462.25	39	73	0	0	0	190	302	1	111.5	1.0	0	0	0	0.0	3.0	0.0	1	116.5	1
6458' 2"	6458.17	6463.67	27	59	0	0	0	222	308	1	115.8	0.0	0	0	0	0.0	0.0	0.0	2	117.8	1
6460' 0"	6460.00	6465.50	29	83	0	2	0	188	302	2	111.0	0.0	1	0	0	0.0	3.0	0.0	2	117.0	2
6463'	6463.00	6468.50	73	186	0	0	0	43	302	4	20.8	0.0	0	0	0	0.0	3.0	0.0	2	25.8	4
6465' 3"	6465.25	6470.75	41	160	0	1	0	100	302	6	84.3	0.0	0	0	0	0.0	6.0	1.0	1	92.3	10
6467' 8"	6467.66	6473.16	55	176	0	0	0	71	302	3	100.5	0.0	0	0	0	0.0	2.0	0.0	1	103.5	4
6472' 4"	6472.33	6477.83	34	163	0	0	0	106	303	1	100.3	0.0	0	2	0	0.0	3.0	0.0	0	105.3	1
6475' 2"	6475.17	6480.67	68	152	0	0	0	80	300	3	95.0	0.0	1	0	1	0.0	3.0	0.0	0	100.0	6
6477' 0"	6477.00	6482.50	3	23	0	0	0	287	313	0	101.3	0.0	0	1	0	0.0	2.0	1.0	2	107.3	0
6481'	6481.00	6486.50	32	78	0	0	1	195	306	1	99.5	0.0	0	1	0	0.0	1.0	0.0	1	102.5	2
6483' 10"	6483.83	6489.33	21	99	0	1	0	182	303	0	100.5	0.0	0	0	3	0.0	4.0	0.0	0	107.5	0
6487' 3"	6487.25	6492.75	33	156	0	0	0	116	305	3	99.0	2.0	0	3	0	0.0	0.0	0.0	0	104.0	3
6489' 6"	6489.50	6495.00	67	163	0	1	0	70	301	1	87.0	1.0	0	2	6	0.0	4.0	1.0	0	101.0	4
6491' 6"	6491.50	6497.00	53	110	0	2	0	35	200	0	16.5	0.0	0	0	0	0.0	2.0	0.0	0	18.5	0
6495' 6"	6495.50	6501.00																			
6499' 0"	6499.00	6504.50	104	133	0	0	1	62	300	2	45.8	1.0	0	2	0	0.0	3.0	0.0	0	51.8	2
6502' 4"	6502.33	6507.83	42	154	0	2	0	113	311	1	95.3	0.0	0	3	2	0.0	2.0	1.0	2	105.3	1
6503' 3"	6503.25	6508.75	84	141	0	1	0	76	302	1	39.8	0.0	0	0	0	0.0	0.1	0.0	0	39.9	1
6505' 1"	6505.08	6510.58	69	197	0	0	1	35	302	1	22.3	0.0	0	0	0	0.0	0.0	0.0	0	22.3	1
6507' 8"	6507.66	6513.16	73	182	0	2	0	44	301	1	93.5	0.0	0	0	0	0.0	6.0	0.0	1	100.5	10
6511' 6"	6511.50	6517.00	74	142	0	6	0	79	301	5	90.0	1.0	0	2	3	0.0	6.0	1.0	0	103.0	7
6514' 6"	6514.50	6520.00	94	148	0	0	1	61	304	2	41.3	0.0	0	0	0	0.0	3.0	0.0	0	44.3	2
6516' 8"	6516.66	6522.16	82	178	0	0	0	40	300	3	19.3	0.0	0	0	0	0.0	0.0	0.0	0	19.3	3
6519' 5"	6519.41	6524.91	16	36	0	0	0	17	69	4	10.3	0.0	0	0	0	0.0	0.0	0.0	0	10.3	4
6522' 3"	6522.25	6527.75	13	13	0	0	0	11	37	0	8.5	0.0	0	0	0	0.0	0.0	0.0	0	8.5	0
6525' 3"	6525.25	6530.75	65	146	0	3	0	92	306	5	88.0	4.0	1	0	3	0.0	5.0	1.0	2	104.0	6
6528' 11"	6528.92	6534.42	67	134	0	0	0	99	300	2	88.5	1.0	0	0	0	0.0	10.0	2.0	1	102.5	2
6531'	6531.00	6536.50	65	166	0	1	0	69	301	2	98.8	0.0	0	0	0	0.0	1.0	1.0	0	100.8	11
6533' 2"	6533.17	6538.67	55	133	0	2	0	111	301	3	99.8	0.0	0	0	2	0.0	1.0	2.0	0	104.8	6

Appendix 1

6539' 11"	6539.92	6545.42	5	4	0	0	0	1	10	0	1.0	0.0	0	0	0	0.0	0.0	0.0	0	1.0	0
6542' 7"	6542.58	6548.08	4	7	0	0	0	3	14	0	3.0	0.0	0	0	0	0.0	0.0	0.0	0	3.0	0
6546' 5"	6546.41	6551.91	108	58	0	0	0	134	300	2	152.0	0.0	0	0	0	0.0	1.0	0.0	0	153.0	2
6548' 11"	6548.92	6554.42	102	93	0	0	0	107	302	3	114.0	0.0	0	0	0	0.0	3.0	0.0	0	117.0	9
6552' 3"	6552.25	6557.75	164	95	0	0	0	51	310	1	117.5	0.0	0	0	0	0.0	0.1	0.0	0	117.6	11
6554' 10"	6554.83	6560.33	93	173	0	0	0	37	303	3	104.3	0.0	0	0	0	0.0	0.0	2.0	0	106.3	15
6557' 7"	6557.58	6563.08	48	115	0	0	0	141	304	0	118.5	1.0	0	0	0	0.0	0.1	0.0	0	119.6	9
6560' 9"	6560.75	6566.25	76	138	0	2	0	86	302	3	78.8	0.0	0	0	0	0.0	0.1	0.0	0	78.9	11
6563' 5"	6563.41	6568.91	81	83	0	0	0	138	302	5	12.8	0.0	0	0	0	0.0	0.1	0.0	0	12.9	2
6564' 9"	6564.66	6570.16	87	126	0	0	0	91	304	5	79.3	0.0	0	2	0	0.0	0.1	0.0	0	81.4	16
6568' 3"	6568.25	6573.75	85	166	0	2	3	46	302	2	42.3	0.0	0	0	0	0.0	0.1	0.0	0	42.4	7
6571' 2"	6571.17	6576.67									97.3	0.0	0	0	4	0.0	7.0	0.0	0	108.3	11
6573' 8"	6573.66	6579.16	91	89	0	1	0	120	301	3	91.5	0.0	0	12	0	0.0	1.0	0.0	0	104.5	7
6577' 1"	6577.08	6582.58	86	88	0	1	3	124	302	6	107.0	1.0	0	3	0	0.0	4.0	0.0	0	115.0	10
6579' 10"	6579.83	6585.33	56	82	0	0	0	173	311	2	104.8	0.0	0	2	0	0.0	3.0	0.0	1	110.8	3
6582' 7"	6582.58	6588.08	65	85	0	0	1	154	305	2	113.5	1.0	0	0	0	0.0	1.0	1.0	0	116.5	1
6586' 3"	6586.25	6591.75	89	153	0	0	1	58	301	4	69.5	0.0	0	1	0	0.0	6.0	1.0	0	77.5	9
6590'	6590.00	6595.50	56	141	0	0	0	108	305	5	91.3	0.0	0	2	0	3.0	5.0	0.0	0	101.3	5
6592' 2"	6592.17	6597.67	48	158	0	0	0	99	305	2	121.3	0.0	0	0	0	0.0	0.1	0.0	0	121.4	6
6598' 6"	6598.50	6604.00																			
6601' 7"	6601.58	6607.08	66	194	0	1	0	42	303	0	106.3	1.0	0	0	0	0.0	4.0	2.0	0	113.3	11
6604' 11"	6604.92	6610.42	54	174	0	0	0	80	308	1	114.0	1.0	1	1	0	0.0	1.0	0.0	0	118.0	8
6608' 1"	6608.08	6613.58	55	89	0	0	0	157	301	2	103.5	0.0	1	1	0	0.0	1.0	0.0	0	106.5	2
6610'	6610.00	6615.50	55	134	0	0	0	115	304	0	99.0	0.0	0	0	0	0.0	2.0	0.0	0	101.0	10
6611' 7"	6611.58	6617.08	79	86	0	0	0	137	302	2	88.5	1.0	1	0	0	0.0	0.1	0.0	2	92.6	2
6612' 4"	6612.33	6617.83	128	111	0	1	0	63	303	2	37.3	0.0	0	0	0	0.0	0.0	1.0	1	39.3	2
6612' 8"	6612.66	6618.16	199	45	0	0	0	58	302	5	25.5	0.0	0	0	0	0.0	2.0	0.0	0	27.5	5
6613' 1"	6613.08	6618.58	121	72	0	2	0	108	303	5	63.5	1.0	1	0	0	0.0	1.0	0.0	0	66.5	5
6613' 6"	6613.50	6619.00	105	70	0	1	0	129	305	9	83.3	0.0	0	0	0	0.0	0.1	0.0	0	83.4	9
6614' 1"	6614.08	6619.58	126	76	0	0	0	102	304	3	80.3	0.0	0	0	0	0.0	0.1	1.0	0	81.4	3
6614' 5"	6614.41	6619.91	53	121	0	0	0	128	302	3	81.0	0.0	0	0	0	0.0	2.0	0.0	0	83.0	3
6614' 9"	6614.75	6620.25	103	145	0	0	1	60	309	5	93.5	0.0	0	0	0	0.0	2.0	0.0	0	95.5	20
6615'	6615.00	6620.50	69	131	0	0	0	102	302	2	49.8	0.0	0	0	0	0.0	0.1	0.0	0	49.9	2
6615' 4"	6615.33	6620.83	69	135	0	1	0	100	305	9	42.3	0.0	0	0	0	0.0	2.0	0.0	0	44.3	9
6615' 7"	6615.58	6621.08	56	169	0	1	0	78	304	15	41.3	0.0	0	0	0	0.0	0.1	0.0	0	41.4	15
6615' 11"	6615.92	6621.42	60	155	0	0	0	90	305	15	101.3	0.0	0	0	0	0.0	0.1	0.0	0	101.4	26
6616' 3"	6616.25	6621.75	63	151	0	0	0	89	303	10	55.5	0.0	0	0	0	0.0	1.0	0.0	0	56.5	10
6616' 7"	6616.58	6622.08	65	74	0	1	0	174	314	8	110.0	0.0	0	0	0	0.0	2.0	0.0	0	112.0	8
6617' 2"	6617.17	6622.67	59	182	0	1	0	61	303	5	38.0	0.0	0	3	0	1.0	1.0	0.0	0	43.0	5
6617' 7"	6617.58	6623.08	81	139	0	0	0	83	303	9	49.0	0.0	0	0	0	0.0	2.0	1.0	0	52.0	9
6618'	6618.00	6623.50	102	114	0	1	0	88	305	14	40.8	0.0	0	1	0	0.0	0.0	0.0	0	41.8	14
6618' 5"	6618.41	6623.91	84	120	0	0	0	100	304	5	69.0	0.0	0	1	0	0.0	1.0	0.0	0	71.0	5
6618' 7"	6618.58	6624.08	87	157	0	0	0	48	292	3	27.8	0.0	0	0	0	0.0	1.0	1.0	0	29.8	3
6619'	6619.00	6624.50	119	63	0	0	0	135	317	7	104.0	0.0	0	0	0	1.0	0.0	0.0	0	105.0	16
6619' 5"	6619.41	6624.91	67	159	0	0	0	79	305	8	106.0	0.0	0	0	0	0.0	0.1	0.0	0	106.1	23
6623'	6623.00	6628.50	36	142	0	0	0	141	319	4	111.5	0.0	0	1	0	0.0	3.0	0.0	0	115.5	8
6626' 5"	6626.41	6631.91	73	144	0	1	2	89	309	6	91.0	0.0	0	1	0	0.0	5.0	0.0	0	97.0	18
6629' 4"	6629.33	6634.83	51	82	0	0	0	178	311	3	123.0	0.0	0	0	0	0.0	1.0	0.0	0	124.0	3
6631' 8"	6631.66	6637.16	32	135	0	1	0	138	306	0	117.5	0.0	0	0	0	0.0	6.0	0.0	0	123.5	4
6634' 5"	6634.41	6639.91	103	142	0	1	0	58	304	6	97.5	1.0	0	0	0	0.0	0.1	0.0	0	98.6	14
6637' 4"	6637.33	6642.83	96	143	0	2	3	57	301	6	94.0	0.0	0	0	0	0.0	2.0	1.0	0	97.0	18
6641'	6641.00	6646.50	77	72	0	0	0	154	303	9	108.0	0.0	0	0	0	0.0	0.1	0.0	1	109.1	9
6644'	6644.00	6649.50	80	94	0	0	0	129	303	8	133.8	2.0	0	0	0	0.0	1.0	1.0	3	140.8	8
6647'	6647.00	6652.50	81	120	0	0	0	104	305	17	99.8	0.0	0	0	0	0.0	4.0	0.0	1	104.8	34
6648' 6"	6648.50	6654.00	141	67	0	0	0	101	309	7	99.0	1.0	0	0	0	0.0	2.0	0.0	0	102.0	16
6652' 7"	6652.58	6658.08	182	82	0	2	0	42	308	11	94.0	1.0	0	1	0	0.0	3.0	1.0	0	100.0	24
6655' 7"	6655.58	6661.08	89	154	0	0	0	62	305	4	104.0	1.0	0	0	0	0.0	0.1	0.0	0	105.1	14

Appendix 1

Depths			absolute data					relative data						
core depth (f)	core depth (decimal f)	log depth (f)	sample weight	*lycopodium* spores/g	black particles/g	brown phytoclasts/g	organic-walled phytoplankton/g	% black particles of all counted particles	% brown phytoclasts of all counted particles	% organic-walld phytoplankton of all counted particles	log (marine/terrestrial ratio)	% *Impagidinium* group	log (peridinioid/gonyaulacoid ratio)	number marine phytoplankton diversity
6433' 4"	6433.33	6438.83	169.0	74.2	0.0	0.0	0.0	100.0	0.0	0.0		0.0		0
6433' 7"	6433.58	6439.08	169.0	74.2	10946.4	334.0	0.0	96.7	3.0	0.0		0.0		0
6434' 7"	6434.58	6440.08	169.0	74.2	1187.4	175.4	0.0	87.1	12.9	0.0		0.0		0
6436' 10"	6436.83	6442.33	169.0	74.2	1524.7	546.5	8.4	71.7	25.7	0.4	-1.796	0.0		0
6438' 2"	6438.17	6443.67	169.0	74.2	397.3	205.2	2.2	62.3	32.2	0.3	-2.037	0.0		0
6438' 10"	6438.83	6444.33	158.0	79.4	3162.0	754.1	0.0	80.2	19.1	0.0		0.0		0
6439'	6439.00	6444.50	159.0	78.9	23348.6	394.4	0.0	97.7	1.7	0.0		0.0		0
6439' 4"	6439.33	6444.83	125.0	100.3	15501.9	150.5	0.0	99.0	1.0	0.0		0.0		0
6440' 6"	6440.60	6446.10	112.0	112.0	2891.2	81.4	0.0	94.4	2.7	0.0		0.0		0
6441' 11"	6441.92	6447.42	200.0	62.7	6062.0	229.9	0.0	95.7	3.6	0.0		0.0		0
6443' 5"	6443.41	6448.91	200.0	62.7	5163.1	313.6	5.2	93.6	5.7	0.4	-1.204	0.0		0
6444' 10"	6444.83	6450.33	200.0	62.7	19063.8	439.0	0.0	97.7	2.3	0.0		0.0		0
6446' 6"	6446.50	6452.00	190.0	66.0	3670.2	290.4	13.2	92.4	7.3	0.3	-1.342	0.0		0
6448' 2"	6448.17	6453.67	200.0	62.7	2116.5	2477.0	0.0	45.5	53.2	0.0		0.0		0
6449' 6"	6449.50	6455.00	160.0	78.4	5761.5	1489.4	2639.0	48.8	12.6	37.8	0.452	2.0	-1.066	16
6451' 10"	6451.83	6457.33	185.0	67.8	11525.1	6440.5	1813.5	55.2	30.8	13.6	-0.356	5.1	-1.103	24
6454' 4"	6454.33	6459.83	200.0	62.7				9.2	22.8	66.4	0.436	2.4	-1.256	19
6456' 9"	6456.75	6462.25	200.0	62.7	2445.7	4577.8	6992.2	12.9	24.2	60.8	0.363	0.0	-0.917	19
6458' 2"	6458.17	6463.67	200.0	62.7	1693.2	3699.9	7258.7	8.8	19.2	70.9	0.541	1.5	-0.951	22
6460' 0"	6460.00	6465.50	200.0	62.7	909.3	2602.5	3480.4	9.6	27.5	59.1	0.287	5.4	-0.544	23
6463'	6463.00	6468.50	172.0	72.9	1330.8	3390.7	378.3	24.2	61.6	11.5	-0.749			
6465' 3"	6465.25	6470.75	200.0	62.7	428.5	1672.3	528.3	13.6	53.0	30.2	-0.269	4.2	-0.492	16
6467' 8"	6467.66	6473.16	200.0	62.7	1149.7	3679.0	1575.6	18.2	58.3	22.8	-0.412	5.0	-1.091	24
6472' 4"	6472.33	6477.83	200.0	62.7	2132.1	10221.7	6286.7	11.2	53.8	33.3	-0.221	3.0	-1.034	22
6475' 2"	6475.17	6480.67	200.0	62.7	1421.4	3177.3	992.9	22.7	50.7	25.6	-0.299	6.8	-0.692	16
6477' 0"	6477.00	6482.50	200.0	62.7				1.0	7.3	86.6	0.841	1.5	-0.781	18
6481'	6481.00	6486.50	200.0	62.7	2006.7	4891.4	3119.8	10.5	25.5	61.9	0.349	2.8	-0.925	23
6483' 10"	6483.83	6489.33	161.0	77.9				6.9	32.7	57.8	0.215	0.5	-1.456	23
6487' 3"	6487.25	6492.75	191.0	65.7	722.3	3414.6	2166.9	10.8	51.1	36.9	-0.151	4.0	-1.978	15
6489' 6"	6489.50	6495.00	200.0	62.7	4201.6	10221.7	1363.9	22.3	54.2	21.6	-0.414	5.2	-1.615	23
6491' 6"	6491.50	6497.00	200.0	62.7				26.5	55.0	15.6	-0.569			
6495' 6"	6495.50	6501.00	200.0	62.7										
6499' 0"	6499.00	6504.50	200.0	62.7	3260.9	4170.2	1434.5	34.7	44.3	18.7	-0.398	1.1	-1.178	16
6502' 4"	6502.33	6507.83	200.0	62.7	2633.8	9657.3	5973.1	13.5	49.5	33.6	-0.198	5.0	-1.258	19
6503' 3"	6503.25	6508.75	200.0	62.7	5267.6	8842.1	2492.7	27.8	46.7	25.1	-0.273	5.0	-1.225	13
6505' 1"	6505.08	6510.58	200.0	62.7	4327.0	12353.9	1395.3	22.8	65.2	11.6	-0.753			
6507' 8"	6507.66	6513.16	200.0	62.7	4577.8	11413.2	586.3	24.3	60.5	13.6	-0.660	9.6	-0.949	22
6511' 6"	6511.50	6517.00	192.0	65.3	966.8	1855.2	839.9	24.6	47.2	24.0	-0.332	6.9	-1.484	20
6514' 6"	6514.50	6520.00	200.0	62.7	2947.4	4640.5	1293.4	30.9	48.7	18.7	-0.430	6.1	-1.588	13
6516' 8"	6516.66	6522.16	200.0	62.7	1714.1	3720.8	402.4	27.3	59.3	13.3	-0.648			
6519' 5"	6519.41	6524.91	200.0	62.7	250.8	564.4	160.7	23.2	52.2	24.6	-0.326			
6522' 3"	6522.25	6527.75	200.0	62.7				35.1	35.1	29.7	-0.073			
6525' 3"	6525.25	6530.75	200.0	62.7	815.2	1831.1	919.7	21.2	47.7	27.5	-0.264	4.8	-1.747	22
6528' 11"	6528.92	6534.42	200.0	62.7	2100.8	4201.6	2774.9	22.3	44.7	28.8	-0.229	4.8	-1.486	23
6531'	6531.00	6536.50	200.0	62.7	2038.1	5204.9	563.0	21.6	55.1	22.5	-0.396	10.1		18

Appendix 1

6533' 2"	6533.17	6538.67	200.0	62.7	1149.7	2780.1	1042.6	18.3	44.2	35.8	-0.108	8.5	-1.659	19
6539' 11"	6539.92	6545.42	200.0	62.7				50.0	40.0	10.0	-0.602			
6542' 7"	6542.58	6548.08	200.0	62.7				28.6	50.0	21.4	-0.368			
6546' 5"	6546.41	6551.91	200.0	62.7	3386.3	1818.6	4766.0	36.0	19.3	44.4	0.354	1.3	-1.176	28
6548' 11"	6548.92	6554.42	200.0	62.7	2132.1	1944.0	794.3	33.8	30.8	34.5	0.037	3.3	-2.343	25
6552' 3"	6552.25	6557.75	200.0	62.7	10284.4	5957.5	669.9	52.9	30.6	16.4	-0.271	14.3	-2.003	24
6554' 10"	6554.83	6560.33	200.0	62.7	1944.0	3616.3	435.8	30.7	57.1	12.0	-0.680	11.0	-1.393	16
6557' 7"	6557.58	6563.08	200.0	62.7			825.7	15.8	37.8	46.3	0.088	9.9	-1.099	23
6560' 9"	6560.75	6566.25	200.0	62.7	1588.7	2884.7	448.9	25.2	45.7	28.4	-0.213	13.3	-1.834	19
6563' 5"	6563.41	6568.91	200.0	62.7	1015.9	1041.0	399.8	26.8	27.5	45.3	0.212			
6564' 9"	6564.66	6570.16	200.0	62.7	1091.2	1580.3	310.6	28.6	41.4	29.2	-0.161	23.0		18
6568' 3"	6568.25	6573.75	200.0	62.7	2665.2	5204.9	378.5	28.1	55.0	15.2	-0.572	7.1	-1.594	14
6571' 2"	6571.17	6576.67	200.0	62.7			554.4					4.4	-1.872	16
6573' 8"	6573.66	6579.16	200.0	62.7	1902.2	1860.4	819.7	30.2	29.6	34.9	0.001	4.4	-1.202	22
6577' 1"	6577.08	6582.58	200.0	62.7	898.8	919.7	671.0	28.5	29.1	38.6	0.068	3.0	-1.715	23
6579' 10"	6579.83	6585.33	200.0	62.7	1755.9	2571.1	2189.6	18.0	26.4	52.6	0.253	3.1	-2.006	22
6582' 7"	6582.58	6588.08	200.0	62.7	2038.1	2665.2	7117.6	21.3	27.9	49.6	0.232	8.6	-1.238	28
6586' 3"	6586.25	6591.75	200.0	62.7	1395.3	2398.7	484.3	29.6	50.8	17.3	-0.488	6.1	-1.638	22
6590'	6590.00	6595.50	200.0	62.7	702.4	1768.4	1144.5	18.4	46.2	31.9	-0.193	3.8	-1.147	20
6592' 2"	6592.17	6597.67	200.0	62.7	1505.0	4954.1	1267.3	15.7	51.8	32.4	-0.204	6.2	-1.296	26
6598' 6"	6598.50	6604.00	200.0	62.7										
6601' 7"	6601.58	6607.08	200.0	62.7			605.7	21.8	64.0	13.1	-0.695	1.9	-1.717	23
6604' 11"	6604.92	6610.42	200.0	62.7	3386.3	10911.5	893.6	17.5	56.5	25.3	-0.348	10.1	-1.022	25
6608' 1"	6608.08	6613.58	200.0	62.7	1724.5	2790.6	3245.2	18.3	29.6	50.7	0.224	7.0	-1.381	26
6610'	6610.00	6615.50	200.0	62.7			620.8	18.1	44.1	37.1	-0.082	10.9	-0.968	24
6611' 7"	6611.58	6617.08	200.0	62.7	2477.0	2696.5	2774.9	26.2	28.5	43.8	0.177	8.2		22
6612' 4"	6612.33	6617.83	200.0	62.7	4013.4	3480.4	1169.5	42.2	36.6	19.7	-0.285	8.7	-1.359	12
6612' 8"	6612.66	6618.16	200.0	62.7	2495.9	564.4	319.8	65.9	14.9	17.8	0.039	8.8	-0.889	18
6613' 1"	6613.08	6618.58	200.0	62.7	1517.6	903.0	796.4	39.9	23.8	34.6	0.148	7.5	-0.780	17
6613' 6"	6613.50	6619.00	200.0	62.7	731.6	487.7	580.1	34.4	23.0	42.2	0.258	11.4	-1.868	21
6614' 1"	6614.08	6619.58	200.0	62.7	2633.8	1588.7	1677.5	41.4	25.0	33.1	0.114	5.6	-1.402	20
6614' 5"	6614.41	6619.91	200.0	62.7	1107.9	2529.3	1693.2	17.5	40.1	41.4	0.003	6.1	-1.166	19
6614' 9"	6614.75	6620.25	200.0	62.7	1291.8	1818.6	293.2	33.3	46.9	19.0	-0.399	9.6	-1.010	20
6615'	6615.00	6620.50	200.0	62.7	2163.5	4107.5	1559.9	22.8	43.4	33.7	-0.110	12.1	-1.641	15
6615' 4"	6615.33	6620.83	200.0	62.7	480.8	940.7	294.4	22.6	44.3	31.3	-0.168	5.9	-1.201	19
6615' 7"	6615.58	6621.08	200.0	62.7	234.1	706.5	172.5	18.4	55.6	25.6	-0.340	5.5	-1.114	20
6615' 11"	6615.92	6621.42	200.0	62.7	250.8	648.0	244.2	19.7	50.8	29.5	-0.237	15.1	-2.059	26
6616' 3"	6616.25	6621.75	200.0	62.7	395.1	946.9	348.0	20.8	49.8	28.9	-0.242	6.3	-1.239	17
6616' 7"	6616.58	6622.08	200.0	62.7	509.5	580.1	862.3	20.7	23.6	54.4	0.340	11.1	-0.658	26
6617' 2"	6617.17	6622.67	200.0	62.7	740.0	2282.6	476.6	19.5	60.1	17.8	-0.547	8.6	-1.365	12
6617' 7"	6617.58	6623.08	200.0	62.7	564.4	968.5	341.4	26.7	45.9	25.8	-0.264	6.6	-1.308	20
6618'	6618.00	6623.50	200.0	62.7	456.9	510.6	182.5	33.4	37.4	28.2	-0.135	22.1	-1.405	23
6618' 5"	6618.41	6623.91	200.0	62.7	1053.5	1505.0	865.4	27.6	39.5	32.0	-0.102	6.5	-1.298	32
6618' 7"	6618.58	6624.08	200.0	62.7	1818.6	3281.8	580.1	29.8	53.8	15.3	-0.554	5.1	-0.827	15
6619'	6619.00	6624.50	200.0	62.7	1066.1	564.4	407.6	37.5	19.9	42.2	0.318	9.4	-0.737	27
6619' 5"	6619.41	6624.91	200.0	62.7	525.2	1246.4	289.0	22.0	52.1	25.9	-0.304	21.5	-1.920	24
6623'	6623.00	6628.50	200.0	62.7	564.4	2226.2	874.0	11.3	44.5	42.7	-0.033	27.6	-1.363	19
6626' 5"	6626.41	6631.91	200.0	62.7	763.0	1505.0	317.0	23.6	46.6	27.0	-0.262	24.7	-0.975	25
6629' 4"	6629.33	6634.83	200.0	62.7	1066.1	1714.1	2571.1	16.4	26.4	56.8	0.326	3.9	-0.620	26
6631' 8"	6631.66	6637.16	200.0	62.7			1842.1	10.5	44.1	42.9	-0.036	6.2	-0.982	29
6634' 5"	6634.41	6639.91	200.0	62.7	1076.5	1484.1	436.7	33.9	46.7	19.1	-0.393	6.9		18
6637' 4"	6637.33	6642.83	200.0	62.7	1003.4	1494.6	327.5	31.9	47.5	18.4	-0.433	2.7	-1.785	20
6641'	6641.00	6646.50	200.0	62.7	536.5	501.7	752.5	25.4	23.8	50.3	0.317	10.6	-1.382	22
6644'	6644.00	6649.50	200.0	62.7	627.1	736.8	1048.4	26.4	31.0	41.1	0.101	11.2	-1.376	26
6647'	6647.00	6652.50	200.0	62.7	298.8	442.7	184.0	26.6	39.3	32.5	-0.101	5.0		20
6648' 6"	6648.50	6654.00	200.0	62.7	1263.2	600.2	388.0	45.6	21.7	32.0	0.157	25.3		12
6652' 7"	6652.58	6658.08	200.0	62.7	1037.6	467.5	245.6	59.1	26.6	13.0	-0.334	8.0	-1.048	18
6655' 7"	6655.58	6661.08	200.0	62.7	1395.3	2414.3	465.8	29.2	50.5	20.3	-0.396	17.3	-1.758	23

Appendix 1

Depths			1st count, kerogen particles and pyrite								2nd count, palynomorphs										
core depth (f)	core depth (decimal f)	log depth (f)	black particles	brown phytoclasts	leaf cuticles	resin	fungal hyphae	palynomorphs	SUM	*Lycopodium* spores	dinoflagellates	other marine algae	foraminifera linings	non-mar. algae, fungal spores and sclerotia	degraded palynomorphs	thick-walled sporomorphs	other non-saccate sporomorphs	saccate pollen	zoomorphs	SUM	*Lycopodium* spores
6809' 3"	6809.25	6814.00	195	89	0	1	1	19	305	5	2.8	0.0	0	4	0	0.0	13.0	0.0	0	19.8	9
6812' 5"	6812.41	6817.16	202	70	0	0	0	28	300	3	0.0	0.0	0	3	1	0.0	21.0	0.0	0	25.0	3
6814' 2"	6814.17	6818.92	232	51	0	2	0	19	304	11	3.3	0.0	0	11	2	0.0	2.0	0.0	0	18.3	11
6817' 7"	6817.58	6822.33	235	60	0	1	0	8	304	2	1.0	0.0	0	5	1	0.0	2.0	0.0	0	9.0	2
6818' 8"	6818.66	6823.41	206	50	0	6	0	11	273	7	0.5	0.0	0	4	2	0.0	4.0	0.0	0	10.5	7
6820'	6820.00	6824.75	272	26	1	0	0	4	303	26	0.5	0.0	0	3	0	0.0	0.0	0.0	0	3.5	26
6821' 1"	6821.08	6825.83	151	103	1	6	2	13	276	44	0.5	0.0	0	3	0	0.0	8.0	0.0	0	11.5	44
6823' 4"	6823.33	6828.08	195	90	3	2	0	15	305	30	1.5	0.0	0	7	0	0.0	4.0	1.0	0	13.5	30
6824' 10"	6824.83	6829.58	208	43	0	1	1	20	273	58	0.0	0.0	0	19	1	0.0	0.0	0.0	0	20.0	58
6826' 8"	6826.66	6831.41	243	70	0	2	0	18	333	17	1.0	0.0	0	14	0	0.0	3.0	0.0	0	18.0	17
6827' 11"	6827.92	6832.67	143	48	0	1	0	30	222	30	0.0	0.0	0	30	0	0.0	0.0	0.0	0	30.0	30
6830'	6830.00	6834.75	79	203	0	1	0	42	325	12	1.0	0.0	0	36	0	0.0	5.0	0.0	0	42.0	12
6833' 6"	6833.50	6838.25	28	92	0	2	1	180	303	0	105.0	0.0	0	2	0	0.0	0.0	0.0	0	107.0	0
6836' 10"	6836.83	6841.58	47	124	0	0	0	139	310	0	103.3	0.0	1	0	0	1.0	1.0	1.0	0	107.3	0
6839' 3"	6839.25	6844.00	96	157	0	2	1	47	303	4	89.0	1.0	0	7	0	1.0	4.0	0.0	0	102.0	8
6841' 11"	6841.92	6846.67	55	156	0	0	0	95	306	6	92.5	0.0	0	7	0	1.0	2.0	1.0	1	104.5	14
6845' 10"	6845.83	6850.58	51	158	0	0	0	92	301	1	95.3	0.0	0	5	0	0.0	5.0	1.5	1	107.8	3
6847' 10"	6847.83	6852.58	48	158	0	0	0	98	304	1	93.5	0.0	0	3	0	0.0	3.0	0.0	1	100.5	1
6859' 10"	6859.83	6864.58	94	146	0	0	0	62	302	0	36.0	0.0	1	7	0	0.0	3.0	0.0	0	47.0	0
6863' 4"	6863.33	6868.08	63	144	0	0	1	97	305	2	50.8	0.0	0	3	0	0.0	4.0	0.0	0	57.8	2
6866' 3"	6866.25	6871.00	30	112	0	0	2	157	301	0	93.5	0.0	0	4	0	0.0	0.0	0.0	0	97.5	0
6869' 4"	6869.33	6874.08	63	163	0	0	1	74	301	2	31.8	0.0	0	11	0	0.0	1.0	0.0	0	43.8	2
6872' 8"	6872.66	6877.41	91	178	0	0	2	31	302	0	14.3	0.0	0	2	0	0.0	0.0	0.0	0	16.3	0
6875' 4"	6875.33	6880.08	52	130	0	0	0	18	200	1	12.0	0.0	0	0	0	0.0	0.0	0.0	0	12.0	1
6877' 8"	6877.66	6882.41	66	196	0	0	2	36	300	2	18.0	1.0	0	3	0	0.0	0.0	0.0	2	24.0	2
6881' 5"	6881.40	6886.15	54	144	0	0	0	106	304	3	55.5	0.0	0	8	0	0.0	0.0	0.0	1	64.5	3
6883' 11"	6883.92	6888.67	55	210	0	0	1	36	302	2	16.0	1.0	0	4	1	0.0	0.0	0.0	0	22.0	2
6887' 3"	6887.25	6892.00	47	127	0	2	4	129	309	3	73.8	0.0	0	1	0	0.0	2.0	0.0	0	76.8	3
6889' 4"	6889.33	6894.08	69	161	0	0	1	71	302	3	41.0	0.0	0	6	0	0.0	1.0	0.0	1	49.0	3
6890' 8"	6890.66	6895.41	58	164	0	0	0	85	307	1	97.8	0.0	1	2	0	0.0	0.0	0.0	0	100.8	2
6894'	6894.00	6898.75	41	135	0	1	0	125	302	4	100.3	0.0	2	0	0	0.0	1.0	0.0	0	103.3	8
6897' 11"	6897.92	6902.67	56	184	0	0	0	61	301	2	34.5	0.0	1	0	0	0.0	0.0	0.0	0	35.5	2
6900' 9"	6900.75	6905.50	78	157	0	0	0	70	305	1	37.0	0.0	0	4	0	0.0	0.0	0.0	0	41.0	1
6903' 9"	6903.75	6908.50	68	170	0	0	3	62	303	1	37.3	0.0	1	1	0	0.0	0.0	0.0	0	39.3	1
6906' 10"	6906.83	6911.58	66	159	0	0	0	76	301	3	40.3	0.0	0	0	0	0.0	0.0	0.0	0	40.3	3
6910' 3"	6910.25	6915.00	58	184	0	0	1	58	301	6	38.5	0.0	0	8	0	0.0	0.0	0.0	0	46.5	6
6912' 5"	6912.41	6917.16	57	108	0	1	0	140	306	2	97.0	0.0	0	3	0	0.0	1.0	0.0	0	101.0	2
6916' 4"	6916.33	6921.08	44	56	0	0	0	202	302	3	142.0	0.0	1	2	0	0.0	1.0	3.0	0	149.0	3
6919' 2"	6919.17	6923.92	85	64	0	2	0	155	306	7	103.3	0.0	1	0	0	0.0	0.0	0.0	1	105.3	7
6920' 9"	6920.75	6925.50	36	64	0	1	0	200	301	14	117.5	0.0	0	0	0	0.0	1.0	1.0	0	119.5	14
6923' 10"	6923.83	6928.58	144	68	0	1	0	95	308	10	100.3	0.0	1	0	0	0.0	1.0	0.0	0	102.3	13
6926' 2"	6926.17	6930.92	25	35	0	0	0	244	304	4	138.3	0.0	0	0	0	0.0	0.0	0.0	0	138.3	4
6928' 7"	6928.58	6933.33	50	91	0	0	0	164	305	18	112.8	0.0	0	0	0	1.0	0.0	0.0	0	113.8	18
6932' 5"	6932.41	6937.16	41	66	0	0	0	198	305	9	133.0	0.0	0	0	0	0.0	0.0	0.0	0	133.0	9
6935' 10"	6935.83	6940.58	70	60	0	0	0	171	301	6	77.3	0.0	0	2	0	0.0	1.0	0.0	0	80.3	6
6938' 4"	6938.33	6943.08	61	50	0	0	0	202	313	14	115.8	0.0	0	0	0	1.0	1.0	0.0	0	117.8	14

Appendix 2

6941' 2"	6941.17	6945.92	95	47	0	0	0	162	304	2	103.8	0.0	0	0	0	0.0	2.0	1.0	0	106.8	2
6943' 3"	6943.25	6948.00	71	41	0	0	0	194	306	8	116.5	0.0	2	0	0	0.0	0.0	1.0	0	119.5	8
6948' 1"	6948.08	6952.83	54	57	0	1	0	197	309	5	101.0	0.0	0	0	0	0.0	0.0	0.0	0	101.0	5
6950' 5"	6950.41	6955.16	116	73	0	0	0	113	302	5	96.8	2.0	0	0	0	0.0	2.0	0.0	0	100.8	9
6952' 11"	6952.92	6957.67	40	50	0	0	0	220	310	7	127.3	1.0	0	1	0	0.0	0.0	0.0	0	129.3	7
6956' 10"	6956.83	6961.58	53	75	0	1	1	174	304	8	108.5	2.0	2	0	0	0.0	1.0	2.0	0	115.5	8
6960' 2"	6960.17	6964.92	38	49	0	0	0	226	313	2	159.5	0.0	1	0	0	0.0	0.0	0.0	1	161.5	2
6963' 2"	6963.17	6967.92	39	40	0	0	0	236	315	11	125.8	0.0	0	0	0	0.0	0.0	0.0	1	126.8	11
6965'2"	6965.17	6969.92	41	59	0	0	0	202	302	8	114.3	0.0	0	1	0	0.0	0.0	1.0	0	116.3	8
6968' 7"	6968.58	6973.33	102	52	0	0	0	150	304	10	101.0	0.0	0	0	0	0.0	0.0	0.0	0	101.0	12
6972' 2"	6972.17	6976.92	91	85	0	0	0	128	304	0	97.5	0.0	1	0	0	0.0	2.0	0.0	0	100.5	0
6975' 2"	6975.17	6979.92	78	56	0	0	0	170	304	7	117.8	0.0	0	0	0	0.0	0.0	1.0	0	118.8	7

Appendix 2

Depths			absolute data					relative data						
core depth (f)	core depth (decimal f)	log depth (f)	sample weight	*lycopodium* spores/g	black particles/g	brown phytoclasts/g	organic-walled phytoplankton/g	% black particles of all counted particles	% brown phytoclasts of all counted particles	% organic-walld phytoplankton of all counted particles	log (marine/terrestrial ratio)	% *Impagidinium* group	log (peridinioid/gonyaulacoid ratio)	number marine phytoplankton diversity
6809' 3"	6809.25	6814.00	200.0	62.7	2445.7	489138	19.2	63.9	29.2	0.9	-1.608	0.0		0
6812' 5"	6812.41	6817.16	200.0	62.7	4222.5	844494.7	0.0	67.3	23.3	0.4	-1.937	0.0		0
6814' 2"	6814.17	6818.92	200.0	62.7	1322.6	264522.2	18.5	76.3	16.8	1.8	-1.085	0.0		0
6817' 7"	6817.58	6822.33	200.0	62.7	7368.4	1473685	31.4	77.3	19.7	0.6	-1.578	0.0		0
6818' 8"	6818.66	6823.41	200.0	62.7	1845.5	369093.1	4.5	75.5	18.3	1.0	-1.391	0.0		0
6820'	6820.00	6824.75	200.0	62.7	656.0	131208.6	1.2	89.8	8.6	0.2	-1.726	0.0		0
6821' 1"	6821.08	6825.83	200.0	62.7	215.2	43041.86	0.7	54.7	37.3	0.2	-2.343	0.0		0
6823' 4"	6823.33	6828.08	200.0	62.7	407.6	81523	3.1	63.9	29.5	0.5	-1.813	0.0		0
6824' 10"	6824.83	6829.58	200.0	62.7	224.9	44978.21	0.0	76.2	15.8	0.4	-1.806	0.0		0
6826' 8"	6826.66	6831.41	200.0	62.7	896.4	179276.8	3.7	73.0	21.0	0.3	-1.949	0.0		0
6827' 11"	6827.92	6832.67	200.0	62.7	298.9	59783.53	0.0	64.4	21.6	0.0		0.0		0
6830'	6830.00	6834.75	200.0	62.7	412.8	82568.17	5.2	24.3	62.5	0.3	-2.389	0.0		0
6833' 6"	6833.50	6838.25	200.0	62.7				9.2	30.4	58.3	0.254	3.1	-1.008	21
6836' 10"	6836.83	6841.58	200.0	62.7				15.2	40.0	43.2	0.024	2.7	-0.880	18
6839' 3"	6839.25	6844.00	200.0	62.7	1505.0	301008	697.6	31.7	51.8	13.7	-0.601	8.7	-1.398	22
6841' 11"	6841.92	6846.67	200.0	62.7	574.8	114968.3	414.3	18.0	51.0	27.5	-0.298	3.5	-0.594	24
6845' 10"	6845.83	6850.58	200.0	62.7	3198.2	639642	1991.0	16.9	52.5	27.0	-0.317	3.4	-0.426	20
6847' 10"	6847.83	6852.58	200.0	62.7	3010.1	602016	5863.4	15.8	52.0	30.0	-0.257	3.5	-0.411	21
6859' 10"	6859.83	6864.58	200.0	62.7				31.1	48.3	15.7	-0.513	0.7	-1.553	13
6863' 4"	6863.33	6868.08	200.0	62.7	1975.4	395073	1591.3	20.7	47.2	27.9	-0.265	3.9	-0.910	15
6866' 3"	6866.25	6871.00	200.0	62.7				10.0	37.2	50.0	0.097	0.3	-0.559	18
6869' 4"	6869.33	6874.08	200.0	62.7	1975.4	395073	995.5	20.9	54.2	17.8	-0.536	14.2		12
6872' 8"	6872.66	6877.41	200.0	62.7				30.1	58.9	9.0	-0.830	7.0	-0.821	7
6875' 4"	6875.33	6880.08	200.0	62.7	3260.9	652184	752.5	26.0	65.0	9.0	-0.859	10.0	-1.033	4
6877' 8"	6877.66	6882.41	200.0	62.7	2069.4	413886	564.4	22.0	65.3	9.5	-0.858	4.2	-1.237	12
6881' 5"	6881.40	6886.15	200.0	62.7	1128.8	225756	1160.1	17.8	47.4	30.0	-0.241	4.1	-1.249	17
6883' 11"	6883.92	6888.67	200.0	62.7	1724.5	344905	501.7	18.2	69.5	9.8	-0.868	10.9	-1.154	8
6887' 3"	6887.25	6892.00	200.0	62.7	982.5	196491.3	1541.6	15.2	41.1	40.1	-0.047	3.7	-1.038	19
6889' 4"	6889.33	6894.08	150.0	83.6	1923.1	288466	1142.7	22.8	53.3	19.7	-0.466	6.7		12
6890' 8"	6890.66	6895.41	200.0	62.7	3637.2	727436	3065.0	18.9	53.4	26.9	-0.299	6.4	-1.865	25
6894'	6894.00	6898.75	200.0	62.7	642.8	128555.5	785.8	13.6	44.7	40.2	-0.045	10.7	-1.952	21
6897' 11"	6897.92	6902.67	200.0	62.7	1755.9	351176	1081.7	18.6	61.1	19.7	-0.479	8.0		8
6900' 9"	6900.75	6905.50	200.0	62.7	4891.4	978276	2320.3	25.6	51.5	20.7	-0.414	4.1		21
6903' 9"	6903.75	6908.50	200.0	62.7	4264.3	852856	2335.9	22.4	56.1	19.4	-0.461	0.7		14
6906' 10"	6906.83	6911.58	200.0	62.7	1379.6	275924	841.4	21.9	52.8	25.2	-0.321	8.7		13
6910' 3"	6910.25	6915.00	200.0	62.7	606.2	121239.3	402.4	19.3	61.1	16.0	-0.609	11.0	-0.991	19
6912' 5"	6912.41	6917.16	200.0	62.7	1787.2	357447	3041.4	18.6	35.3	43.9	0.070	6.7		25
6916' 4"	6916.33	6921.08	200.0	62.7	919.7	183949.3	2968.3	14.6	18.5	63.7	0.480	4.2	-1.338	35
6919' 2"	6919.17	6923.92	200.0	62.7	761.5	152295.7	925.0	27.8	20.9	49.7	0.357	4.4	-1.597	31
6920' 9"	6920.75	6925.50	200.0	62.7	161.3	32250.86	526.3	12.0	21.3	65.3	0.459	8.5	-1.128	27
6923' 10"	6923.83	6928.58	200.0	62.7	903.0	180604.8	483.6	46.8	22.1	30.2	0.129	6.5	-1.319	37
6926' 2"	6926.17	6930.92	200.0	62.7	391.9	78387.5	2167.4	8.2	11.5	80.3	0.843	5.2	-0.706	39
6928' 7"	6928.58	6933.33	200.0	62.7	174.2	34838.89	392.8	16.4	29.8	53.3	0.245	5.8	-1.005	35
6932' 5"	6932.41	6937.16	200.0	62.7	285.7	57135.78	926.7	13.4	21.6	64.9	0.477	8.1	-1.388	33
6935' 10"	6935.83	6940.58	200.0	62.7	731.6	146323.3	807.4	23.3	19.9	54.7	0.394	1.9	-1.703	26
6938' 4"	6938.33	6943.08	200.0	62.7	273.2	54647.29	518.5	19.5	16.0	63.4	0.570	3.2	-1.447	35

Appendix 2

6941' 2"	6941.17	6945.92	200.0	62.7	2978.7	595745	3253.1	31.3	15.5	51.8	0.485	5.8	-1.551	25
6943' 3"	6943.25	6948.00	200.0	62.7	556.6	111310.3	913.2	23.2	13.4	61.8	0.655	4.7	-1.501	35
6948' 1"	6948.08	6952.83	200.0	62.7	677.3	135453.6	1266.7	17.5	18.4	63.8	0.531	12.4	-1.058	32
6950' 5"	6950.41	6955.16	160.0	78.4	1818.6	290974.4	842.7	38.4	24.2	36.7	0.168	8.3	-1.374	26
6952' 11"	6952.92	6957.67	176.0	71.3	407.2	71668.57	1295.4	12.9	16.1	70.4	0.626	4.7	-1.385	33
6956' 10"	6956.83	6961.58	200.0	62.7	415.5	83090.75	850.5	17.4	24.7	54.8	0.318	11.1	-0.700	25
6960' 2"	6960.17	6964.92	200.0	62.7	1191.5	238298	5001.1	12.1	15.7	71.3	0.649	3.9	-1.055	24
6963' 2"	6963.17	6967.92	200.0	62.7	222.3	44467.09	716.9	12.4	12.7	74.3	0.748	7.6	-1.123	29
6965'2"	6965.17	6969.92	200.0	62.7	321.4	64277.75	895.6	13.6	19.5	65.7	0.502	4.8	-1.492	30
6968' 7"	6968.58	6973.33	200.0	62.7	639.6	127928.4	527.8	33.6	17.1	49.3	0.460	5.0	-1.329	23
6972' 2"	6972.17	6976.92	200.0	62.7				29.9	28.0	40.8	0.156	4.6		22
6975' 2"	6975.17	6979.92	200.0	62.7	698.8	139753.7	1054.9	25.7	18.4	55.5	0.468	3.4	-1.181	29

Appendix 2